Graduate University of Advanced Technology

Faculty of Science and Modern Technology

Department of Chemistry

Theoretical and experimental investigation of synthesize NiO nanoparticle and nanocomposite; Application of them for electrochemical drug analysis

A Thesis Submitted as a Partial Fulfillment of the Requirements for the Degree of Master of Science in Mathematics (M.Sc.)

Prepared by:

Afsaneh Lal Sanati

Supervisors:

Dr. Hassan Karimi-Maleh
Dr. Mehdi Yoosefian

Advisor:

Dr. Mohammad Mahani

Dr. Hassan Karimi-maleh
Assistant Professor Of Analytical Chemistry
Graduate University Of Advanced Technology, Kerman Iran
Email : h.karimi.maleh@Gmail.com
Tel : +989132540112

September 2014

Abstract

In first section, we study synthesis of nanoparticle and nanocomposite NiO based compound at a carbon nanotubes as a substrate. Synthesis nanoparticle and nanocomposite were characterized using different methods such as XRD, TEM, SEM and EDAX. Results shows good synthesize of nanoparticle and nanocomposite in low size. Finally we used the NiO/CNTs nanocomposite at a carbon paste electrode in the presence of ionic liquids as a sensor for determination of Morphine, Diclofenac and NADH.

Result shows that in the presence of nanostructure current density can be improved for drug analysis. Different thermodynamic and kinetic parameter was determined for drug at a surface of modified electrode.

In secondary section, we report our findings on relative energies, geometric properties and the intramolecular hydrogen bond strength of 48 possible conformers of Droxidopa (DD) by means of the quantum chemistry method (DFT). These were carried out at the B3LYP/6-311++G^{**} level of theory in all conformers of Droxidopa. Harmonic vibrational frequencies were estimated at the same level to account the zero point vibrational energy (ZPVE) correction. Hydrogen bond energies for all conformers of Droxidopa were obtained from the Espinosa method. Solvent effects are estimated by the polarizable continuum model (PCM) at the B3LYP/6-311++G** level of theory. The ‘‘atoms in molecules’’ theory of Bader was used to analyze critical points and to study the nature of hydrogen bond in these molecules. Also Natural bond orbital (NBO) analysis was also performed for better understanding the nature of intramolecular interactions. Natural Bond Orbital analysis data, the electron density and laplacian properties as well as ν (O…H) and ɣ (O…H) have been used to evaluate the hydrogen bonding interactions**.** The calculated highest occupied molecular orbital (HOMO) and lowest unoccupied molecular orbital (LUMO) with frontier orbital gap are presented. In Continue were examined to the adsorption of nickel oxide on functionalized carbon nanotubes (5,5).

Keywords: NiO nanoparticle, NiO/CNT nanocomposite, DFT method, Morphine, Diclofenac, Deroxidopa

Contents page

1. Chapter One (Introduction) 11

1.1. First study 12

1.2. Second study 14

1.3. Third study 15

1.4. Forth study 16

1.5. Fifth study 17

1.6. Sixth study 18

2. Chapter Two (Experimental) 21

2.1. Experimental of first study 22

2.1.1. Apparatus for first study 22

2.1.2. Preparation of the modified electrode for first study 23

2.1.3. Preparation of real samples for first study 23

2.2. Chemicals for second study 23

2.2.1. Apparatus for second study 23

2.2.2. Synthesis of NiO/NPs for second study 24

2.2.3. Preparation of the modified electrode for second study 24

2.2.4. Preparation of real samples for second study 24

2.3. Chemicals for third study 25

2.3.1. Apparatus for third study 25

2.3.2. Synthesis of ZnO/CNTs for third study 25

2.3.3. Preparation of the sensor for third study 26

2.3.4. Preparation of real samples for third study 26

2.4. Chemicals for forth study 26

2.4.1. Apparatus for forth study 27

2.4.2. Synthesis of ZnO/NPs for forth study 27

2.4.3. Preparation of the sensor for forth study 28

2.4.4. Preparation of real samples for forth study 28
2.4.5. Dichlorophenolindophenol (DCPIP) titration method [33] for forth study 28
2.5. Chemicals for fifth study 29
2.5.1. Apparatus for fifth study 29
2.5.2. Synthesis of NiO/NPs for fifth study 29
2.5.3. Preparation of the modified electrode for fifth study 29
2.5.4. Preparation of real samples for fifth study 30
2.6. Computational Details for sixth study 30
3. Chapter three (Results and Discussion) 32
3.1. Optimization of NiO/CNTs and the ionic liquid ratio for first study 33
3.1.1. NiO/CNTs characterization for first study 33
3.1.2. Voltammetric investigation for first study 35
3.1.3. Chronoamperometric measurements for first study 40
3.1.4. Impedance characterization for first study 40
3.1.5. Calibration plot and limit of detection for first study 42
3.1.6. Stability and reproducibility of the modified electrode for first study 42
3.1.7. Simultaneous determination of morphine and Diclofenac for first study 42
3.1.8. Interference studies for first study 43
3.1.9. Real sample analysis for first study 44
3.2. Optimization of NiO/NPs and the ionic liquid ratio in second study 45
3.2.1. NiO/NPs characterization in second study 46
3.2.2. Electrochemical investigation in second study 47
3.2.3. Analytical features in second study 54
3.2.4. Interference studies in second study 55
3.2.5. Stability and reproducibility of the biosensor in second study 55
3.2.6. Real sample analysis in second study 56
3.3. Nanostructures characterization for third study 56

3.3.1. Voltammetric study for third study 58
3.3.2. Calibration plot and limit of detection for third study 63
3.3.3. Stability and reproducibility for third study 65
3.3.4. Interference study for third study 65
3.3.5. Real-life sample analysis study for third study 66
3.4. X-Ray diffraction and TEM of ZnO nanoparticles for forth study 67
3.4.1. Electrochemical investigation for forth study 69
3.4.2. Linear dynamic range and limit of detection for forth study 74
3.4.3. Stability and reproducibility for forth study 74
3.4.4. Interference study for forth study 75
3.5. Real sample analysis for forth study 75
3.5.1. X-Ray diffraction and TEM of NiO nanoparticles for fifth study 76
3.5.2. Electrochemical investigation for fifth study 77
3.6. Molecular geometry for sixth study 84
3.6.1. H-bond energies for sixth study 86
3.6.2. Charge Density Properties for sixth study 87
3.6.3. NBO analysis for sixth study 90
4. Chapter Four (Conclusion) 92
4.1. First study 93
4.2. Second study 93
4.3. Third study 93
4.4. Forth study 94
4.5. Fifth study 94
4.6. Sixth study 94

Table of Figures

Figure 1-1The structure of (A) morphine; and (B) diclofenac 13
Figure 1-2The geometry of Droxidopa and the numbering of the atoms 19
Figure 3-1A) XRD patterns of as-synthesized NiO/CNTs nanocomposite. B) EDAX analysis for NiO/CNTs nanocomposite..... 34
Figure 3-2TEM image of NiO/CNTs..... 35
Figure 3-3The mechanism for electrooxidation of morphine at a surface of modified electrode 36
Figure 3-4Current–pH curve for electro- oxidation of 100.0 μM morphine at IL/NiO/CNTCPE with a scan rate of 100 mV s −1 . Inset: influence of pH on cyclic voltammograms of morphine at a surface of the modified electrode (pH 5, 6, 7, and 8, respectively) 37
Figure 3-5 Cyclic voltammograms of a) CPE, b) NiO/CNT/CPE, c) IL/CPE and d) IL/NiO/CNTCPE 38
Figure 3-6 Plot of I pa versus ν 1/2 for the oxidation of morphine at IL/NiO/CNTCPE. Inset shows..... 39
Figure 3-7Chronoamperograms obtained at IL/NiO/CNTCPE in the presence of a) 200, b) 300, ... 40
Figure 3-8 Nyquistplots of CPE (a),NiO/CNT/CPE (b), IL/CPE (c), andIL/NiO/CNTCPE (d)in the..... 41
Figure 3-9The plots of the electrocatalytic peak current as a function of morphine concentration. Inset; SWVs of IL/NiO/CNTCPE in 0.1 M PBS (pH 7.0) containing different concentrations of morphine – diclofenac in μM. a–f: 1.63 + 2.0; 60.0 + 10.0; 100.0 + 15.0; 150 43
Figure 3-10(A) Current vs. % NiO/NPs curve at a surface of carbon paste electrode in the presence of fix amount (10% ILs) for electrooxidation of 700 μmol L −1 at pH 7.0. (B) Current vs. % ILs at a curve surface of carbon paste electrode in the presence of fix amount (10% NiO/NPs) for electrooxidation of 700 μmol L −1 at pH 7.0..... 46
Figure 3-11((A) XRD . (C) TEM image of NiO nanparticles patterns of as-synthesized NiO nanparticles. (B) EDAX analysis for NiO nanoparticle..... 47
Figure 3-12Current–pH curve for electro-oxidation of 450 μmol L −1 NADH at IL/NiO/NPs/CPE with a scan rate of 100 mV s −1 . Inset: influence of pH on cyclic voltammograms of NADH at a surface of the modified electrode, (pH 5–8, respectively). 48

Figure 3-13 Cyclic voltammograms of (a) IL/NiO/NPs/CPE, (b) IL/CPE, (c) NiO/NPs/CPE and 50
Figure 3-14Plot of I pa versus v 1/2 for the oxidation of NADH at IL/NiO/NPs/CPE. Inset shows cyclic voltammograms of NADH at IL/NiO/NPs/CPE at different scan rates (from inner to outer) of 5, 10, 30, 60, 100, 150 and 200 mV s −1 in 0.1 M phosphate buffer, pH 7.0. 51
Figure 3-15(A) Chronoamperograms obtained at IL/NiO/NPs/CPE in the presence of (a) 400; (b) 500; and (c) 600 μmol L −1 NADH in the buffer solution (pH 7.0). (B) Cottrell's plot for the data from the chronoamperograms 52
Figure 3-16Nyquist plots of CPE (a), NiO/NPs/CPE (b), IL/CPE (c), and IL/NiO/NPs/CPE (d) in the presence of 500 μmol L −1 NADH. Conditions: pH, 7.0; Edc, +0.56 V vs. Ag/AgCl; Eac , 5 mV; frequency range, 0.1–100,000 Hz. 53
Figure 3-17(A) SWVs of IL/NiO/NPs/CPE in 0.1 mol L^{-1} phosphate buffer solution (pH 7.0) containing different concentrations of NADH. Inner to outer voltammograms correspond to 0.03, 0.3, 5.0, 50.0, 100.0, 200.0, 400.0, 500.0, 700.0 and 900.0 μmol L^{-1} of NADH. (B) Plot of the peak current as a function of NADH concentration in the range. Error bar obtained for three separate experimental..... 54
Figure 3-18A) TEM image of ZnO nanoparticles deposited on sidewalls of MWCNTs. B) EDAX analysis for ZnO/CNTs nanocomposite. C) SEM image of ZnO nanoparticles and D) SEM image of multiwall carbon nanotubes..... 57
Figure 3-19XRD patterns of as-synthesized ZnO/CNTs nanocomposite..... 58
Figure 3-20 Current–pH curve for electrooxidation of 450 μmol L −1 NE at ZnO/CNTs/ 59
Figure 3-21Cyclic voltammograms of a) CPE, b) ZnO/CNTs/CPE, c) IL/CPE and d) ZnO/CNTs/IL/CPE in the presence of 350 μmol L −1 NE at pH 6.0, respectively 60
Figure 3-22 Plot of I pa versus v 1/2 for the oxidation of NE at ZnO/CNTs/IL/CPE. Inset shows cyclic voltammograms of NE at ZnO/CNTs/IL/CPE at different scan rates (from inner to outer) of 5, 10, 20, 30, 50, 100, 150 and 200 mV s −1 in 0.1 M phosphate buffer, pH 6. 62
Figure 3-23 A) Chronoamperograms obtained at ZnO/CNTs/IL/CPE in the presence of a) 300; b) 350; and c) 450 μmolL−1 NE in the buffer solution (pH 6.0). B) Cottrell's plot for the data from the chronoamperograms (n = 3)..... 63
Figure 3-24 Plot of the peak current as a function of NE concentration in the range (n = 3). Inset) 64

Figure 3-25 XRD patterns of ZnO nanoparticles. 68
Figure 3-26 TEM image of ZnO nanoparticles. 69
Figure 3-27 Current–pH curve for electrooxidation of 50.0 μM AA at ZnO/NP/IL/CPE with a scan rate of 50 mV s -1 . Inset) influence of pH on cyclic voltammograms of AA at a surface of the modified electrode, (pH 4, 5, 6, 7, and 8, respectively). 70
Figure 3-28 Cyclic voltammograms of a) at ZnO/NP/IL/CPE, b) IL/CPE, c) at ZnO/NP/CPE and d) CPE in presence of 100 μM AA at a pH 7.0, respectively. Inset: the current density derived from cyclic voltammograms responses of 100 μM AA at pH 7.0 at the surface of different electrodes with a scan rate of 50 mV s^{-1} 71
Figure 3-29 Plot of I pa versus ν 1/2 for the oxidation of AA at ZnO/NP/IL/CPE. Inset shows cyclic voltammograms of AA at ZnO/NP/IL/CPE at different scan rates of 50, 70, 100, 150, 200, 250, 420 and 480 mV s –1 in 0.1 M phosphate buffer, pH 7.0. 72
Figure 3-30 Tafel plot for ZnO/NP/IL/CPE in 0.1 M PBS (pH 7.0) with a scan rate of 50 mV s −1 in the presence of 50 μM AA 73
Figure 3-31 A) Chronoamperograms obtained at ZnO/NP/IL/CPE in the presence of a) 300; b) 400; c) 500; d) 600 and e) 700 μM AA in the buffer solution (pH 7.0). B) Cottrell's plot for the data from the chronoamperograms 74
Figure 3-32 SEM image of NiO/NPs. 77
Figure 3-33 XRD patterns of as-synthesized NiO nanoparticle. 77
Figure 3-34 Mechanism for electro-oxidation of NB 78
Figure 3-35 Current–pH curve for electro-oxidation of 100.0 μM NB at NiO/NPs/CPE with a scan rate of 50 mV s^{-1} 79
Figure 3-36 Cyclic voltammograms of (a) NiO/NPs/CPE, and (b) CPE in the presence of 100 μM NB at pH 7.0, respectively. 80
Figure 3-37 Tafel plot for NiO/NPs/CPE in 0.1 MPBS (pH 7.0) at the scan rateof 50 mV s −1 in the presence of 100.0 μM NB 81
Figure 3-38 The plots of the electrocatalytic peak current as a function of NB concentration. Inset shows the SWVs of NiO/NPs/CPE in 0.1 M phosphate buffer solution (pH 7.0) containing different concentrations of NB. From inner to outer correspond to 0.8, 5.0, 50.0 83
Figure 3-39 The relationship between the E HB (in kJ/mol) and dielectric constant. 84

Figure 3-40 The molecular graphs of Droxidopa obtained from the B3LYP/6-311++G(d,p) wave function. 88
Figure 3-41 The contour map of Droxidopa in vacuum and in five solvents obtained from the B3LYP/6 311++G(d,p) wave function in plane with three selected points: A(2.42, 3.06, 2.07), B(7.33, 1.88, 0.82), and C(7.97, −1.56, −1.52)..... 89

Table 3-1 Interference study for the determination of 15.0 μM morphine under the optimized conditions 44
Table 3-2Determination of morphine in drug and urine samples 45
Table 3-3Comparison of the efficiency of some modified electrodes used in the electrocatalysis of NADH. 55
Table 3-4Interference study for the determination of 10.0 μmol L −1 NADH under the optimized conditions 55
Table 3-5Determination of NADH in real samples (n = 3) 56
Table 3-6Comparison of the efficiency of some electrochemical methods in the determination of NE 65
Table 3-7Interference study for the determination of 10.0μmol L −1 NE under the optimized conditions 66
Table 3-8Determinationof NE in drug, and urine samples (n = 3). 67
Table 3-9 Interference study for the determination of 10.0 μM AA under the optimized conditions 75
Table 3-10 Determination of AA in real samples (n=3) 76
Table 3-11 Ability of propose sensor for determination of NB in real samples 83

Chapter One

Introduction

1.1. First study

The science of nanomaterials has created great excitement and expectation in the recent years at the nano-scale fundamental properties changes [1–3]. Oxide nano-materials were used as catalysts in the preparation of electrochemical sensor [4–7] and starting materials for preparing advanced structural ceramics [8]. On the other hand, nanocomposite of a variety of shapes, sizes and compositions is changing nowadays the bioanalytical measurement.

Morphine (Fig. 1A) is the mainly abundant alkaloid found in opium. In clinical medicine, morphine is regarded as the gold standard or benchmark of analgesics used to relieve severe or agonizing pain and suffering [9]. On the other hand, morphine is on the banned list for athletic doping. An advantage of using morphine would be to reduce pain during an intense athletic event-pain that could reduce performance. Studies show that if an athlete is given morphine during training (which is legal), then abstains long enough for the morphine to clear the system, and then takes a saline injection (placebo) on the day of competition, the athlete experiences reduced pain [10]. So, a fast and sensitive method for sensitive and selective determination of morphine in pharmaceutical and biological sample is very important. The determination of morphine has been carried out with various detection techniques such as high performance liquid chromatography [11,12], UV–Vis spectroscopy [13], gas chromatography–mass spectroscopy [14,15], fluorimetry [16–19], chemiluminescence [20–22], surface plasma resonance (SPR) [23], and electrochemical methods [24–31].

Diclofenac (Fig. 1B) is a synthetic nonsteroidal anti-inflammatory drug (NSAID), has been proven as a safe and efficacious drug in the treatment of a variety of inflammatory and rheumatoid disorders [32]. Diclofenac is well absorbed after oral administration with extensive hepatic metabolism. This compound exhibits a terminal half-life of 1–2 h, volume of distribution of 0.17 l/kg, 99% protein binding and enters the synovial fluid [33]. The determination of small amounts of Diclofenac in pharmaceutical preparations is very important for medical and pharmaceutical needs where it is used for the treatment of various diseases. Therefore it is vital to develop a simple, fast, selective and cost-effective method of determining the trace amounts of diclofenac in different pharmaceutical formulations.

Diclofenac as a NSAID has been shown to decrease morphine consumption after operation in adults. The addition of regular doses of Diclofenac may reduce the need for morphine after abdominal surgery [34]. Therefore, the design of a simple, fast and inexpensive method for determination of these compounds in biological and pharmaceutical samples seems essential.

Room temperature ionic liquids (RTILs) are beginning to be used as new kind of binder to make an ionic liquid modified electrode. Because RTILs have many specific electrochemical properties such as wide electrochemical window, high ionic conductivity and good solubility [35–37], they have been recognized as a useful non-aqueous media for various electrochemical processes [38–41].

To the best of our knowledge, only one study has been reported on the voltammetric determination of morphine in the presence of diclofenac using modified electrodes [29], which is the focus of the present study.Compared with previous report for determination of diclofenac using vinylferrocene/multiwall carbon nanotube paste electrodes [29]; the modified electrode has not any mediator in electrode matrix and simple prepared. Also, the propose sensor has the comparable dynamic range, limit of detection and sensitivity for morphine and diclofenac analysis. In continuation of our studies on the preparation of chemically modified electrodes [42–46], a novel ionic liquid modified NiO/CNTs carbon paste electrode for the voltammetric determination of morphine was investigated using square wave voltammetry. We have also evaluated the analytical performance of the modified electrode for quantification of morphine in the presence of diclofenac in some real samples.

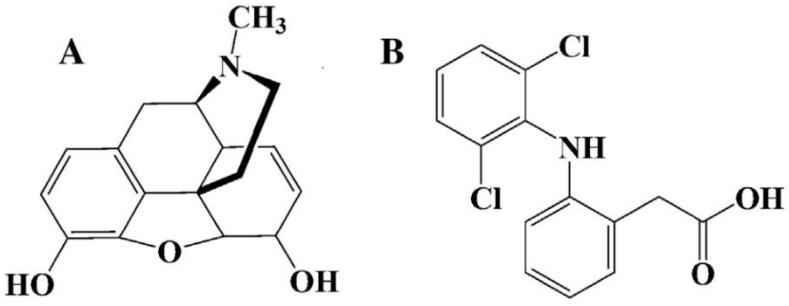

Figure 1-1The structure of (A) morphine; and (B) diclofenac

1.2. Second study

NADH is an important coenzyme produced in vivo during dehydrogenase based enzymatic reactions and it has a number of essential roles in biological systems [1]. It acts as a coenzyme in redox reactions, as a donor of Adenosine diphosphate (ADP)-ribose moieties in ADP-ribosylation reactions, as a precursor of the second messenger molecule cyclic ADP-ribose, as well as acting as a substrate for bacterial DNA ligases and a group of enzymes called sirtuins that use NAD + to remove acetyl groups from proteins. In addition to these metabolic functions, NAD + emerges as an adenine nucleotide that can be released from cells spontaneously and by regulated mechanisms [2] and can so have important extracellular roles [3]. The electrochemical oxidation of NADH has attracted considerable attention due to its importance both as a cofactor for dehydrogenase enzymes and its role in the electron-transfer chain in biological system and also due to the need to expand voltammetric biosensors for substrates of NAD + -dependent dehydrogenases [4]. According to the above points, it is very important to create suitable conditions for the analysis of NADH in pharmaceutical and biological samples. Many modified electrodes have been so far reported for its determination [4,5,1,6,7].

Room temperature ionic liquids exhibit unusual and promising properties for electrochemical applications, such as ionic conductivity and non-volatility [8–13]. Furthermore, due to their considerably high ionic conductivity, broad electrochemical window and fast ion mobility [11–13], ionic liquids have also been utilized as electrolyte, binder and solvents in the electrochemical preparations of modified electrodes [14–17]. Room temperature ionic liquids-based electrochemical sensors have also been extensively reported for direct electron transfer of different types of compounds such as ascorbic acid, Sudan I, morphine, epinephrine, methyldopa, norepinephrine and benserazide [18–24]. Results suggested that the use of ILs could increase the sensitivity of response and facilitate efficient direct electron transfer of various electro-active compounds [25–28].

Nanostructured materials such as carbon nanotubes, nanoparticles and nanocomposite have also been incorporated into electrochemical sensors for biological and pharmaceutical analyses over the last decade [29–34]. In between, NiO nanoparticles are an important multifunctional material with applications such as gas sensors and catalysts. The various applications of NiO are due to the specific chemical, surface and microstructural properties of this material [35].

A review of literature showed that there are a few studies reported on the voltammetric determination of NADH using modified ionic liquid electrodes [4,36–38], which is the focus of the present study. However there is no report available on the voltammetric determination of NADH using NiO nanoparticle modified electrode. Further in the present study no mediator for NADH analysis has been used and it has the best dynamic range, limit of detection and sensitivity for its analysis. In this study, we describe the synthesis and application of NiO/NP as a novel nanosensor and 1-methyl-3-butylimidazolium bromide as a suitable binder in a carbon paste matrix for the voltammetric determination of NADH. We also evaluate the analytical performance of the modified electrode for the voltammetric determination of NADH in real samples such as water, urine and serum.

1.3. Third study

Noradrenaline (NE) is a neurotransmitter belonging to a catecholamine type hormone [1] that is manufactured as a drug. Also called norepinephrine, especially by those in the medical field, this hormone acts on the parts of the brain involved with responsiveness and fear. This neurotransmitter is released into the blood from the adrenal medulla and from nerves called adrenergic nerves [2]. Also, NE is a drug belonging to the stimulants that are on the World Anti-Doping Agency's 2005 Prohibited List. It is also critical in mental disease, heart failure; DNA breaks in cardiac myoblast cells, and diabetes. Recent reports have indicated that NE enhances adhesion of human immunodeficiency virus-1 (HIV-1)-infected leukocytes to cardiac micro-vascular endothelial cells and also accelerates HIV replication via protein kinase [3]. Therefore, the quantitative determination of NE concentration in different human fluids, such as plasma and urine, is important for developing nerve physiology, pharmacological research and life sciences. Numerous electrochemical methods have been developed to determine NE due to its electroactive nature [4–9]. Electroanalytical methods have attracted more attention in recent years for environmental and biological compounds determination due to their sensitivity, accuracy, lower cost, and simplicity [10–16]. In recent years, nanostructured materials such as nanocomposites have also been incorporated into electrochemical sensors for biological and pharmaceutical analyses [17–21]. While they have many properties similar to other types of materials, they offer unique advantages including enhanced electron transfer, large edge

plane/basal plane ratios and rapid kinetics of the electrode processes [22–25]. Nanocomposites of a variety of shapes, sizes and compositions are changing modern bioanalytical measurement [26–28].

Recently, room temperature ionic liquid (RTIL) has been used as a new agent for binding to chemically modified electrodes [29–31]. RTIL is composed entirely of ions and exists as a liquid at room temperature with the characteristics of negligible vapor pressure and good solubility and chemical stability. As a new green medium, RTIL has many unique electrochemical properties, such as higher ionic conductivity and wider electrochemical windows [32–38].

In this study, we describe synthesis and application of novel ZnO/CNTs nanocomposite modified carbon ionic liquid paste electrode, which utilizes 1,3-dipropylimidazolium bromide as a binder. The electrochemical behavior of NE at a CPE, an ionic liquid modified carbon paste electrode (IL/CPE), a ZnO/CNT carbon paste electrode (ZnO/CNT/CPE) and a ZnO/CNT/IL/CPE was investigated. The results showed the superiority of ZnO/CNT/IL/CPE to the other electrodes in terms of both provision of better reversibility and higher sensitivity. Finally, ZnO/CNT/IL/CPE was successfully applied for the determination of NE in real samples.

1.4. Forth study

Compared to conventional electrodes, chemically modified electrodes (CMEs) offer unique well recognized advantages, especially in situations where the target analyte requires high overpotential, i.e. electrocatalysis, and also electroanalysis [1-4]. This characteristic of chemically modified electrodes arises from the advantageous combination of conventional electrochemical techniques with the chemical, structural and other specific properties of the modifying layer(s) [5-8].

A new room temperature ionic liquid has been used as a new kind of modifier for a chemically modified electrode [9-12]. This room temperature ionic liquid is composed entirely of ions and exists as a liquid at room temperature with the characteristics of negligible vapor pressure and good solubility and chemical stability. As a new green media, the room temperature ionic liquid

has many unique optical and electrochemical properties, such as higher ionic conductivity and wider electrochemical windows [13–18].

Ascorbic acid (AA), also known as vitamin C, is found in numerous natural sources. Its determination has received great attention in analytical chemistry due to the wide use in soft drinks and drugs [19]. It is also important clinically to determine its concentration in blood, urine [20] and tissues. Its quantification in foods and beverages has received increasing importance [21-23].

For the determination of ascorbic acid, several analytical methods have been proposed such as chromatography [24, 25], spectrophotometry [26, 27], mass spectrometry [28], flow injection [29, 30], chemiluminescence and electrochemical methods [31, 32] have been proposed for its determination in different matrices and at different levels. In this study, we describe the synthesis and application of a novel ZnO/NPs modified carbon ionic liquid paste electrode, which utilizes 1, 3- dipropylimidazolium bromide as a binder.

The electrochemical behavior of AA at ZnO/NPs modified carbon ionic liquid electrode (ZnO/NPs/IL/CPE), at carbon paste electrode modified with ionic liquid (CP/ILE), at ZnO/NPs paste electrode (ZnO/NPs/CPE), and at carbon paste electrode (CPE) was investigated. The results showed the superiority of ZnO/NPs/IL/CPE to the other electrodes in terms of better reversibility and higher sensitivity. The proposed method is selective and sensitive enough for the determination of AA in real samples such as fruit juices, vegetables and tablet samples with good reproducibility.

1.5. Fifth study

Nalbuphine is a semi-synthetic opioid used commercially as an analgesic under a variety of trade names, including Nubain. Nalbuphine is a semi- synthetic opioid agonist-antagonist analgesic of the phenanthrene series [1]. It is chemically related to the widely used opioid antagonists, naloxone and naltrexone, and the potent opioid analgesic, oxymorphone. It is available in two concentrations, 10 mg and 20 mg of nalbuphine hydrochloride per mL. Both strengths contain 0.94% sodium citrate hydrous, 1.26% citric acid anhydrous, 0.1% sodium metabisulfite, and

0.2% of a 9:1 mixture of methylparaben and propylparaben as preservatives; pH is adjusted, if necessary, with hydrochloric acid. The 10 mg/mL strength contains 0.1% sodium chloride. So, determination of NB is very important in pharmaceutical and biological samples [2].

Nanoscience represent new and enabling platforms that promise to provide a broad range of novel uses and improved technologies for environmental, biological and other scientific applications [3]. One of the reasons behind the intense interest is that nanotechnology permits the controlled synthesis of materials where at least one dimension of the structure is less than 100 nm. Recently, nanostructured materials have also been incorporated into electrochemical sensors for biological and pharmaceutical analyses [4–6]. While they have many properties similar to other types of carbon, they offer unique advantages including enhanced electron transfer, large edge plane/basal plane ratios and rapid kinetics of the electrode processes. In between, NiO/NPs are an important multifunctional material with applications such as varistors, gas sensors, SAW devices, transparent electrodes and catalysts. The various applications of NiO/NPs are due to the specific chemical, surface and microstructural properties of this material [7-9].

In continuation of our studies on chemically modified electrodes [10–17], we describe the synthesis and application of NiO/NPS as a novel nanosensor in a carbon paste matrix for the voltammetric determination of NB. We also evaluate the analytical performance of the modified electrode for the voltammetric determination of NB in real samples such as drug, urine and serum.

1.6. Sixth study

The importance of hydrogen bond cannot be overstated. It is strong enough to influence the arrangement of molecules in crystals and even the geometry of molecules participating in these interactions [1–8] They influence the physicochemical properties [9–13] and play relevant roles in important aspects of biological activity mechanisms like selective binding, molecular recognition and in specific activities (e.g., anti-tumor activity) [14,15]. The presence of a solvent affects molecular properties such as bond length, electron population on atoms, energy level separations, [16,17] relative stabilities of different conformers of a molecule or different isomers, [18,19] polarizabilities, dipole moments, NMR and ESR parameters. [20,21]

Its influence on important aspects of the mechanisms of biological activities, such as molecular recognition [22] or interactions with the receptor [23] and the fact that biological activities occur in some medium within living organisms [24] provide strong motivation for the study of the solvent effects on the characteristics of biologically active molecules. The current study investigates the influence of the presence of a medium (solvent) on the characteristics of the intramolecular hydrogen bond (IHB) typical of Droxidopa (figure 2). The study in solution aims at verifying whether and to what extent those patterns remain valid, or new patterns emerge, under different types of solute–solvent interactions.

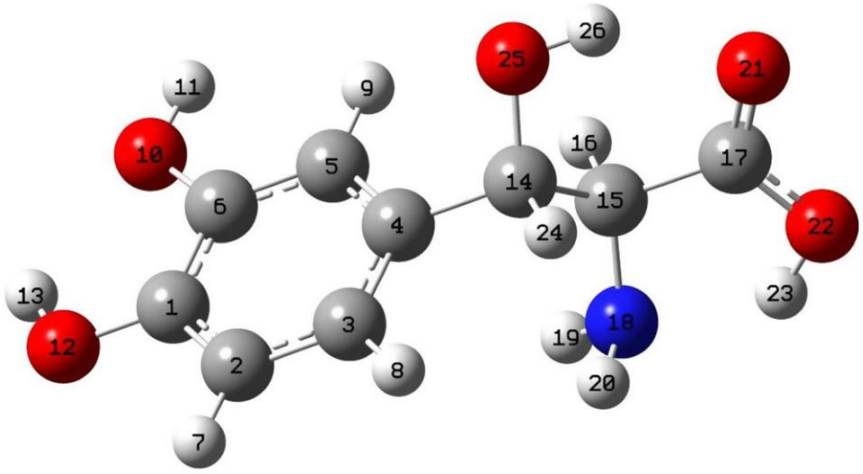

Figure 1-2The geometry of Droxidopa and the numbering of the atoms

Droxidopa is an international nonproprietary name (INN) for a synthetic amino acid precursor of norepinephrine, whose systematic (IUPAC) name is (2R,3S)- 2-amino-3-(3,4-dihydroxyphenyl)-3-hydroxypropanoic acid (L-DOPS). Droxidopa is a psychoactive drug and a synthetic amino acid precursor that acts as a prodrugto the neurotransmitters norepinephrine (noradrenaline) and epinephrine (adrenaline). 25 Unlike norepinephrine and epinephrine themselves, L-DOPS is capable of crossing the protective blood–brain barrier (BBB) [25].

Data from clinical studies and post-marketing surveillance programs conducted in Japan show that the most commonly reported adverse drug reactions with Droxidopa are increased blood

pressure, nausea, and headache. In clinical studies to date, data suggest that Droxidopa is well tolerated and effective as a norepinephrine precursor [26].

Five solvents exerting different types of interactions with the solute molecules are selected: water and ethanol (which are capable of forming intermolecular H-bonds with the solute, with both donor and acceptor roles, and also among themselves), tetrahydrofuran and dimethyl sulfoxide (which can only form intermolecular H-bonds with the solute, with acceptor role), and carbon tetrachloride (which cannot form H-bonds).

Their different dielectric constants (78.4 for water, 46.7 for dimethyl sulfoxide, 24.6 for ethanol, 7.6 for tetrahydrofuran, 2.3 for carbon tetrachloride) enable informative comparisons from the results of continuum model (PCM 27,28) calculations. Their different polarities adequately cover the polarity range of possible environments in which Droxidopa molecules maybe preferably present within a living organism, according to preference of individual compounds for more or less polar solvents.

Chapter Two

Experimental

2.1. Experimental of first study

All chemicals used were analytic reagent grade purchased from Merck (Darmstadt, Germany) unless otherwise stated. Doubly distilled water was used throughout. Morphine sulfate and diclofenac were from Sigma. Other reagents were used without further purification.

A 1.0×10^{-2} M morphine solution was preparing daily by dissolving 0.19 g morphine sulfate in water and the solution was diluted to 25 mL with water in a 25-mL volumetric flask. The solution was kept in refrigerator at 4 °C in dark. More dilute solutions were prepared by serial dilution with water.

A 1.0×10^{-3} M Diclofenac solution was prepared daily by dissolving 0.032 g Diclofenac in water and the solution was diluted to100 mL with water in a 100 mL volumetric flask. The solution was kept in a refrigerator at 4 °C and in dark. More dilute solutions were prepared by serial dilution with water.

Phosphate buffer solutions (sodium dihydrogen phosphate and disodium monohydrogen phosphate plus sodium hydroxide, 0.1 mol L^{-1}), PBS, with different pH were used.

Spectrally pure graphite powder (particle size b50 μm), and high viscous paraffin oil (density = 0.88 kg L^{-1}) from Merck were used as the substrate for the preparation of the working electrodes.

2.1.1. Apparatus for first study

Cyclic voltammetry, chronoamperometry, square wave voltammetry, and impedance spectroscopy were performed in an analytical system, Autolab PGSTAT 302 N, potentiostat/galvanostat connected to a three electrode cell, Metrohm Model 663 VA stand, linked with a computer (Pentium IV, 1200 MHz) and run with GPES and FRA 4.9 software. For impedance measurements, a frequency range of 100 kHz to 1.0 Hz was employed.TheACvoltageamplitudeusedwas5 mV, and the equilibrium time was 5 min. A conventional three-electrode cell assembly consisting of a platinum wire as an auxiliary electrode and an (Ag/AgCl/KCl sat) electrode as a reference electrode was used. The working electrode was either an unmodified carbon paste electrode (CPE), NiO/CNTs carbon paste electrode (NiO/CNT/CPE), or IL/CPE an IL/NiO/CNTCPE.

2.1.2. Preparation of the modified electrode for first study

IL/NiO/CNTCPE was prepared by mixing of 0.25 g of [MBIDZ]Cl, 0.70 g of the liquid paraffin, 0.35 g of NiO/CNTs, and 0.70 g of graphite powder. Then the mixture was mixed well for 50 min until a uniformly wetted paste was obtained. A portion of the paste was filled firmly into one glass tube as described above to prepare IL/NiO/CNTCPE. Electrical contact was made by pushing a copper wire down the glass tube into the back of the mixture. When necessary, a new surface was obtained by pushing an excess of the paste out of the tube and polishing it on a weighing paper.

2.1.3. Preparation of real samples for first study

Urine samples were stored in a refrigerator at 4 °C immediately after collection. Ten milliliters of each sample was centrifuged for 15 min at 2500 rpm. The supernatant was filtered using a 0.45 μm filter and then diluted five times with PBS (pH 7.0). The solution was transferred into the voltammetric cell to be analyzed without any further pretreatment. Standard addition method was used for the determination of morphine in real samples. For pharmaceutical analyses, 0.10 mL of commercial injection solution (APP Pharmaceuticals, LLC Schaumburg), contained 0.5 mg mL^{-1} of morphine was mixed with 10 mL of 0.1 mol L −1 phosphate buffer (pH 7.0) before analysis.

2.2. Chemicals for second study

All chemicals used were of analytical reagent grade purchased from Merck (Darmstadt, Germany) unless otherwise stated. Double distilled water was used throughout for all experiments. Phosphate buffer (sodium dihydrogen phosphate and disodium monohydrogen phosphate plus sodium hydroxide, 0.1 mol L −1) solutions (PBS) with different pH values were used. High viscosity paraffin (d = 0.88 kg L −1) and pure graphite powder (particle size < 50 μm) from Merck was used for the preparation of the carbon paste electrodes**.**

2.2.1. Apparatus for second study

Cyclic voltammetry, electrochemical impedance spectroscopy, and square wave voltammetry were performed in an analytical system, Autolab with PGSTAT 302N (Eco Chemie, the

Netherlands). The system was run on a PC using GPES and FRA 4.9 software. For impedance measurements, a frequency range of 100 kHz to 0.1 Hz was employed. The AC voltage amplitude used was 5 mV, and the equilibrium time was 15 min. A conventional three-electrode cell assembly consisting of a platinum wire as an auxiliary electrode and an Ag/AgCl/KCl sat electrode as a reference electrode was used. The working electrode was either an IL/NiO/NPs/CPE. X-ray powder diffraction studies were carried out using a STOE diffractometer with Cu–Ka radiation (l = 1.54 ˚ A).

2.2.2. Synthesis of NiO/NPs for second study

0.6 M aqueous solution of nickel nitrate Ni (NO 3) 2 and a 0.4 M aqueous solution of sodium hydroxide (NaOH) were prepared in distilled water. The beaker containing NaOH solution was heated at the temperature of about 60 ◦ C and Ni (NO 3) 2 solutions were added drop wise (slowly for 2.0 h) to the above heated solution under high-speed stirring. The beaker was sealed at this condition for 2 h. The precipitated Ni (OH) 2 were cleaned with deionized water and ethanol then calcined at 350 ˚C for 2.0 h for synthesis of NiO/NPs**.**

2.2.3. Preparation of the modified electrode for second study

IL/NiO/NPs/CPE was prepared by mixing 0.2 g of 1-methyl-3- butylimidazolium bromide, 0.7 g of liquid paraffin, 0.2 g of NiO/NPs and 0.9 g of graphite powder. Then the mixture was mixed well for 45 min until a uniformly wetted paste was obtained. A portion of the paste was filled firmly into a glass tube (geometrical area; 0.09 cm 2) as described above to prepare IL/NiO/NPs/CPE. Whenever required, a new surface was obtained by pushing an excess of the paste out of the tube and polishing it on a weighing paper.

2.2.4. Preparation of real samples for second study

Urine samples were stored in a refrigerator immediately after collection. Ten milliliters of the sample was centrifuged for 45 min at 2000 rpm. The supernatant was filtered using a 0.45 µm filter and then diluted 5 times with the phosphate buffer, pH 7.0. The solution was transferred into the voltammetric cell to be analyzed without any further pretreatment. The standard addition

method was used for NADH determination in real samples. Also, water and serum samples were directly subjected to the voltammetric measurement after filtering using a 0.45 μm filter.

2.3. Chemicals for third study

All chemicals used were of analytical reagent grade purchased from Merck (Darmstadt, Germany) unless otherwise stated. Doubly distilled water was used throughout. Phosphate buffered salines (PBS; sodium dihydrogen phosphate and disodium monohydrogen phosphate plus sodium hydroxide, 0.1 mol L^{-1}) at different pH values were used. High viscosity paraffin (d = 0.88 kg L −1) from Merck was used as the pasting liquid for the preparation of the carbon paste electrodes.

2.3.1. Apparatus for third study

Cyclic voltammetry, chronoamperometry, and square wave voltammetry were performed using a -Autolab with PGSTAT (Eco Chemie, the Netherlands). The system was run on a PC using NOVA software. A conventional three-electrode cell assembly consisting of a platinum wire as an auxiliary electrode and an Ag/AgCl/KCl sat electrode as a reference electrode was used. The working electrode was a CPE, ZnO/CNTs/IL/CPE, ZnO/CNTs/CPE or IL/CPE. X-ray powder diffraction studies were carried out using a STOE diffractometer with Cu-Ka radiation (k = 1.54˚A). Samples for transmission electron microscopy (TEM) analysis were prepared by evaporating a hexane solution of dispersed particles on amorphous carbon coated copper grids.

2.3.2. Synthesis of ZnO/CNTs for third study

The commercial multi-walled carbon nanotubes with tube diameters of about 10–20 nm were used. The preparation of ZnO/CNTs catalysts includes three steps. First, the chemical pre-treatment of carbon nanotubes is required. A definite amount of carbon nanotubes was introduced into 40 cm 3 of nitric acid and sulfuric acid (3:1 in volume) solution, then 10 cm 3 of ethanol was dropped into the solution slowly, and the solution was agitated in a shaker at 70 ◦ C and 150 rpm for 24 h. In the second step, certain amounts of purified CNTs (6 g) were dispersed into distilled water solution of NaOH (0.5 M; 100 ml) by ultrasonication for 15 min. The third step is the supporting of zinc oxide on carbon nanotubes by a direct deposition process. 7.4 g

$ZnO(NO_3)_2 \cdot 2H_2O$ was dissolved in 100 cm^3 distilled water. In the constant magnetic stirring, the solution of $ZnO(NO_3)_2 \cdot 2H_2O$ was added drop wise to the solution of CNTs at 50 ◦ C through a dropping funnel. The rate of addition of the salt solution was kept approximately at 20 ml/h. After completion of the precipitation procedure, the mixture was stirred at room temperature for 12 h, washed and filtered continually in distilled water (pH 7.5), and dried at 120 ◦ C. The solid samples were then calcined at 200 ◦ C for 1 h.

2.3.3. Preparation of the sensor for third study

ZnO/CNTs/CPE was prepared by hand-mixing of 0.80 g of graphite powder and 0.20 g ZnO/CNT plus paraffin at a ratio of 70:30 (w/w) and mixed well for 40 min until a uniformly wetted paste was obtained. The paste was then packed into a glass tube. Electrical contact was made by pushing a copper wire down the glass tube into the back of the mixture. When necessary, a new surface was obtained by pushing an excess of the paste out of the tube and polishing it on a weighing paper. ZnO/CNTs/IL/CPE was prepared by mixing of 0.3 g of 11, 3-dipropylimidazolium bromide, 0.7 g of the liquid paraffin, 0.20 g of ZnO/CNTs, and 0.80 g of graphite powder. Then the mixture was mixed well for 50 min until a uniformly wetted paste was obtained. A portion of the paste was filled firmly into one glass tube as described above to prepare ZnO/CNTs/IL/CPE.

2.3.4. Preparation of real samples for third study

Injection solution was prepared (1.0 mg mL^{-1}, Darou Pakhsh Company, Iran) and then 1.0 mL of the solution plus 10 mL of 0.1 mol L^{-1} PBS (pH 6.0) was used for the analysis. Urine samples were stored at 4 ◦ C immediately after collection (from the Sari Health Centre). Ten milliliters of the sample was centrifuged for 20 min at 1500 rpm. The supernatant was filtered out using a 0.45 μm filter and then diluted 5 times with the PBS (pH 6.0). The solution was transferred into the voltammetric cell for analysis without any further pretreatment. The standard addition method was used for the determination of NE in real-life samples.

2.4. Chemicals for forth study

All chemicals used were of analytical reagent grade purchased from Merck (Darmstadt, Germany) unless otherwise stated. Doubly distilled water was used throughout. Ascorbic acid was used from Merck.

A 1.0 × 10 –3 mol L –1 ascorbic acid solutions was prepared daily by dissolving 0.0176 g ascorbic acid (Merck) in water and the solution was diluted to 100 mL with water in a 100-mL volumetric flask. The solution was kept in a refrigerator at 4 0 C in dark. Phosphate buffer (sodium dihydrogen phosphate and disodium monohydrogen phosphate plus sodium hydroxide, 0.1 mol L^{-1}) solutions (PBS) with different pH values were used. High viscosity paraffin (d = 0.88 kg L^{-1}) from Merck was used as the pasting liquid for the preparation of the carbon paste electrodes. Chemicals and solutions

2.4.1. Apparatus for forth study

Cyclic voltammetry, chronoamperometry, and differential pulse voltammetry were performed in an analytical system, µ-Autolab with (µ3AUT 71226) PGSTAT (Eco Chemie, the Netherlands). The system was run on a PC using NOVA software. A conventional three-electrode cell assembly consisting of a platinum wire as an auxiliary electrode and an Ag/AgCl/KClsat electrode as a reference electrode was used. The working electrode was a CPE, ZnO/NPs/CPE, CP/ILE or a ZnO/NPs/IL/CPE. X-ray powder diffraction studies were carried out using a STOE diffractometer with Cu-Ka radiation (k = 1.54 Å). Samples for transmission electron microscopy (TEM) analysis was prepared by evaporating a hexane solution of dispersed particles on amorphous carbon coated copper grids.

2.4.2. Synthesis of ZnO/NPs for forth study

To prepare of ZnO/NPs, in a typical experiment, a 0.25M aqueous solution of zinc nitrate (Zn $(NO_3)_2.4H_2$ O) and 0.5 M aqueous solution of sodium hydroxide (NaOH) were prepared in distilled water. Then, the beaker containing NaOH solution was heated at the temperature of about 55◦C. The Zn $(NO_3)_2$ solutions were added drop wise (slowly for 1.5 h) to the above-heated solution under high-speed stirring. The beaker was sealed at this condition for 2 h. The precipitated ZnO/NPs were cleaned with deionized water and ethanol then calcined at 200 ◦ C for 2 hours.

2.4.3. Preparation of the sensor for forth study

ZnO/NPs/IL/CPE was prepared by mixing of 0.2 g of 1,3-dipropylimidazolium bromide, 0.8 g of the liquid paraffin, 0.2 g of ZnO/NP, and 0.9 g of graphite powder. Then the mixture was mixed well for 50 min until a uniformly wetted paste was obtained. A portion of the paste was filled firmly into one glass tube as described above to prepare ZnO/NPs/IL/CPE. When necessary, a new surface was obtained by pushing an excess of the paste out of the tube and polishing it on a weighing paper.

2.4.4. Preparation of real samples for forth study

Fresh juices were obtained using a mechanical squeezer. The juices obtained were filtered into a beaker and acidified (pH =2) using citric or sulfuric acid. A 1.0 mL portion of the filtrate was added to the supporting electrolyte solution in voltammetric cell. Vegetable juices were obtained using a grater (polymer material) and a centrifuge respectively, a 1.0 mL portion of vegetable juice was subjected for the voltammetric measurement. In all cases the amounts of vitamin C in the samples were evaluated by the standard addition method.

For the tablets, an accurately weighed portion of finely powdered sample obtained from three tablets, equivalent to about 50 mg of ascorbic acid dissolved in 100 mL water with ultrasonication. Then, 0.1 mL of the solution plus 9.9 mL of the buffer (pH 7.0) was used for the analysis with standard addition method.

2.4.5. Dichlorophenolindophenol (DCPIP) titration method [33] for forth study

The indophenol solution was standardized by titration with 2.0 mL of standard ascorbic acid solution and 5 mL of HPO_3+HOAc solution to the end point (a persistent rosypink color). The consumption of the blank was determined by titration indophenol solution with 7 mL of HPO_3HOAc solution plus a given amount of water equivalent to the volume indophenol solution used in the previousstandardization titration. For sample titration, a 100 mL portion of the juice was mixed with an equal volume of HPO_3+HOAc solution before filtering. A volume of the filtrate equivalent to about 250 mg of ascorbic acid was then titrated with indophenols solution using the same procedure as described above including the titration of the blank.

2.5. Chemicals for fifth study

All chemicals used were of analytical reagent grade purchased from Merck (Darmstadt, Germany) unless otherwise stated. Doubly distilled water was used throughout. Phosphate buffer (sodium dihydrogen phosphate and disodium monohydrogen phosphate plus sodium hydroxide, 0.1 mol L^{-1}) solutions (PBS) with different pH values were used. High viscosity paraffin (d = 0.88 kg L^{-1}) and pure graphite powder (particle size<50 μm) from Merck was used for the preparation of the carbon paste electrodes.

2.5.1. Apparatus for fifth study

Cyclic voltammetry, chronoamperometry, and square wave voltammetry were performed in an analytical system, Autolab with PGSTAT 302N (Eco Chemie, the Netherlands). A conventional three-electrode cell assembly consisting of a platinum wire as an auxiliary electrode and an Ag/AgCl/KCl sat electrode as a reference electrode was used. The working electrode was either a NiO/NPs/CPE.

2.5.2. Synthesis of NiO/NPs for fifth study

To prepare the NiO/NPs, in a typical experiment, a 0.6 M aqueous solution of nickel nitrate $Ni(NO_3)_2$ and a 0.4 M aqueous solution of sodium hydroxide (NaOH) were prepared in distilled water. Then, the beaker containing NaOH solution was heated at the temperature of about 60°C. The Ni $(NO_3)_2$ solutions were added drop wise (slowly for 2.0 h) to the above heated solution under high-speed stirring. The beaker was sealed at this condition for 2 h. The precipitated $Ni(OH)_2$ were cleaned with deionized water and ethanol then calcined at 350 ∘ C for 2.0 hours for synthesis of NiO/NPs.

2.5.3. Preparation of the modified electrode for fifth study

NiO/NPs/CPE was prepared by mixing 0.5 g of liquid paraffin, 0.2 g of NiO/NPs and 0.8 g of graphite powder. Then the mixture was mixed well for 45 min until a uniformly wetted paste was obtained. A portion of the paste was filled firmly into a glass tube (geometrical area; 0.09 cm^2)

as described above to prepare NiO/NPs/CPE. When necessary, a new surface was obtained by pushing an excess of the paste out of the tube and polishing it on a weighing paper.

2.5.4. Preparation of real samples for fifth study

Urine samples were stored in a refrigerator immediately after collection. Ten milliliters of the sample was centrifuged for 45 min at 2000 rpm. The supernatant was filtered using a 0.45 µm filter and then diluted 5 times with the phosphate buffer, pH 7.0. The solution was transferred into the voltammetric cell to be analyzed without any further pretreatment. The standard addition method was used for NB determination in real samples. Also, water and serum samples were directly subjected to the voltammetric measurement after filtered using a 0.45 µm filter.

2.6. Computational Details for sixth study

All DFT calculations were performed with the Gaussian 03 [29] with the default convergence criteria without any constraint on the geometry. The geometry optimizations were carried out using the B3LYP method with 6-311++G**basis set. Calculations in solution were performed with the polarizable continuum model (PCM) as employed in the Gaussian 03 package, with its default settings for building the cavity around the solute, with simple United Atom Topological Model (UAO) for the atomic radii (default values) and average tesserae area 0.200 Å [2] Calculations used the vacuum optimized geometries as inputs, and performed reoptimization in solution at the same level of theory (reoptimization being the only choice for the study of geometry-related characteristics similar to the parameters of the IHB, besides its general importance for the quality of the description of the solvation phenomenon).

The nature of the intramolecular hydrogen bonds existing within Droxidopa in vacuum and in the five solvents was studied by means of the Bader theory of atoms in molecules (AIM). The calculated electron density, ρ, and its second derivative, $\nabla^2\rho$, were used for describing the nature of the intramolecular O-H...(O)N bonds. The AIM2000 program was used to find the bond critical points (BCPs) and analyze [30]. Finally, for comprehensive understanding of the nature of intramolecular interactions, the natural bond orbital (NBO) method was utilized [31]. For the sake of conciseness, the environment will be denoted with the following acronyms on reporting

values: VAC (vacuum), CC (carbon tetrachloride), THF (tetrahydrofuran), DMSO (dimethyl sulfoxide), ET (ethanol), and AQ (water).

Chapter three

Results and Discussion

3.1. Optimization of NiO/CNTs and the ionic liquid ratio for first study

To obtain the best condition in the preparation of modified electrode, the ratio of NiO/CNTs to ionic liquid in IL/NiO/CNTCPE was optimized. The result showed that with increasing the amount of NiO/CNTs 17.5% w/w and the ionic liquid (IL) in ration of 12.5% (to prepare the modified electrode is the presence of fix amount of morphine), the oxidation peak current for morphine increased and then it's leveled off. Therefore, we selected the second conditions (NiO/CNTs17.5%andIL 12.5%) for preparation of modified electrode.

3.1.1. NiO/CNTs characterization for first study

The XRD patterns of the NiO/CNTs showed diffraction peaks absorbed at 2θ values (Fig. 2A). The prominent peaks were used to calculate the grain size via the Scherrer equation, expressed as follows:

$D = K\lambda / \beta \cos\theta$

Where λ is the wavelength (λ = 1.542 Å) (CuK α), β is the full width at half maximum (FWHM) of the line, and θ is the diffraction angle.

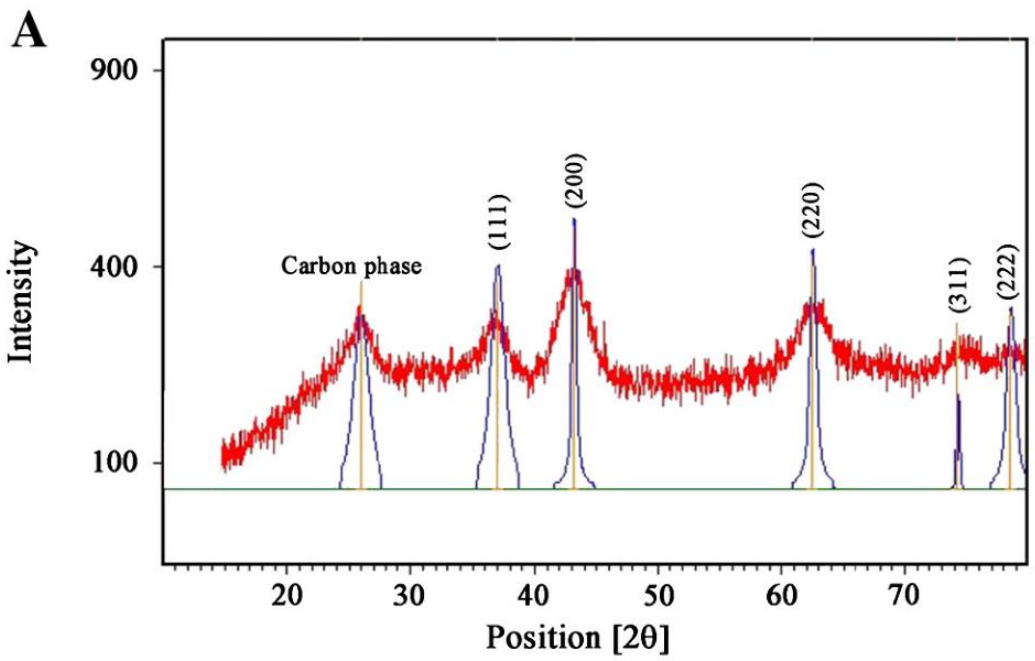

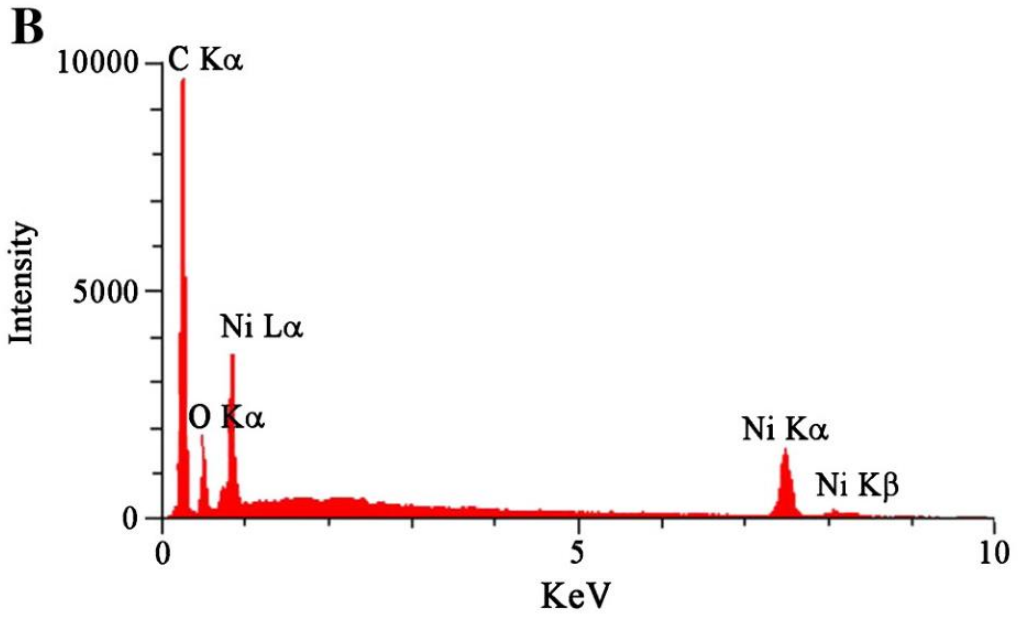

Figure 3-1A) XRD patterns of as-synthesized NiO/CNTs nanocomposite. B) EDAX analysis for NiO/CNTs nanocomposite

The grain size of the NiO nanoparticle was 11.0 nm, and the peaks were observed at the (111), (200), (220), (311) and (222) planes (for FCC structure). These peaks correspond to NiO. On the other hand, it clearly proves the presence of CNTs with a diffraction peak at about 26°. Also, Fig. 2B shows EDAX analysis for NiO/CNTs in the present work. As can be seen, presence of Ni, O and C elements confirms the synthesis of NiO/CNTs nanocomposite carefully. The morphology of the as-grown nanostructures was characterized by TEM. Typical TEM micrograph of the NiO/CNTsis shown in Fig. 3. Results show presence of NiO nanostructure grown on carbon nanotubes. Presence of a covalent bond between NiO nanoparticle and COOH positions at a surface of CNTs can be cause for preparation of NiO/CNTs.

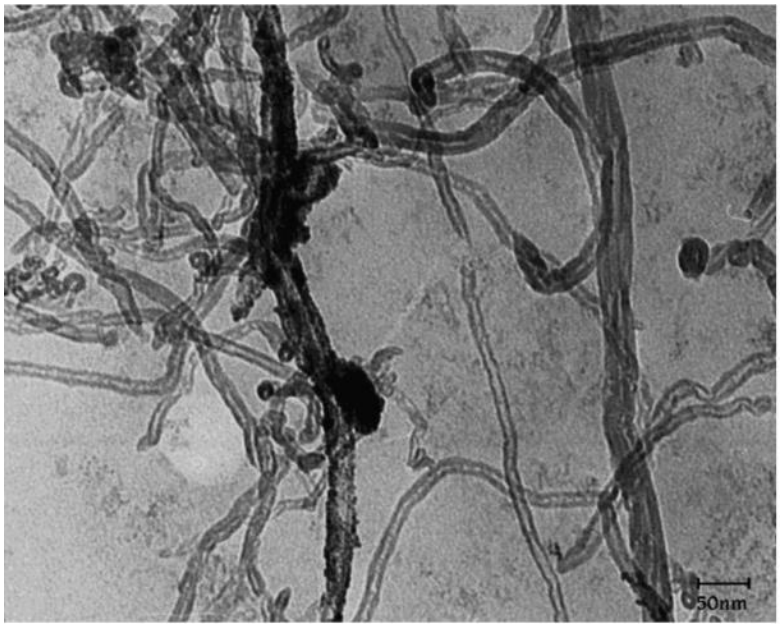

Figure 3-2TEM image of NiO/CNTs

3.1.2. Voltammetric investigation for first study

Morphine can be oxidized at positive potential depending on the electrode type and solution pH (see scheme 1) [4]. In order to ascertain this, the voltammetric response of morphine was obtained in solutions with varying pH from 5.0 to 8.0 (Fig. 4, inset) at the surface of IL/NiO/CNTCPE. The results showed that the peak potential (E) of morphine shifted negatively as the solution pH increased, which indicated that protons were involved in the electrode reaction.

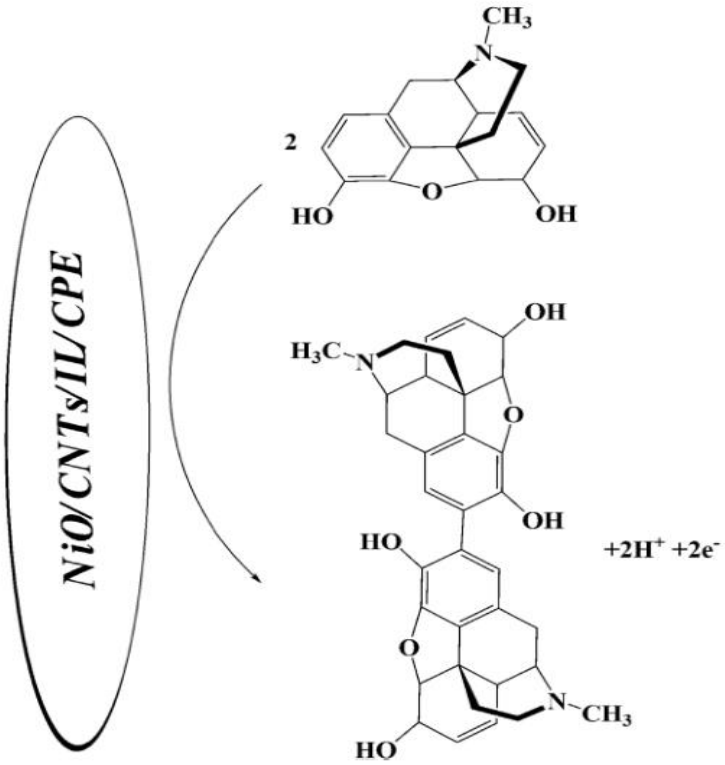

Figure 3-3The mechanism for electrooxidation of morphine at a surface of modified electrode

A good linear relationship between the peak potential (E) and the solution pH was also established (not shown). The linear regression equation was gotten as E(mV)=−63.0pH + k (n=4, r^2 = 0.998). According to the Nernstian slope ($-59.0_x/n$), where x is the hydrogen ion participating the electrode reaction and n is the number of electron transferred ≈ −63.0, the loss of electrons was accompanied by the loss of an equal amount of protons and x = n = 1 [4].

The effect of pH on the anodic peak current was investigated (Fig. 4).

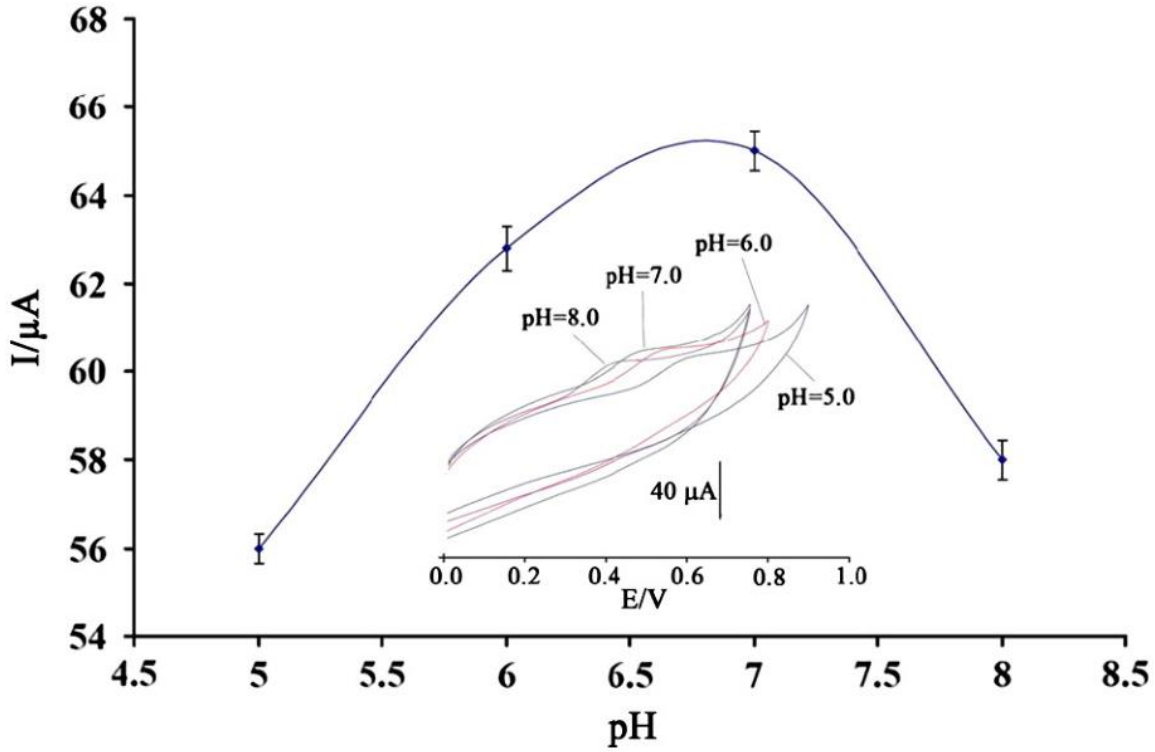

Figure 3-4Current–pH curve for electro- oxidation of 100.0 μM morphine at IL/NiO/CNTCPE with a scan rate of 100 mV s −1 . Inset: influence of pH on cyclic voltammograms of morphine at a surface of the modified electrode (pH 5, 6, 7, and 8, respectively)

The results showed that when the pH exceeded pH 7.0, the peak currents began to decrease and even disappeared with further increasing the buffer pH. Therefore, pH 7.0, PBS, was selected for all the experiments. The direct electrochemistry of morphine at IL/NiO/CNTCPE was investigated by cyclic voltammetry. Fig. 5 showed a typical cyclic voltammograms of different electrodes in a buffer solution (pH 7.0) with scan rate of 100 mV s^{-1}. The results showed that no electrochemical responses were obtained on the bare carbon ionic liquid electrode (IL/CPE) (not shown) indicating that no electroactive substance existed on the electrode surface. For CPE, an electrochemical signal of morphine wa sobtained with the oxidation peak current (I pa) of 30.8 μA and the oxidation potential (E pa) of 0.59 V (Fig. 5, curve a). On the other hand, at NiO/CNT/ CPE, the oxidation peak current (I pa) was obtained as 70.0 μA with oxidation potential (E pa) of 0.53 V(Fig.5, curve b). These small changes in the peak potential indicated that NiO/CNTs showed a little catalytic activity to the morphine oxidation. In addition, at the

surface of unmodified IL/CPE, the oxidation peak appeared at 0.50 V with the peak current of 126.9 μA (Fig. 5, curve c). This indicated that presence of the IL in CPE could enhance the peak currents and decrease the oxidation potential (decreasing the overpotential). The advantages of IL/CPE had been elucidated with higher conductivity, fast electron transfer rate, good antfouling properties and inherent catalytic ability of ILs. So the oxidation peak current increased with decreasing of the over potential at IL/CPE, while at IL/NiO/CNTCPE, the oxidation peak current increased to185.1 μA with theoxidation peakpotential of 0.49 V (Fig. 5, curve d).

The results confirmed that presence of NiO/CNTsonIL/NiO/CNTCPE surface had great improvement on the electrochemical response, which was partly due to excellent characteristics such as good electrical conductivity, high chemical stability and high surface area.

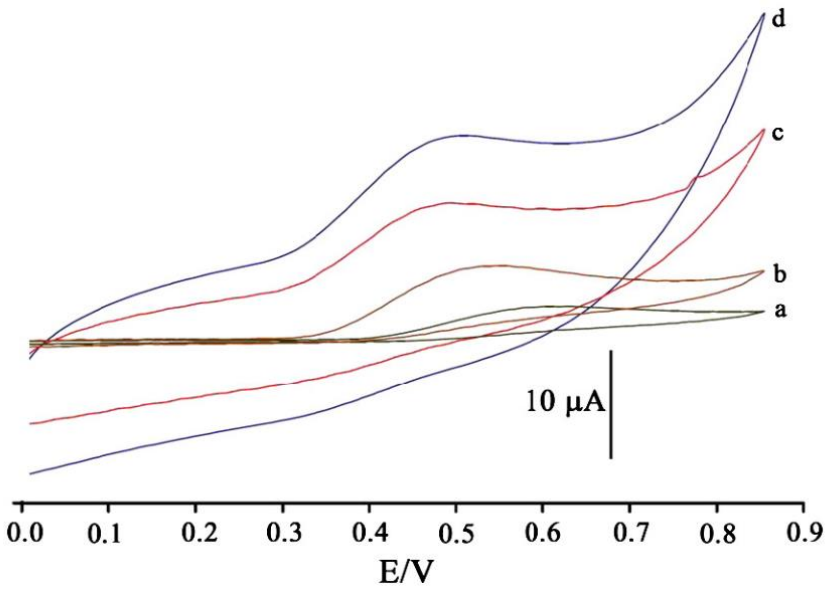

Figure 3-5 Cyclic voltammograms of a) CPE, b) NiO/CNT/CPE, c) IL/CPE and d) IL/NiO/CNTCPE in the presence of 500 μM morphine at pH 7.0, respectively. Conditions: 0.1 mol L^{-1} PBS (pH 7.0); scan rate of 100 mV s^{-1}

The dependence of the current response on the potential scan rate was evaluated by varying the scan rate during the electro-oxidation of morphine. Fig. 6 (inset) depicts the CVs observed for the oxidation of 150 μM morphine at IL/NiO/CNTCPE at different scan rates from 5 to 200 mV s^{-1} .The results confirmed that there is a linear relationship between the peak current (i_p) and the square root of the scan rate ($\nu^{1/2}$) in the scan rates of 5–200 mV s^{-1} (Fig. 6). This indicates that the oxidation of morphine at IL/NiO/CNTCPE is a diffusion-controlled process.

On the other hand, the peak potential shifts in negative direction when the scan rate increases, meaning that the electrochemical reaction is irreversible. At higher scan rate, the dependence of the peak potential (E pa) and ln(ν) showed a linear relationship with a regression equation of:

$E_{pa=}\ 0.0386\ ln\ (\nu) + 0.2973\ (r^2 = 0.9943;\ E_p\ in\ V,\ \nu\ in\ V\ s^{-1})$

According to the following equation [47]:

$E_{pa} = E^{0}/+ m\ [0{:}78 + ln(\ D^{1/2}\ k_s^{-1}) - 0.5\ lnm] + (m/2)\ ln(\nu)$

With

$m = RT/\ [(1–\alpha\ )\ n_\alpha\ F]$

Where E_{pa} is oxidation peak potential, $E^{0/}$ is the formal potential, ν is the sweep rate, and k_s is electron transfer rate constant. A plot of $E_{pa} = f\ (\ln(\nu/V\ s^{-1}))$ yields a straight line with slopes equal to $2(RT/[(1 - \alpha)]\ n_\alpha\ F)$ where R = 8.314 J mol^{-1} $^0K^{-1}$, T = 298 ^{0}K and F = 96485 C mol^{-1}. The value of m = 0.0772 is calculated from Eq. (4). Therefore, the electron transfer coefficient (α) is approximately 0.23 for the irreversible electrode process.

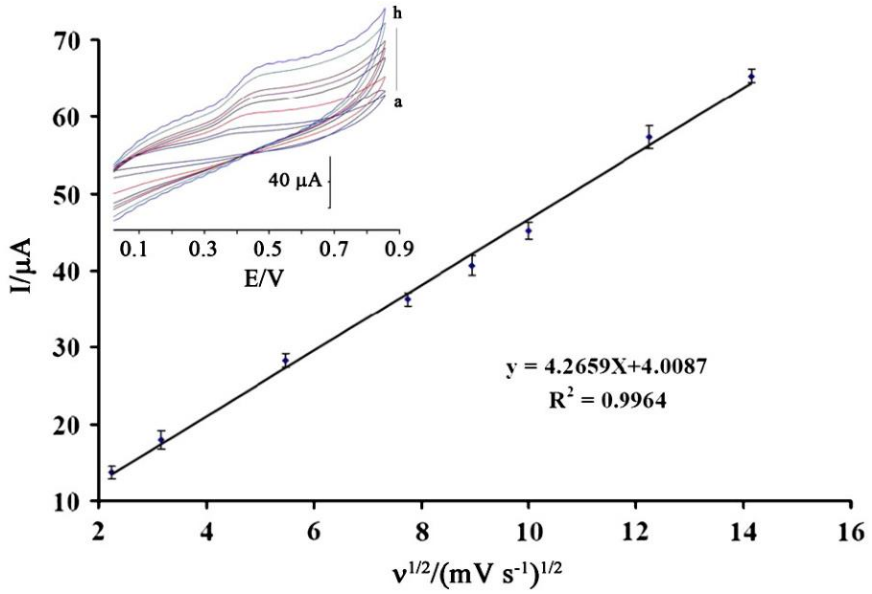

Figure 3-6 Plot of I pa versus ν 1/2 for the oxidation of morphine at IL/NiO/CNTCPE. Inset shows cyclic voltammograms of morphine at IL/NiO/CNTCPE at different scan rates of a) 5, b) 10, c) 30, d) 60, e) 80, f) 100, g) 150 and h) 200 mV s −1 in 0.1 M phosphate buffer, pH 7.0

3.1.3. Chronoamperometric measurements for first study

Chronoamperometric measurements of morphineatIL/NiO/CNTCPE were carriedout bysettingtheworkingelectrodepotentialat0.55 V vs. Ag/AgCl/KCl sat for different concentration of morphine in the buffer solutions, pH 7.0 (Fig. 7). For an electroactive material (morphine in this case) with a diffusion coefficient of D, the current observed for the electrochemical reaction at the mass transport limited condition is described by the Cottrell equation. Experimental plots of I vs. t −1/2 were employed, with the best fits for different concentrations of morphine (Fig.7, inset).The slopes of the resulting straight lines were then plotted vs. morphine concentration. From the resulting slope and Cottrell equation the mean value of the D was found to be 2.8×10^{-5} cm^2/s.

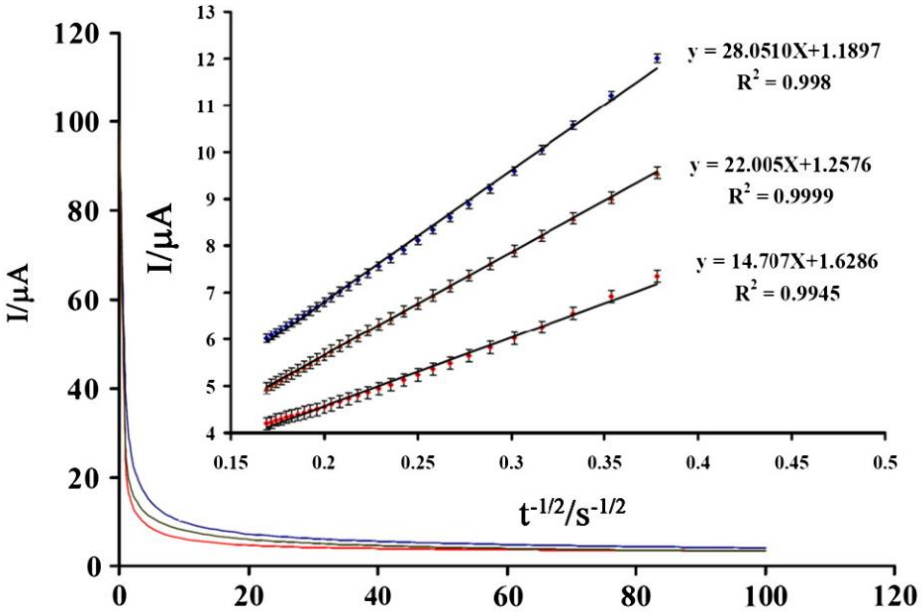

Figure 3-7Chronoamperograms obtained at IL/NiO/CNTCPE in the presence of a) 200, b) 300, and c) 400 μM morphine in the buffer solution (pH7.0). Inset: Cottrell's plot for the data from the chronoamperograms

3.1.4. Impedance characterization for first study

Electrochemical impedance spectroscopy (EIS) was also employed to study the oxidation of morphine at IL/NiO/CNTCPE. Fig. 8 showed the typical results of AC impedance spectra of the unmodified CPE (curve a), NiO/CNT/CPE (curve b), IL/CPE (curve c), and IL/NiO/CNTCPE

(curve d), respectively. Those experiments were done in a solution of 0.1 M PBS containing 400 μM morphine with the frequencies ranging from 100 KHz to 1.0 Hz. On the unmodified CPE, the value of R ct was 14.2 kΩ(curvea) which was due to the presence of non-conductive liquid paraffin in the carbon paste. After NiO/CNTs was added into the carbon paste to get a NiO/CNT/CPE, the value of R ct was decreased to 8.2 kΩ (curve b), which was smaller than that of CPE and was due to the presence of conductive NiO/CNTs in the carbon paste. In continuous, by addition of IL into CPE to get a IL/CPE, the value of R ct was decreased to 3.9 kΩ (curve c), which was much smaller than that of CPE. It was due to the presence of high conductive IL in the carbon paste. On the IL/NiO/CNTCPE (curve d), the value of R ct was equal to 2.1 kΩ, that relative to present NiO/CNTs on the surface of IL/NiO/CNTCPE. All these results indicated that morphine can successfully oxidize on the surface of IL/NiO/CNTCPE.

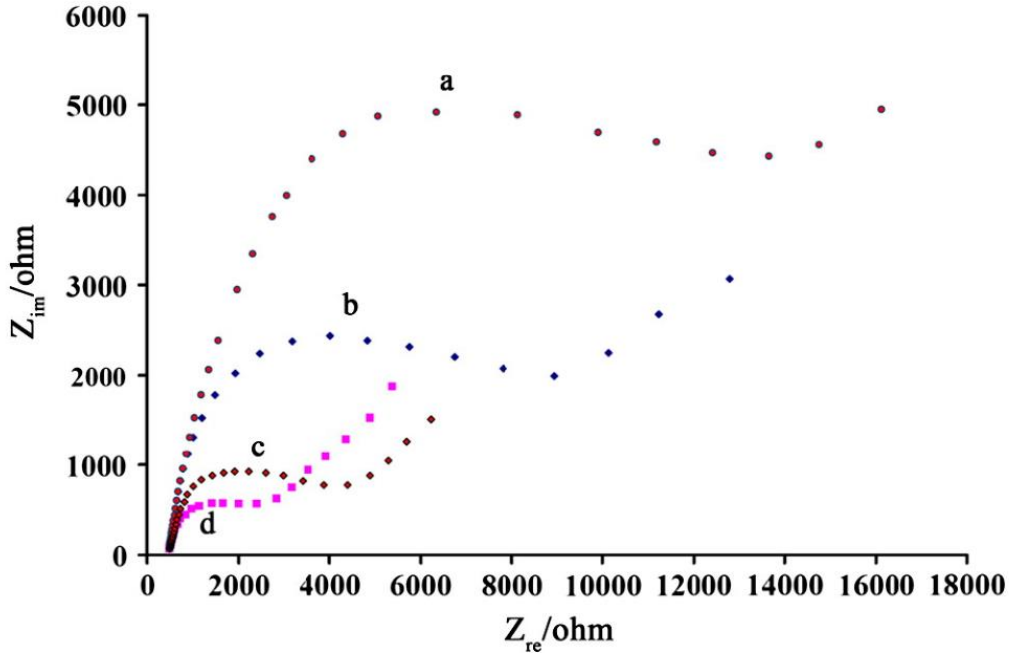

Figure 3-8 Nyquistplots of CPE (a),NiO/CNT/CPE (b), IL/CPE (c), andIL/NiO/CNTCPE (d)in the presence of 400 μM morphine. Conditions: pH, 7.0; E dc , +0.43 V vs. Ag/AgCl; E ac , 5 mV; frequency range, 0.1 to 10,000 Hz

3.1.5. Calibration plot and limit of detection for first study

Since SWV has a much higher current sensitivity and better resolution than cyclic voltammetry, it was used for the determination of morphine in this work. The SW voltammograms clearly show that the plot of peak current vs. morphine concentration is linear for 0.05–520 μM of morphine, the regression equation being $I_p(\mu A) = (0.0521 \pm 0.0055)C_{Morphine} + (2.2410 \pm 0.4351)$ ($r^2 = 0.9922$, n =17), where C is μM concentration of morphine and I_p is the peak current. The detection limit was 0.01 μM morphine according to the definition of $Y_{LOD} = Y_B + 3\sigma$.

3.1.6. Stability and reproducibility of the modified electrode for first study

The stability and reproducibility of any sensor are two important parameters. Our experiments showed that after IL/NiO/CNTCPE was stored for 4 weeks at 4 °C, only a small decrease of peak current sensitivity with a relative standard deviation (RSD) of 1.4% (for 10.0 μM morphine) was observed. This showed good stability of the modified electrode. Furthermore, the reproducibility of the determination was performed with nine successive scans in the solution containing 10.0μM morphine. The RSD values were found to be 2.2% for the analyte, indicating good producibility of the modified electrode. The electrode can be immersed in an aqueous media for 2.0 h with stable response. After that, the background current began to increase, which may be due to the partly leakage of ionic liquid from the electrode and the roughness of the electrode surface was increasing gradually.

3.1.7. Simultaneous determination of morphine and Diclofenac for first study

The main object of this study was to detect morphine and Diclofenac simultaneously using IL/NiO/CNTCPE. This was performed by simultaneously changing the concentrations of morphine and Diclofenac, and recording the SWVs. The voltammetric results showed well defined anodic peaks at potentials of 500 and 680 mV, corresponding to the oxidation of morphine and Diclofenac, respectively. This is indicating that simultaneous determination of these compounds is feasible at IL/NiO/CNTCPE as shown in Fig.9 inset. The sensitivity of the modified electrode towards the oxidation of morphine in the presence of diclofenac was found to be 0.0501 μA/μM (Fig. 9). This is very close to the value obtained in the absence of diclofenac (0.0521 μA/μM) indicating that the oxidation processes of these compounds at the

IL/NiO/CNTCPE are independent and therefore, simultaneous determination of their mixtures is possible without significant interferences.

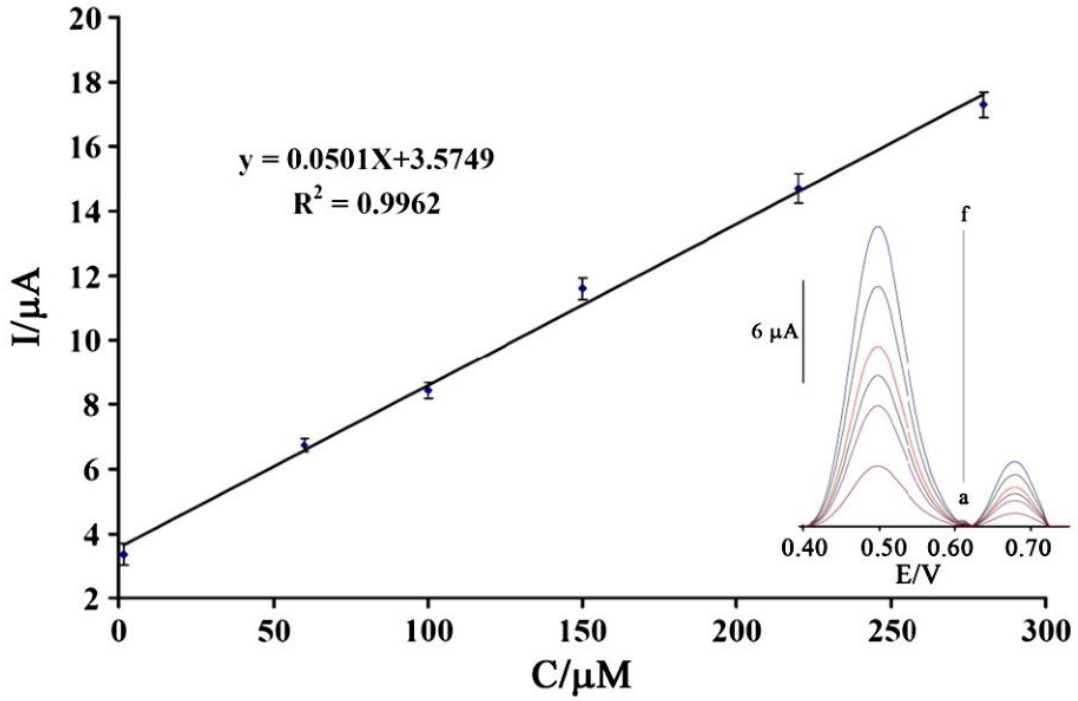

Figure 3-9The plots of the electrocatalytic peak current as a function of morphine concentration. Inset; SWVs of IL/NiO/CNTCPE in 0.1 M PBS (pH 7.0) containing different concentrations of morphine – diclofenac in µM. a–f: 1.63 + 2.0; 60.0 + 10.0; 100.0 + 15.0; 150

3.1.8. Interference studies for first study

In order to evaluate the selectivity of the proposed method in the determination of morphine the influence of various foreign species on the determination of 15.0µM morphine was investigated. Tolerance limit was taken as the maximum concentration of foreign substances that caused an approximate relative error of ±5%. The results are shown in Table 1. These results demonstrate that the modified electrode has a good selectivity for morphine analysis.

Table 3-1 Interference study for the determination of 15.0 μM morphine under the optimized conditions

Species	Tolerance limits (W/W)
Na^{+}, Mg^{2+}, ClO_4^{-}, Li^{+}, Br^{-}, NO_3^{-}, SCN^{-},SO_4^{2-}, Br^{-}, Glucose, Fructose, Lactose, Sucrose, Ca^{+2}	950
Hystidine, Alanine, Phenyl alanine, Methionine, Glycine, Methanol, Tryptophan, L-Theronine, L-isoleucin, L_Orinthime,	700
Starch	Saturation
Ascorbic acid*, Urea; Thiourea, Cysteine	400

* After addition of 1 mmol L^{-1} ascorbic oxidize.

3.1.9. Real sample analysis for first study

In order to evaluate the analytical applicability of the proposed method, also it was applied to the determination of morphine in injection solution and urine samples. Based on the repeated differential pulse voltammetric responses (n = 3) of the diluted analyte and the samples that were spiked with specified concentration of morphine, measurements were made for determination of morphine concentrations in the pharmaceutical, and urine preparations. The results are listed in Table 2. In addition, a published electrochemical method [29] was used for the analysis to confirm the accuracy of the proposed method with a standard procedure (Table2). The results presented in Table2 indicate that the modified electrode retained its efficiency for the determination of morphine in real samples with satisfactory results.

Table 3-2Determination of morphine in drug and urine samples

Sample	Added (μM)	Expected (μM)	Founded (μM)	Published method (μM) [26]	F_{ex}	F_{tab}	t_{ex}	$t_{tab(95\%)}$
Injection solution	-	5.00	4.82 ± 0.44	5.5 ± 0.65	6.5	19	1.8	3.8
	10.0	15.0	15.33 ± 0.55	15.78 ± 0.85	-	-	-	-
	15.0	30.0	29.51 ± 0.63	29.73 ± 0.75	-	-	-	-
Urine	-	-	<Limit of detection	-	-	-	-	-
	20.0	5.0	20.44 ± 0.76	20.57 ± 1.1	9.5	19	2.9	3.8
	20.0	40.0	39.48 ± 0.75	40.22 ± 0.65	-	-	-	-
Urine*	-	-	9.44 ± 0.56	10.11 ± 0.75	10.1	19	3.2	3.8
	10.56	20.0	20.21 ± 0.65	20.57 ± 0.85	-	-	-	-

± Shows the standard deviation.

* Sampling was made after 3.0 h from a man who is sick and used morphine.

3.2. Optimization of NiO/NPs and the ionic liquid ratio in second study

To obtain the best condition in the preparation of modified electrode, the ratio of NiO/NPs to ionic liquid in IL/NiO/NPs/CPE was optimized. For this goal, the oxidations signal of 700 μmol L^{-1} NADH was used for the optimization. We record oxidation signal in the fix amount of ILs and different amount of NiO/NPs and vice versa. The result showed that with increasing the amount of NiO/NPs 10.0% w/w and the ionic liquid (IL) in ration of 10.0% (to prepare the modified electrode is the presence of fix amount of NADH), the oxidation peak current for NADH increased and then it is leveled off (Fig. 1). Therefore, we selected these conditions (NiO/NPs 10.0% and IL 10.0%) for preparation of modified electrode.

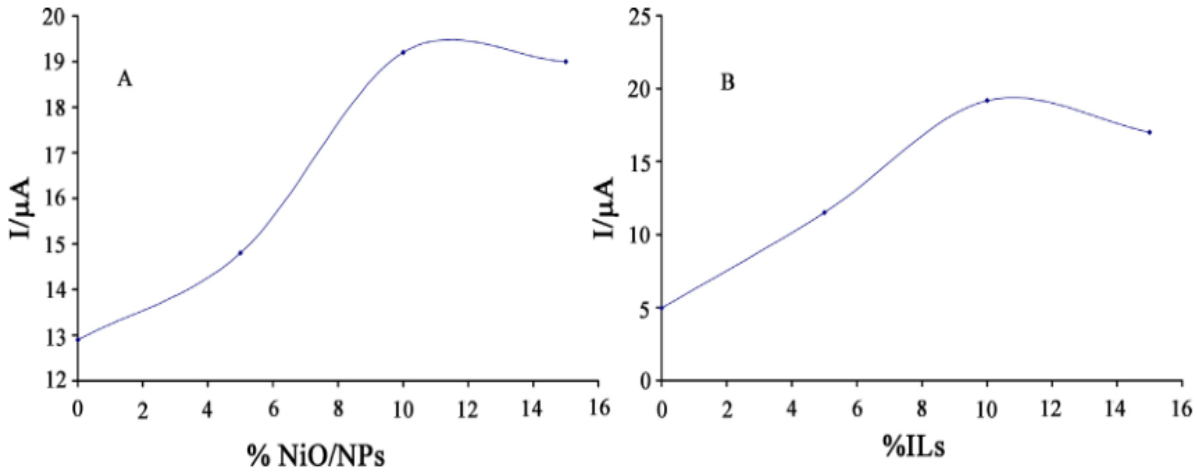

Figure 3-10(A) Current vs. % NiO/NPs curve at a surface of carbon paste electrode in the presence of fix amount (10% ILs) for electrooxidation of 700 µmol L −1 at pH 7.0. (B) Current vs. % ILs at a curve surface of carbon paste electrode in the presence of fix amount (10% NiO/NPs) for electrooxidation of 700 µmol L −1 at pH 7.0

3.2.1. NiO/NPs characterization in second study

Fig. 2A shows the X-ray diffraction (XRD) data for synthesis NiO/NPs. The intensity data were collected over a 2θ range of 10–80 ◦. The average grain size of the samples was estimated with the help of Scherrer equation using the diffraction intensity of (2 0 0) peak. XRD studies confirmed that the synthesized materials were NiO, and all the diffraction peaks agreed with the reported Joint Committee on Powder Diffraction Standards (JCPDS) data, and no characteristic peaks were observed other than NiO [39]. The mean grain size (D = 23 nm) of the particles was determined from the XRD line broadening measurement using Scherrer equation:

$D= K\lambda/ \beta \cos\theta$

Where λ is the wavelength (Cu Kα), β is the full width at the half- maximum (FWHM) of the NiO (2 0 0) line and θ is the diffraction angle. A definite line broadening of the diffraction peaks is an indication that the synthesized materials are in the nanometre range.

Also, Fig. 2B shows EDAX analysis for NiO/NPs in the present work. As can be seen, presence of Ni and O elements confirm the synthesis of NiO/NPs carefully. The morphology of the as-grown nanostructures was characterized by TEM. Typical TEM micrograph of the NiO/NPs is shown in Fig. 2C. Presence of dark point in these figure in nanoscale size confirm synthesis of this nanoparticle carefully. It is clear that in this case, a NiO nanoparticle was successfully prepared.

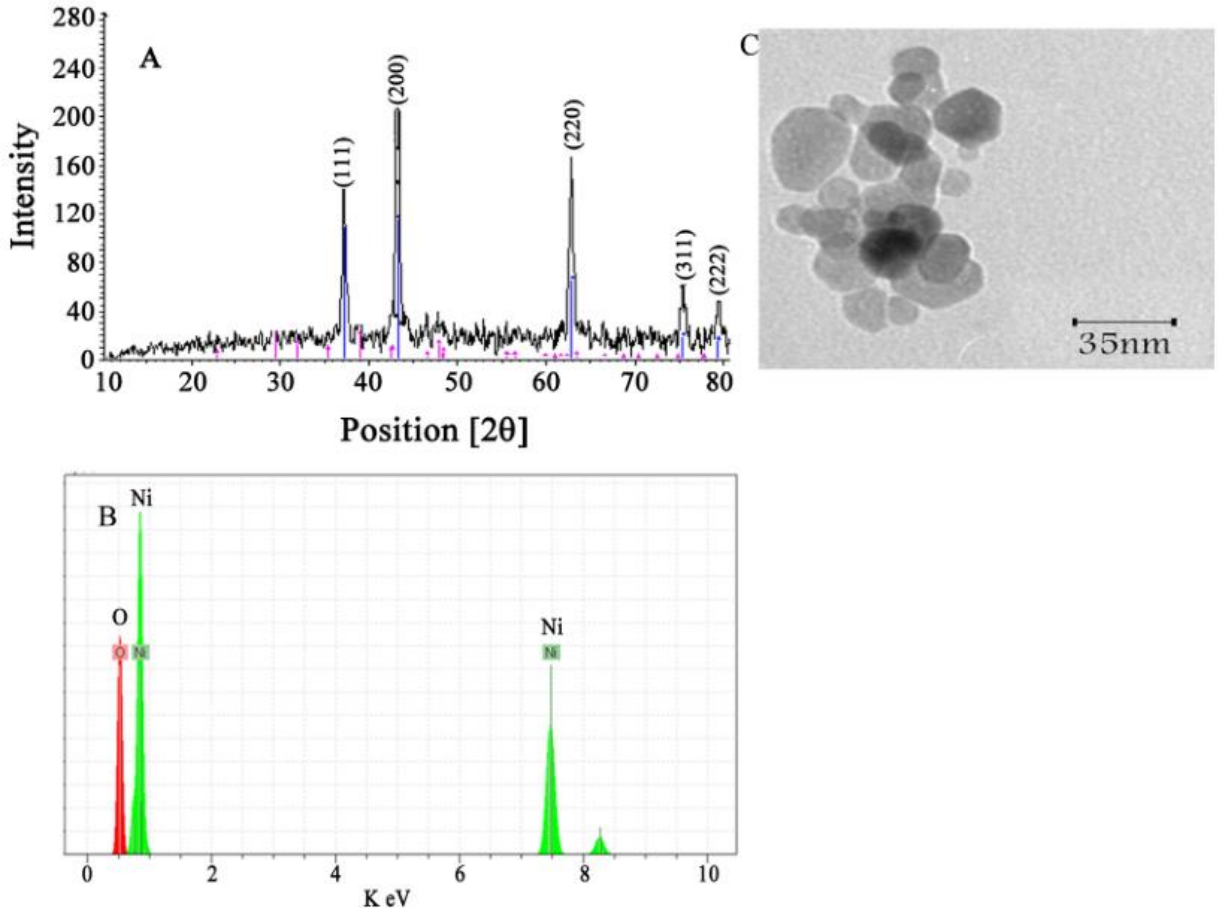

Figure 3-11((A) XRD . (C) TEM image of NiO nanparticles patterns of as-synthesized NiO nanparticles. (B) EDAX analysis for NiO nanoparticle

3.2.2. Electrochemical investigation in second study

The active surface areas of the working electrodes are estimated according to the slope of the I_P versus $v^{1/2}$ plot for a known concentration of $K_4Fe(CN)_6$, based on the Randles–Sevcik equation:

$$I_p = 2.69 \times 10^5 n^{3/2} AD^{1/2} \nu^{1/2} CO$$

Where I_{pa} refers to the anodic peak current, n the electron transfer number, A the surface area of the electrode, D_R the diffusion coefficient, C^0 the concentration of $K_4Fe(CN)_6$ and ν is the scan rate. For 1.0 mmol L^{-1} $K_4Fe(CN)_6$ in 0.10 mol L^{-1} KCl electrolyte with n=1 and $D_R = 7.6\times10^{-6}$ cm s^{-1} and from the slope of the $I_{pa} - \nu^{1/2}$ relation, the microscopic areas were calculated. They were 0.24, 0.19, 0.16 and 0.09 cm 2 for IL/NiO/NPs/CPE, IL/CPE, NiO/NPs/CPE and CPE, respectively. The results show that presence of NiO/NPs and IL together causes the increase of the active surface. According to scientific investigations, nanomaterials have high surface area and can increase current density and sensitivity in modified electrodes [40].

On the other hand, to summarize contrary to the electrodes modified by unsupported organic phase the electrochemical generation of charge in IL deposit may generate the transfer of its component across liquid/liquid interface. These points can increase active surface area for modified electrode [41].

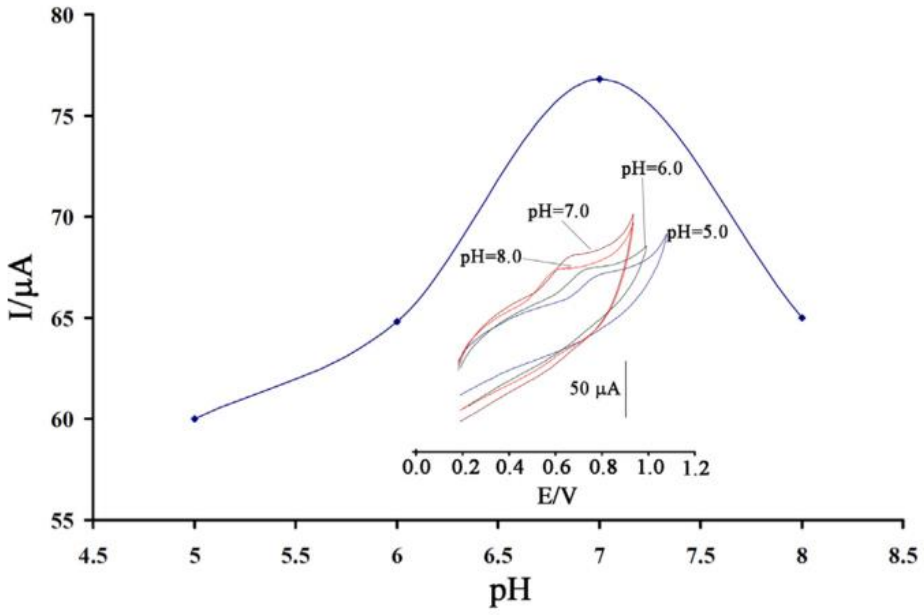

Figure 3-12Current–pH curve for electro-oxidation of 450 μmol L −1 NADH at IL/NiO/NPs/CPE with a scan rate of 100 mV s −1 . Inset: influence of pH on cyclic voltammograms of NADH at a surface of the modified electrode, (pH 5–8, respectively).

The effect of pH was investigated using cyclic voltammetry (Fig. 3 inset) for electro oxidation of NADH at a surface of IL/NiO/NPs/CPE. It was found that the oxidation peak current increased gradually from pH 5.0 to 7.0, and then the current decreased when the pH value increased from 7.0 to 8.0 (Fig. 3).

According to the above point that pH 7.0 was chosen as the optimal experimental condition. The relationship between the oxidation peak potential and pH was also constructed. A linear shift of E pa toward negative potential with an increasing pH can be obtained and obeyed the regression equation of E pa (V) = −0.063 pH + 1.097 (R 2 = 0.991), which indicates that protons are directly involved in the oxidation of NADH. A slope of 63 mV /pH suggests that the number of electron transfer is equal to the proton number involved in the electrode reaction of NADH. Fig.4 (inset) shows the current density derived from the cyclic voltammograms responses of 700 µmol L^{-1} NADH (pH 7.0) at the surface of different electrodes and with a scan rate of 100 mV s^{-1}. The direct electrochemistry of NADH on the modified electrode was investigated by cyclic voltammetry. IL/NiO/NPs/CPE exhibited significant oxidation peak current of 190.1 µA around 635 mV (Fig. 4, curve a). In contrast, low redox activity peak was observed at NiO/NPs/CPE (Fig. 4, curve c) and at unmodified CPE (Fig. 4, curve d) over the same potential range. The NADH oxidation peak potential at NiO/NPs/CPE and at CPE observed was around 670 and 705 mV in contrast to the Ag/AgCl/KCl sat reference electrode and has an oxidation peak current of 90.5 and 49.0 µA, respectively. In addition, at the surface of IL/CPE, the oxidation peak appeared at 653 mV and the peak current achieved was 125.0 µA (Fig. 4, curve b). This indicated that the presence of ILs in CPE could enhance the peak currents and decrease the oxidation potential (decreasing the over potential). A substantial negative shift of the current starting from the oxidation potential for NADH and dramatic increase of current of NADH indicated the catalytic ability of IL/NiO/NPs/CPE to NADH oxidation. The results indicated that the presence of NiO/NPs on IL/NiO/NPs/CPE surface had great improvement on the electrochemical response, which was partly due to the excellent characteristics of NiO/NPs such as good electrical conductivity, high chemical stability and high surface area. The suitable electronic properties of NiO/NPs together with the ionic liquid gave the ability to promote charge transfer reactions, good anti-fouling properties, especially when mixed with a higher conductive compound such as ILs when used as an electrode.

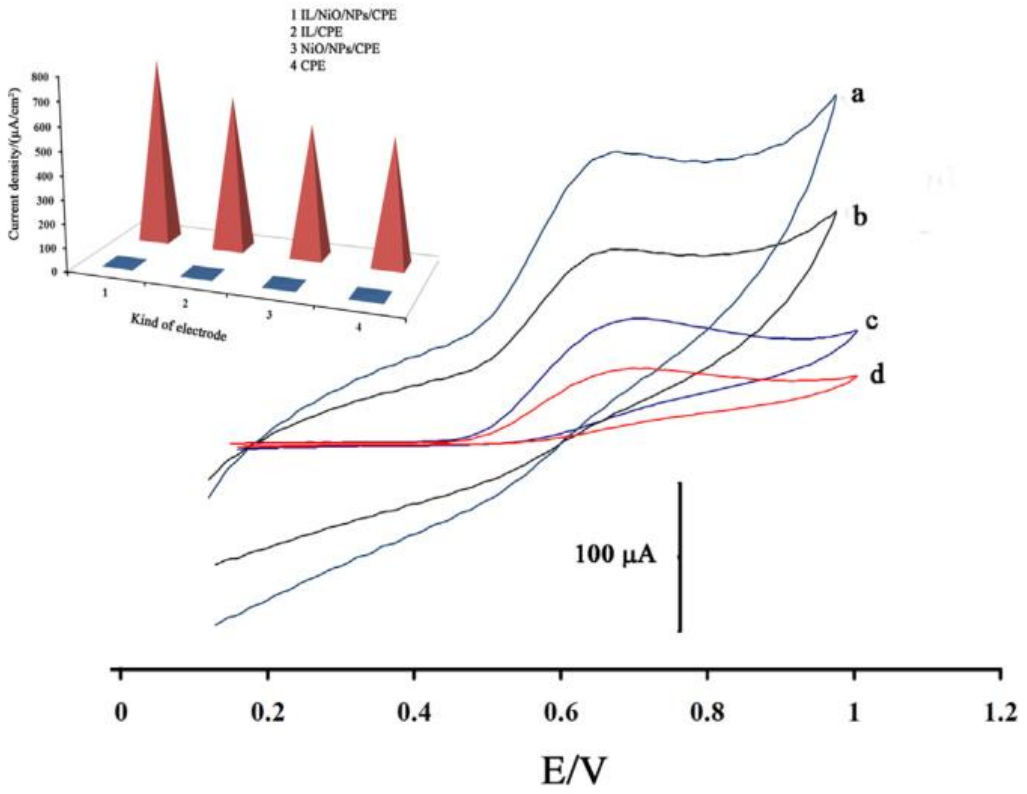

Figure 3-13 Cyclic voltammograms of (a) IL/NiO/NPs/CPE, (b) IL/CPE, (c) NiO/NPs/CPE and (d) CPE in the presence of 700 μmol L −1 NADH at pH 7.0, respectively. Inset: the current density derived from cyclic voltammograms responses of 700 μmol L^{-1} NADH at pH 7.0 at the surface of different electrodes.

Further, the effect of potential scan rate on the peak current of NADH was studied at an optimum condition. It can be seen from Fig. 5 inset that NADH gives an irreversible cyclic voltammograms at a surface of modified electrode. From Fig. 5 inset, it can also be seen that the oxidation peak shifts to a more positive value for NADH with increasing scan rates along with a concurrent increase in current. The cyclic voltammetric results indicate that the anodic peak currents (I_p) of NADH varied linearly with the square root of scan rate ($v^{1/2}$) ranging from 20 mV s^{-1} to 300 mV s^{-1} (Fig. 5) which implies that the oxidation of NADH is diffusion controlled on IL/NiO/NPs/CPE, regarding following equations:

$I_p = 6.551v^{1/2} + 3.213$($r^2 = 0.994$, I in μA, v in mV s^{-1})

The dependence of the peak potential (E_{pa}) and ln(v) showed a linear relationship with a regression equation of:

$E_p = 0.044 \ln(v) + 0.499$($r^2 = 0.993$, E_p in V, v in V s^{-1})

According to the following equation [42]:

$E_{pa} = E^{0/} + m [0.78 + \ln(D^{1/2} k_s^{-1}) - 0.5 \ln m] + m/2 \ln(v)$

With

$m = RT (1 - \alpha)/ n_\alpha F$

The value of m = 0.088 is calculated from Eq. (4). Using the obtained value of m, the electron transfer coefficient (α) is approximately 0.67 for the irreversible electrode process.

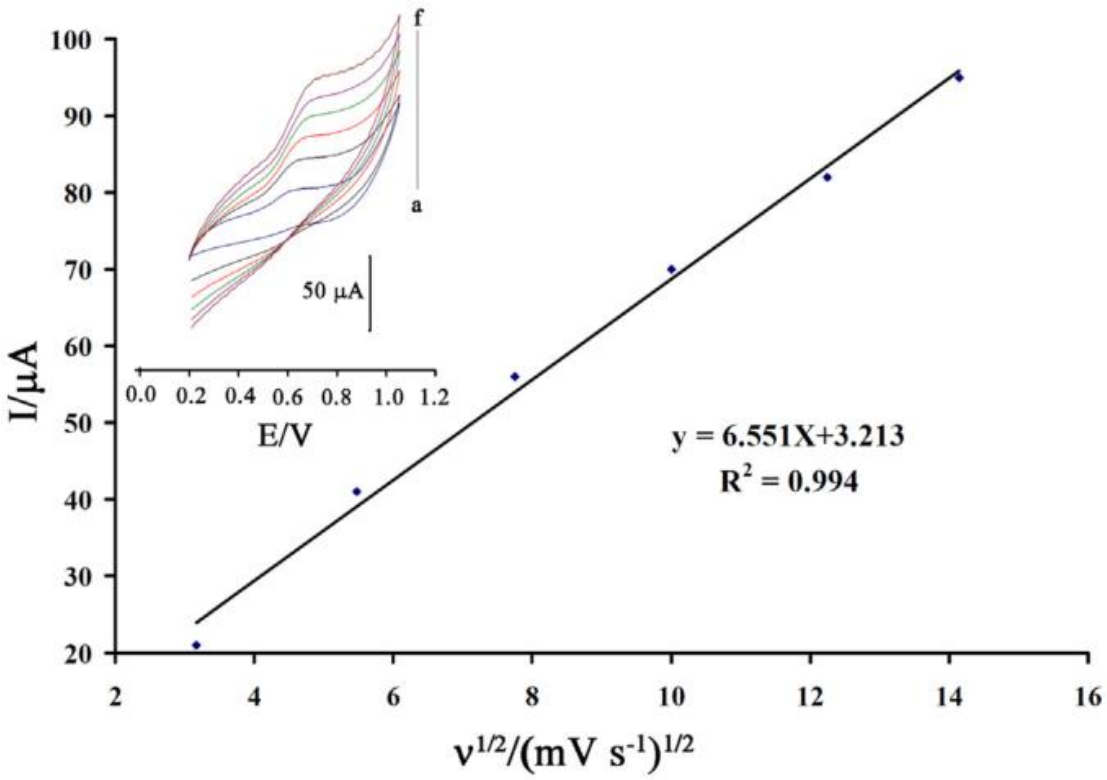

Figure 3-14Plot of I pa versus v 1/2 for the oxidation of NADH at IL/NiO/NPs/CPE. Inset shows cyclic voltammograms of NADH at IL/NiO/NPs/CPE at different scan rates (from inner to outer) of 5, 10, 30, 60, 100, 150 and 200 mV s −1 in 0.1 M phosphate buffer, pH 7.0.

Chronoamperometry results obtained for the various concentrations of NADH solution using IL/NiO/NPs/CPE are shown in Fig. 6A. The plot of current (I) versus $t^{-1/2}$ at various concentrations NADH on IL/NiO/NPs/CPE (Fig. 6B) gives straight lines with different slopes. From the slopes we calculated a diffusion coefficient of 7.23×10^{-5} cm^2 s^{-1} for NADH using the Cottrell equation. Electrochemical impedance spectroscopy (EIS) is one of the most powerful electrochemical techniques frequently used in studying the electron transfer kinetics in modification of electrode surfaces [43–46]. So it was also employed to study the oxidation of NADH at IL/NiO/NPs/CPE in optimum condition. Impedance measurements were performed in the frequency range from 0.1 to 100,000 Hz.

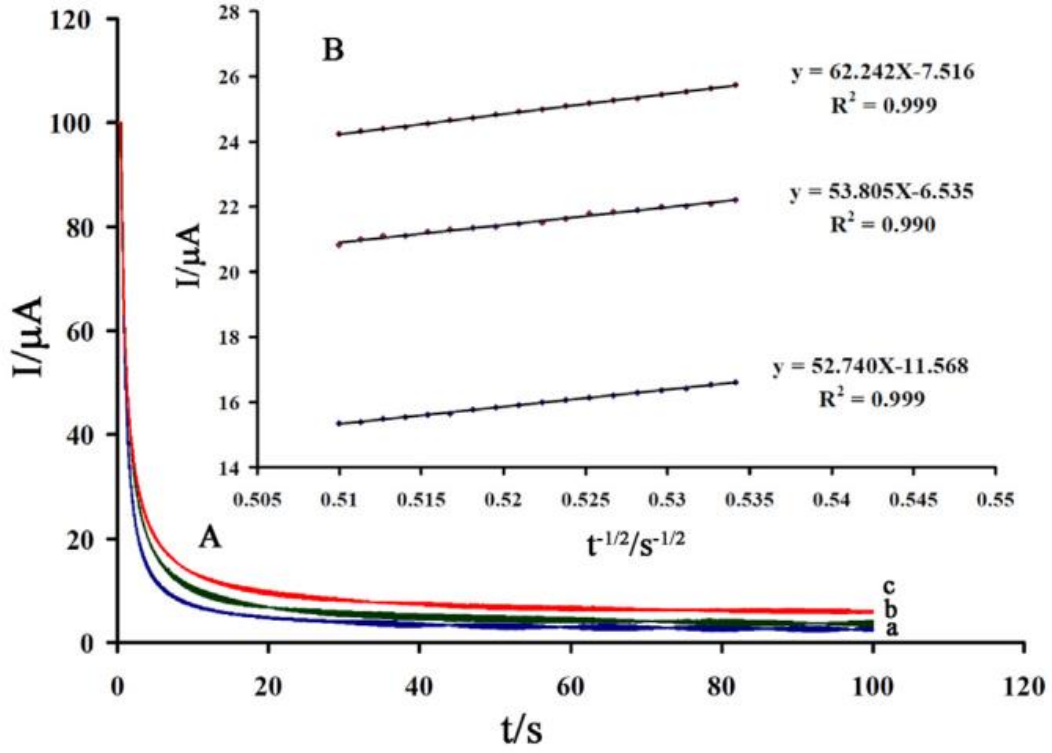

Figure 3-15(A) Chronoamperograms obtained at IL/NiO/NPs/CPE in the presence of (a) 400; (b) 500; and (c) 600 µmol L −1 NADH in the buffer solution (pH 7.0). (B) Cottrell's plot for the data from the chronoamperograms

Fig. 7 shows Nyquist diagrams of the imaginary impedance (Z_{im}) vs. the real impedance (Z_{re}) of the EIS obtained at CPE (curve a); NiO/NPs/CPE (curve b); IL/CPE (curve c) and IL/NiO/NPs/CPE (curve d) in the presence of 500 µmol L^{-1} NADH at pH 7.0, respectively. It

can be seen that the all of the electrodes exhibits an almost straight line that is characteristic of a diffusional limiting step of the electrochemical process. Nyquist diagrams follow the theoretical shapes and include a squeezed semicircle portion, observed at higher frequencies, which corresponds to the electron transfer limited process. The respective semicircle diameters at the high frequency, corresponding to the electron transfer resistance at the electrode surface. The curve corresponding to CPE is a big semicircle plus a straight line (Fig. 7a). For NiO/NPs/CPE, IL/CPE, and IL/NiO/NPs/CPE, R_{ct} decreases dramatically (Fig. 7b–d), indicating that NiO/NPs and IL can act as an effective electron conduction pathway between the electrode and electrolyte. Therefore, IL/NiO/NPs/CPE composite electrode has good electronic conductivity for electro-oxidation of NADH [47–58].

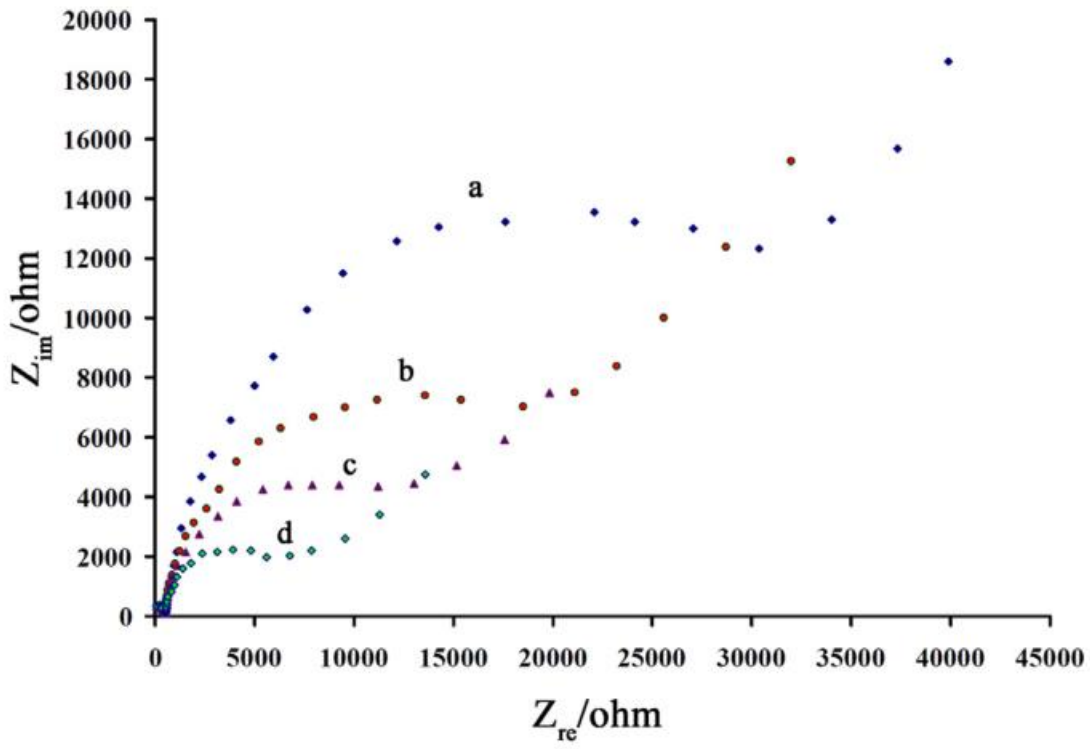

Figure 3-16Nyquist plots of CPE (a), NiO/NPs/CPE (b), IL/CPE (c), and IL/NiO/NPs/CPE (d) in the presence of 500 μmol L −1 NADH. Conditions: pH, 7.0; Edc, +0.56 V vs. Ag/AgCl; Eac , 5 mV; frequency range, 0.1–100,000 Hz.

3.2.3. Analytical features in second study

Square wave voltammetry (SWV) (with amplitude potential of 50 mV and frequency of 10 Hz) was used to determine NADH concentrations (Fig. 8A) at a surface of modified electrode. The data repeat for three time and error bar shows in Fig. 8B. The SW voltammograms clearly show that the plot of peak current vs. NADH concentration is linear for 0.03–900 µmol L^{-1} of NADH, the regression equation being I_p (µA) = (0.0911 ± 0.0034) C NADH + (4.2042 ± 0.573) (r^2 = 0.9941, n = 10), where C is µmol L^{-1} concentration of NADH and I p is the peak current (Fig. 8B). The detection limit was determined at 9.0 nmol L^{-1} NADH according to the definition of $Y_{LOD} = Y_B + 3\sigma$.

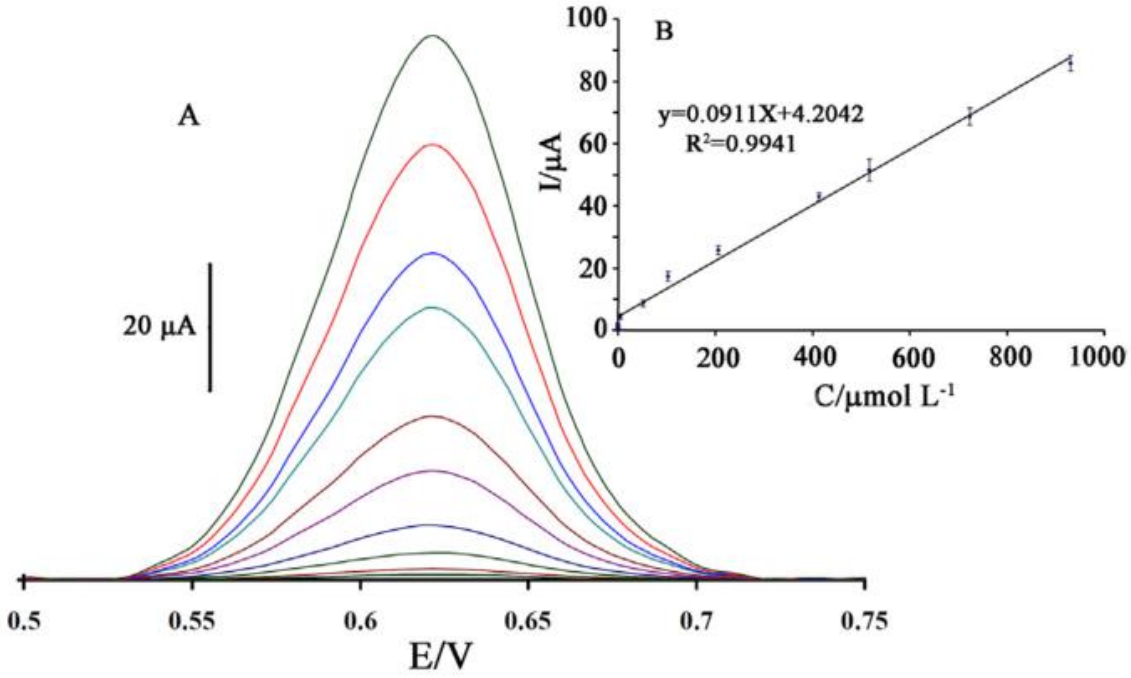

Figure 3-17(A) SWVs of IL/NiO/NPs/CPE in 0.1 mol L^{-1} phosphate buffer solution (pH 7.0) containing different concentrations of NADH. Inner to outer voltammograms correspond to 0.03, 0.3, 5.0, 50.0, 100.0, 200.0, 400.0, 500.0, 700.0 and 900.0 µmol L^{-1} of NADH. (B) Plot of the peak current as a function of NADH concentration in the range. Error bar obtained for three separate experimental.

The detection limit, linear dynamic range, and sensitivity for NADH obtained with the sensor were comparable to or better than those obtained with several other modified electrodes (Table 1). The presence of ionic liquid as a conductive binder and NiO/NPs with high surface area improves electrode conductivity for NADH analysis.

Table 3-3Comparison of the efficiency of some modified electrodes used in the electrocatalysis of NADH.

Electrode	Modifier	Method	pH	LOD ($\mu mol\ L^{-1}$)	LDR ($\mu mol\ L^{-1}$)	Sensitivity ($\mu A/\mu mol\ L^{-1}$)	Ref.
Glassy carbon	IL and MWCNTs	Amperometry	7.0	1100	250–2000	0.0037	[4]
Screen-printed carbon	Graphene oxide	Amperometry	7.0	0.1	0.8–500	0.0025	[5]
Carbon paste	Hematoxylin	Differential pulse voltammetry	7.0	0.08	0.4–600	0.0028	[1]
Glassy carbon	(bis-Phenothiazin-3-yl methane; BPhM)	Amperometry	7.0	0.2	0.2–100.0	0.0018	[6]
Screen-printed carbon	Azure B	Cyclic voltammetry	6.9	0.2	0.5–100	0.0023	[7]
Carbon paste	IL and NiO/NPs	SWV	7.0	0.009	0.03–900	0.0911	This work

3.2.4. Interference studies in second study

In order to evaluate the selectivity of the proposed method in the determination of NADH, the influence of various foreign species on the determination of 10.0 µmol L^{-1} NADH was investigated. Tolerance limit was taken as the maximum concentration of foreign substances that caused an approximate relative error of ± 5%. The results are shown in Table 2. These results demonstrate that the modified electrode has a good selectivity for NADH analysis in the presence of other foreign species.

Table 3-4Interference study for the determination of 10.0 µmol L −1 NADH under the optimized conditions

Selected compounds for interference study	Tolerante limits ($W_{Substance}/W_{NADH}$)
Glucose, Fructose, Lactose, Sucrose, Methanol, Ethanol	900
Tryptophan, Valine, Methionine, Glycine, Lucine, Histidine, Glutamic acid, Alanine, Glycine, Phenylalanine	800
Al^{3+}, Li^{+}, Cl^{-}, CO_3^{2-}, ClO_4^{-}, SO_4^{2-}, SCN^{-}, Na^{+}, Mg^{2+}, K^{+}, Ca^{+2}, Ascorbic acid[a], Thiourea, urea, uric acid	500
Starch	Saturation

[a] After addition of 1 mM ascorbic oxidaze.

3.2.5. Stability and reproducibility of the biosensor in second study

Long-term stability is one of the most important properties for biosensor application. The stability of IL/NiO/NPs/CPE was investigated by SWV. The response currents can retain almost constant upon continuous 15 cyclic sweeps over the applied potential ranging from +0.50 to

+0.75 V. After stored in refrigerator at 4 °C for 60 days, the potentials of oxidation peak in SWVs remained at the same positions and the peak currents decreased by only about 4.1% of its initial current response. Furthermore, the reproducibility of the determination was performed with seven successive scans in the solution containing 10.0 μmol L^{-1}. The RSD values were found to be 2.0% for the analyte, indicating good reproducibility of the modified electrode.

3.2.6. Real sample analysis in second study

In order to evaluate the analytical applicability of the proposed sensor, also it was applied to the determination of NADH in biological samples such as water, serum and urine. Standard addition method was used for measuring NADH concentration in the samples. The results are given in Table 3, confirm that the modified electrode retained its efficiency for the determination of NADH in real samples.

Table 3-5Determination of NADH in real samples (n = 3)

Sample	Added (μmol L^{-1})	Expected (μmol L^{-1})	Founded (μmol L^{-1})	Recovery (%)
Urine	–	–	<Limit of detection	–
	5.0	5.0	5.32 ± 0.51	106.0
	10.0	15.0	15.55 ± 0.75	103.6
Water	–	–	<Limit of detection	–
	20.0	20.0	19.84 ± 0.65	99.2
	20.0	40.0	40.05 ± 0.47	101.7
Serum	–	–	<Limit of detection	–
	30.0	30.0	29.75 ± 0.55	99.2

± shows the standard deviation.

3.3. Nanostructures characterization for third study

The morphology of the as-grown nanostructures was characterized by TEM techniques. Typical TEM micrograph of the ZnO/CNTs is shown in Fig. 1A. Results show the core of particles supported on carbon nanotubes. Since the corresponding XRD pattern presented in Fig. 1A detected only CNTs and ZnO, it was believed that the core and nanotubes of particles should be ZnO and carbon nanotubes, respectively. Fig. 1B shows EDAX analysis for ZnO/CNTs in the present work. As can be seen, presence of Zn, O and C elements confirms the synthesis of ZnO/CNTs nanocomposite carefully. Also, Fig. 1C and 1D show SEM images of ZnO nanoparticle before preparation of nanocomposite and ZnO/CNTs.

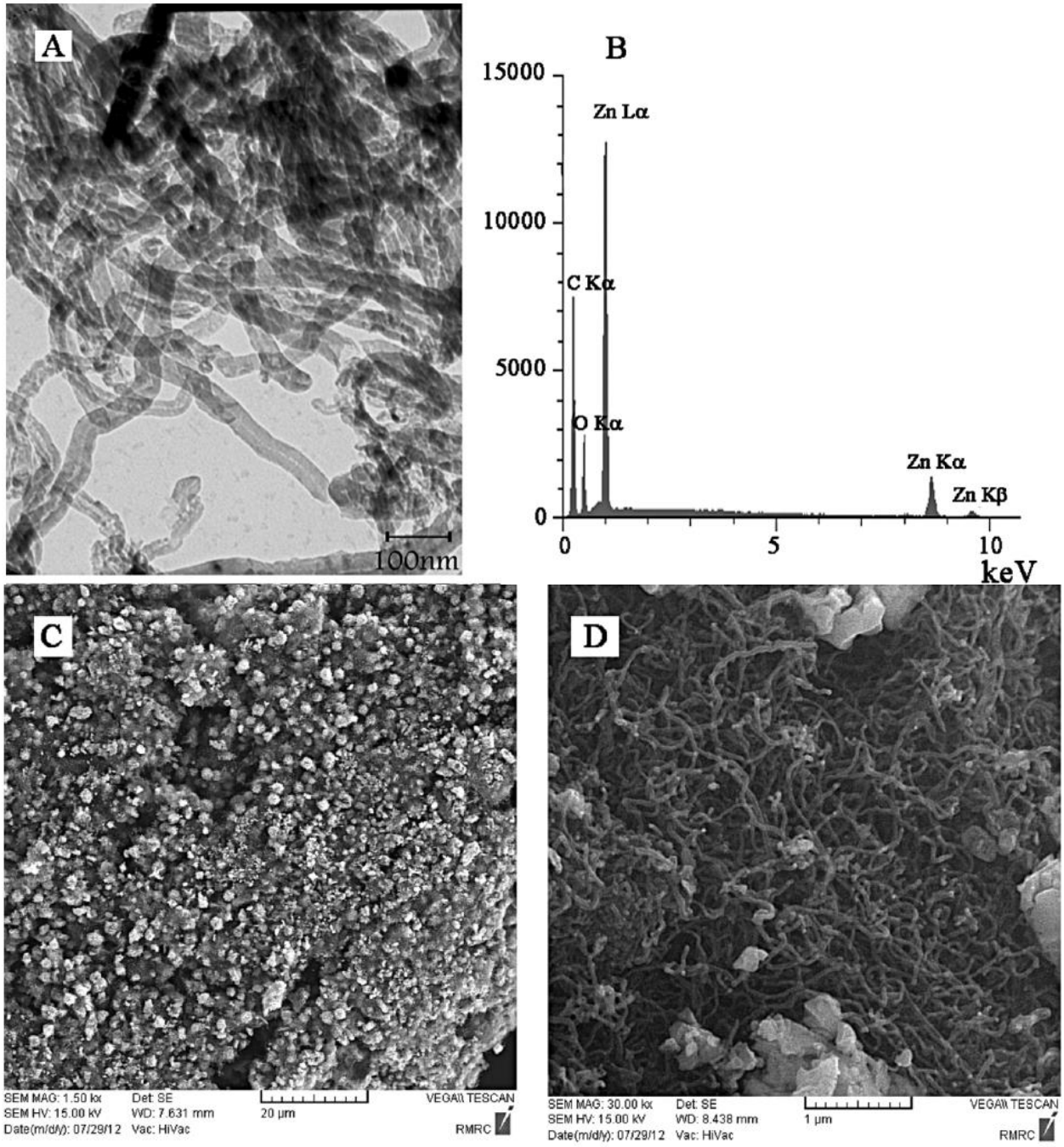

Figure 3-18A) TEM image of ZnO nanoparticles deposited on sidewalls of MWCNTs. B) EDAX analysis for ZnO/CNTs nanocomposite. C) SEM image of ZnO nanoparticles and D) SEM image of multiwall carbon nanotubes

The XRD patterns of the ZnO/CNTs showed diffraction peaks absorbed at 2θ values (Fig. 2). The prominent peaks were used to calculate the grain size via the Scherrer equation, expressed as follows:

$D = K\lambda / \beta \cos\theta$

Where λ is the wavelength (λ = 1.542 ˚ A) (CuK?), β is the full width at half maximum of the line, and θ is the diffraction angle. The grain size of the ZnO nanostructure was 15.0 nm, and the peaks were observed at the (100), (002), (101), (102), (110), (103), (200), (112), (201), (004) and (202) planes. These peaks correspond to ZnO. On the other hand, it clearly proves the presence of CNTs with a diffraction peak at about 26°.

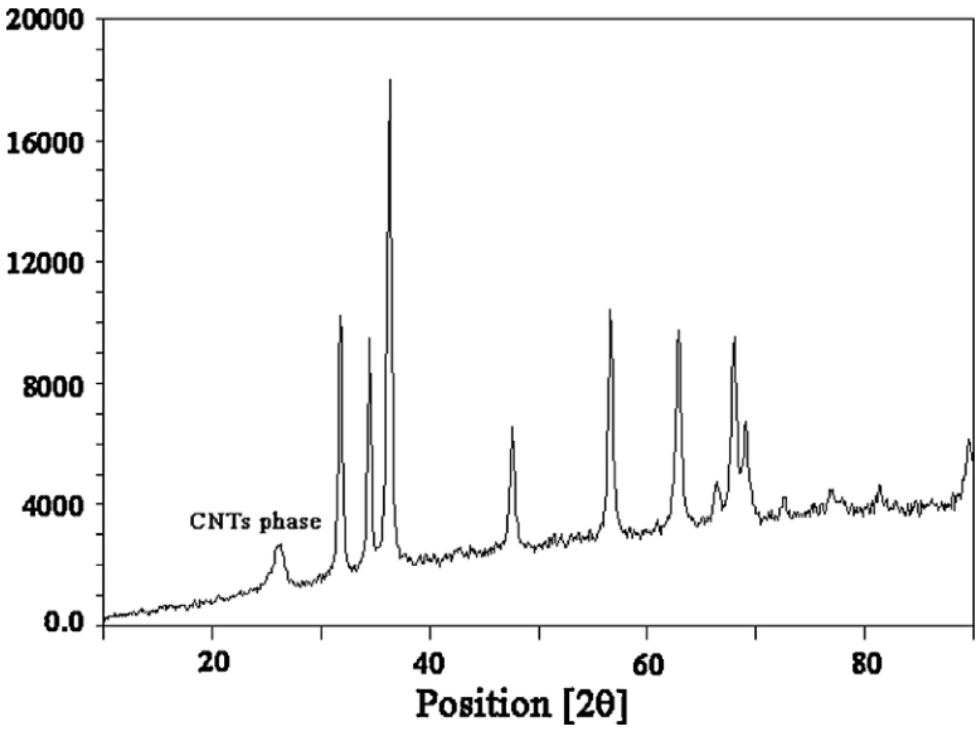

Figure 3-19XRD patterns of as-synthesized ZnO/CNTs nanocomposite

3.3.1. Voltammetric study for third study

The active surface area of the modified electrode was estimated according to the slope of the I_P versus $\nu^{1/2}$ plot for a known con- centration of $K_4Fe(CN)_6$, based on the Randles–Sevcik equation:

$$I_p = 2.69 \times 10^5 \, n^{3/2} \, A D^{1/2} \, \nu^{1/2} \, C_O$$

Where I_p refers to the anodic peak current, n the electron transfer number, A the surface area of the electrode, D_R the diffusion coefficient, C_o the concentration of $K_4Fe(CN)_6$ and ν is the scan

rate. The microscopic areas were calculated from the slope of the I_p $-v^{1/2}$ relation (taking concentration of $K_4Fe(CN)_6$ as 1.0 mmol L^{-1}, concentration of KCl electrolyte as 0.10 mol L^{-1} n = 1, D R = 7.6×10^{-6} cm s^{-1}). The results obtained were 0.2, 0.17, 0.11 and 0.09 cm^2 for ZnO/CNTs/IL/CPE, IL/CPE, ZnO/CNTs/CPE and CPE, respectively. The results further show that the presence of ZnO/CNTs and IL together contributed to an increase in the active surface area of the electrode.

As NE has a catechol moiety, we anticipate that the redox response of NE would be pH dependent. In order to ascertain this, the voltammetric response of NE was obtained in solutions with varying pH from 4.0 to 8.0 at a surface of ZnO/CNTs/IL/CPE. Result shows, the peak potential (E) of the redox couple was pH dependent, with a slope of −62.3 mV/pH unit at 25°C which was equal to the anticipated Nernstian value for a two–electron, two–proton electrochemical reaction. It can be seen that maximum value of the peak current was appeared at pH 6.0 (Fig. 3), so this value was selected throughout the experiments.

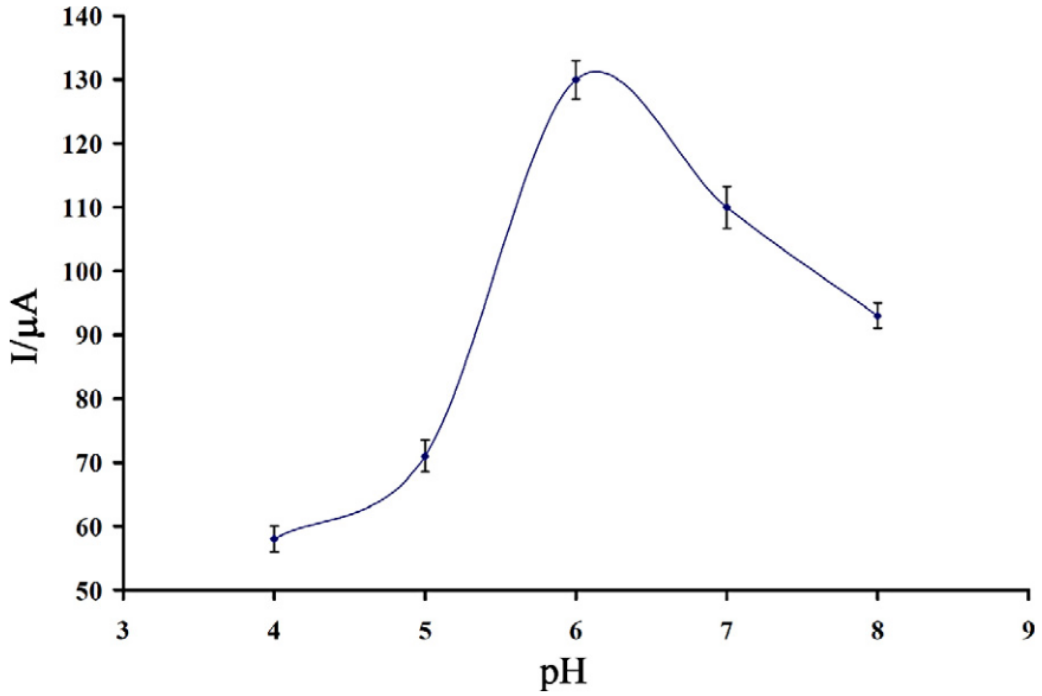

Figure 3-20 Current–pH curve for electrooxidation of 450 μmol L −1 NE at ZnO/CNTs/

The direct electrochemistry of NE on the modified electrode was investigated by cyclic voltammetry. Fig. 4 showed the typical cyclic voltammogram responses of 350 μmol L^{-1} NE at

pH 6.0 at the surface of different electrodes with a scan rate of 100 mV s^{-1}. A peak of 90.8 µA at approximately 430 mV was observed when NE was oxidized to ZnO/CNT/IL/CPE (Fig. 4, curve d). In contrast, a peak current of 24.1 µA and 12.1 µA was observed at the ZnO/CNT/CPE (Fig. 4, curve b) and the unmodified CPE (Fig. 4, curve a), respectively, under the same experimental conditions. In addition, the NE oxidation peak potential was observed to have shifted to 550 mV and 560 mV at the ZnO/CNT/CPE and the unmodified CPE, respectively. Further, the same NE oxidation peak with an enhanced peak current of 50.5 µA has shifted negatively to 380 mV (Fig. 4, curve c), indicating that the presence of ILs on a CPE could enhance the peak current and decrease the oxidation overpotential. A substantial negative shift of the currents and a dramatic increase of current of NE indicated the catalytic ability of ZnO/CNTs/IL/CPE to NE oxidation. Because the high surface area of ZnO/CNTs at a surface of modified electrode it can be increasing conductivity of modified electrode and increasing current sensitivity for determination of NE.

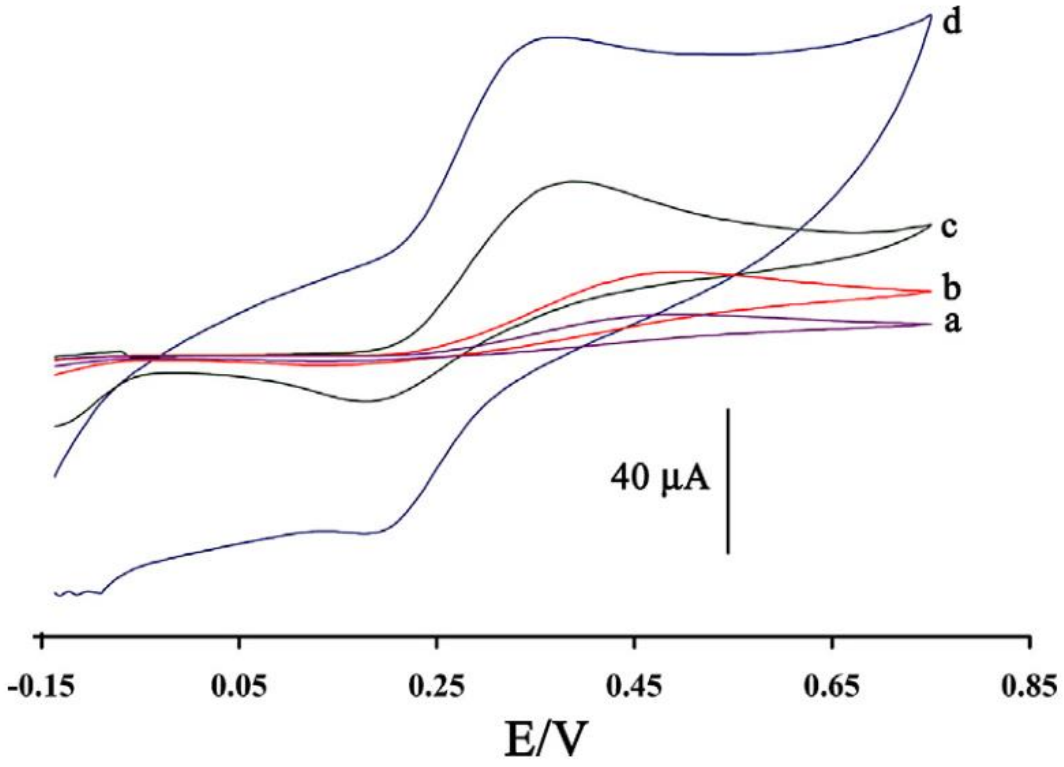

Figure 3-21Cyclic voltammograms of a) CPE, b) ZnO/CNTs/CPE, c) IL/CPE and d) ZnO/CNTs/IL/CPE in the presence of 350 µmol L −1 NE at pH 6.0, respectively

The influence of potential scan rate (v) on I_p (for 300 µmol L^{-1} NE) at ZnO/CNTs/IL/CPE was studied by linear sweep voltammetry at various sweep rates. As shown in Fig. 5, the peak currents of NE grow with the increasing in scan rates and there are good linear relationships between the peak currents and square root of the scan rate ($v^{1/2}$). The results also showed that the action is mass transfer controlled at sufficient over-potentials [39–41]. In addition, with increasing the potential scan rate, the oxidation peak potential gradually shifted towards more positive potentials, suggesting a kinetic limitation in the reaction of NE at a surface of modified electrode (Fig. 5 inset) [42–47]. On the other hand, the peak potential shifts in negative direction when the scan rate increases, meaning that the electrochemical reaction is quasi-reversible. At higher scan rate, the dependence of the peak potential (E_{pa}) and ln(v) showed a linear relationship with a regression equation of:

$E_p = 0.0509 \ln(v) + 0.2696 (r^2 = 0.9945, E_p \text{ in V}, v \text{ in V s}^{-1})$ (3)

According to the following equation:

$E_{pa} = E^0 / + m[0.78 + \ln(D^{1/2} k_s^{-1}) - 0.5 \ln m] + (m/2) \ln(v)$ (4)

With

$m = RT/[(1 - \alpha) n_\alpha F$ (5)

The value of m= 0.1018 is calculated from Eq. (4). Therefore, the electron transfer coefficient (α) is approximately 0.74 for the quasi-reversible electrode process, indicating that two electrons are transferred in the oxidation of NE.

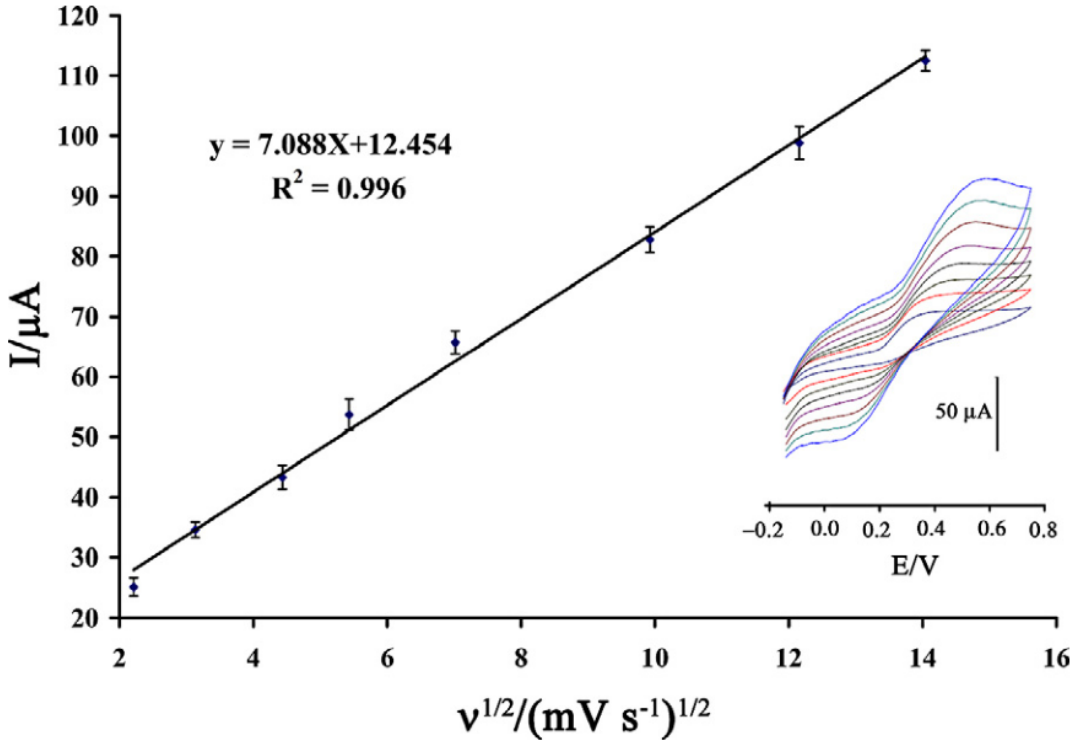

Figure 3-22 Plot of I pa versus v 1/2 for the oxidation of NE at ZnO/CNTs/IL/CPE. Inset shows cyclic voltammograms of NE at ZnO/CNTs/IL/CPE at different scan rates (from inner to outer) of 5, 10, 20, 30, 50, 100, 150 and 200 mV s −1 in 0.1 M phosphate buffer, pH 6.

Chronoamperometry results obtained for the various concentrations of NE solution using ZnO/CNTs/IL/CPE (Fig. 6 A) gives straight lines. The plot of current (I) versus $t^{-1/2}$ for NE solution at various concentrations using ZnO/CNTs/IL/CPE (Fig. 6 A) gives straight lines with different slopes (Fig. 6B). From the slopes we calculated a diffusion coefficient of 3.3×10^{-5} cm^2 s^{-1} (assuming n = 2 and the electrode surface area (A) of 0.2 cm^2) for NE using the Cottrell equation.

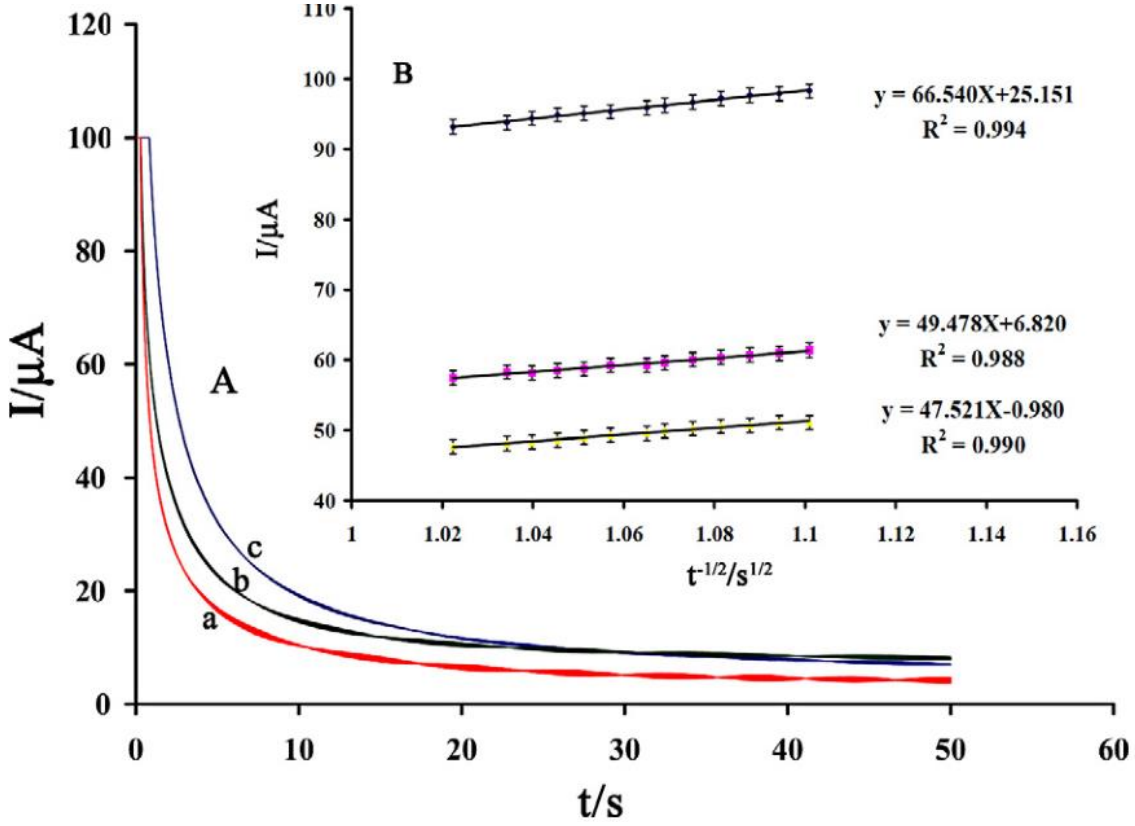

Figure 3-23 A) Chronoamperograms obtained at ZnO/CNTs/IL/CPE in the presence of a) 300; b) 350; and c) 450 µmolL−1 NE in the buffer solution (pH 6.0). B) Cottrell's plot for the data from the chronoamperograms (n = 3)

3.

SWV method was used to prepare the calibration plot (Fig. 7 inset). The plot of the peak current vs. NE concentration consisted of two linear segments with slopes of 2.9464 and 0.3489µA/µmol L^{-1} in the concentration ranges of 0.05 to 8.0 µmol L^{-1} and 8.0 to 450.0 µmol L^{-1} NE, respectively (Fig. 7).

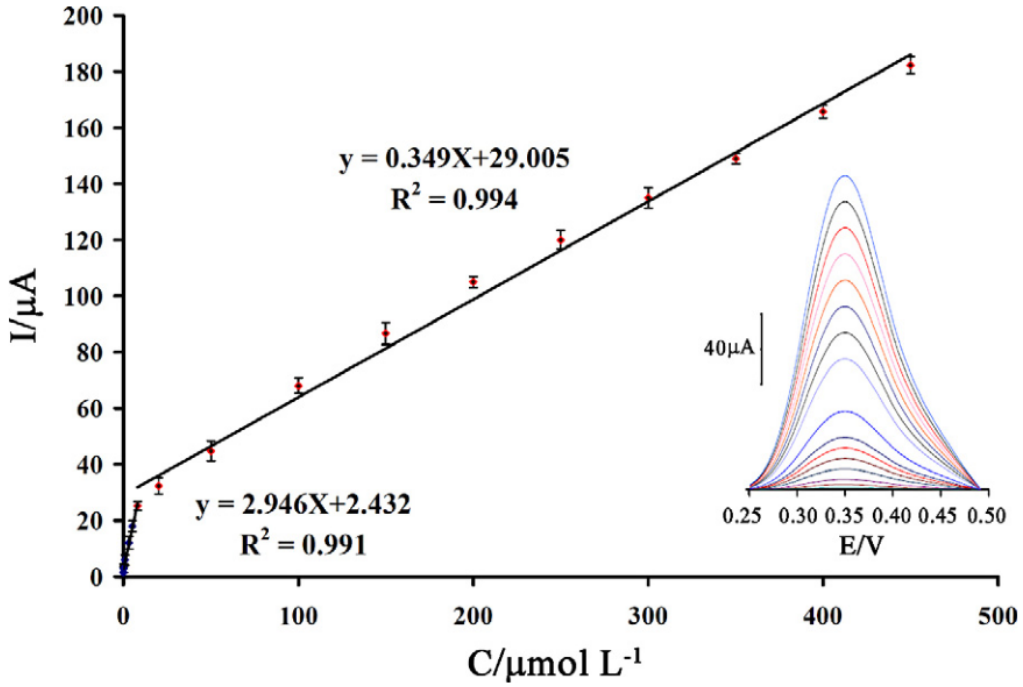

Figure 3-24 Plot of the peak current as a function of NE concentration in the range (n = 3). Inset) SWVs of ZnO/CNTs/IL/CPE in 0.1 mol L −1 phosphate buffer solution (pH 6.0) containing different concentrations of NE. Inner to outer voltammograms correspond to 0.05, 0.3, 0.9, 3.0, 5.0, 8.0, 20.0,

The regression equations were as: for 0.05 to 8.0 μmol L^{-1} NE, I_p = (2.9464 ± 0.2431) C NE + (2.4321 ± 0.4371) (r^2 = 0.9913, n = 6) and for 8.0 to 450.0 μmol L^{-1} NE, I_p = (0.3489 ± 0.00178) C_{NE} + (29.0050 ± 0.9581) (r^2 = 0.9937, n = 11), where C is μmol L^{-1} NE and I_p is the peak current vs. μA. The decrease in the sensitivity (slope) of the second linear segment is likely due to kinetic limitation [48]. The detection limit (3σ) of NE was found to be 0.02 μmol L^{-1}. This value of detection limit, the linear dynamic range, and the sensitivity for NE observed for the ZnO/CNTs/IL/CPE are comparable and even better than those obtained for several other modified electrodes (Table 1).

Table 3-6Comparison of the efficiency of some electrochemical methods in the determination of NE

Electrode	Methods	LOD (µM)	LDR (µM)	Sensitivity µA (µM)$^{-1}$	Ref.
Carbon paste	SWV	0.0094	0.08-550	0.0181	[1]
Carbon paste	DPV	0.21	0.47-500	0.046	[3]
Carbon paste	SWV	8.0	15.0-1000	0.091	[4]
Glassy carbon	SWV	Not report	1.0-50.0	0.35	[5]
Carbon paste	DPV	0.15	0.52-530	0.035	[6]
Glassy carbon	DPV	0.05	0.3-10	1.45	[7]
Glassy carbon	DPV	0.2	3.0-30	0.5616	[8]
Carbon paste	SWV	0.002	0.005-450.0	2.9464	This

3.3.3. Stability and reproducibility for third study

The repeatability and stability of ZnO/CNTs/IL/CPE was investigated by cyclic voltammetric measurements of 20.0 µmol L^{-1} NE. The relative standard deviation (RSD%) for five successive assays was 0.95%. When using six different electrodes, the RSD% for seven measurements was 1.5%. When the electrode stored in the laboratory, the modified electrode retains 98% of its initial response after a week and 95% after 30 days. These results indicate that ZnO/CNTs/IL/CPE has good stability and reproducibility, and could be used for NE.

3.3.4. Interference study for third study

The influence of various substances as potentially interfering compounds with the determination of NE was studied under the optimum conditions 10.0 µmol L^{-1} 1 NE at pH 6.0. The potentially interfering substances were chosen from the group of substances commonly found with NE in pharmaceutical samples. The tolerance limit was defined as the maximum concentration of the interfering substance that caused an error less than ±5% for the determination of NE. The results are shown in Table 2. Those results confirm the suitable selectivity of the proposed method for determination of these compounds.

Table 3-7Interference study for the determination of 10.0μmol L −1 NE under the optimized conditions

Species	Tolerante limits ($W_{Substance}/W_{NE}$)
Glucose, Fructose, Lactose, Sucrose	1000
Tryptophan, Thiourea,Valine, Methionine, Glycine, Lucine, Histidine, Glutamic acid, Alanine, Glycine, Phenylalanine, Ascorbic acid*, Thiourea, urea, uric acid	900
Li^+, Cl^-, CO_3^{2-}, ClO_4^-, SO_4^{2-}, SCN^-, Na^+, Mg^{2+}, K^+, Ca^{+2}	700
Starch	Saturation
Serotonin	100
Dopamine	20

*After addition of 1 mM ascorbic oxidaze

3.3.5. Real-life sample analysis study for third study

In order to evaluate the analytical applicability of the proposed method, it was applied to the determination of NE in injection solution and urine samples. Based on the repeated square wave voltammetric responses (n = 3) of the diluted analyte and the samples that were spiked with specified concentration of NE, measurements were made for determination of NE concentrations in the pharmaceutical and urine preparations. The results are listed in Table 2. In addition, a published capillary lectrochromatographic method [49–71] was used for the analysis to confirm the accuracy of the proposed method with a standard procedure (Table 3). The results presented in Table 2 indicate that the modified electrode retained its efficiency for the determination of NE in real samples with satisfactory results.

Table 3-8Determinationof NE in drug, and urine samples (n = 3).

Sample	Added(μmol L^{-1})	Expected(μmol L^{-1})	Founded(μmol L^{-1})	Published method (μmol L^{-1}) [50]	F_{ex}	F_{tab}	t_{ex}	$t_{tab(95\%)}$
Ampoule	--	5.0	5.2±0.4	5.4±0.7	7.5	19	2.4	3.8
	15.0	15.0	14.8±0.5	15.3±0.7	--	--	--	--
Urine	--	--	<Limit of detection	--	--	--	--	--
	10.0	10.0	10.8±0.9	10.9±1.71	10.5	19	3.1	3.8
	20.0	20.0	20.7±0.8	19.9±1.0	--	--	--	--
Urine*	--	--	8.9±0.8	8.5±0.8	8.5	19	2.6	3.8

±Shows the standard deviation.

*Sampling was made after 3.0 h from a man who used NE.

3.4. X-Ray diffraction and TEM of ZnO nanoparticles for forth study

The X-ray diffraction data were recorded by using Cu K α radiation (1.5406 A 0). The intensity data were collected over a 2θ range of 20–80 ◦ . The average grain size of the samples was estimated with the help of Scherrer equation using the diffraction intensity of (101) peak. X-ray diffraction studies confirmed that the synthesized materials were ZnO with wurtzite phase, and all the diffraction peaks agreed with the reported JCPDS data, and no characteristic peaks were observed other than ZnO. The mean grain size (D=17 nm) of the particles was determined from the XRD line broadening measurement using Scherrer equation:

$D=K\lambda/(\beta \cos\theta)$ (1)

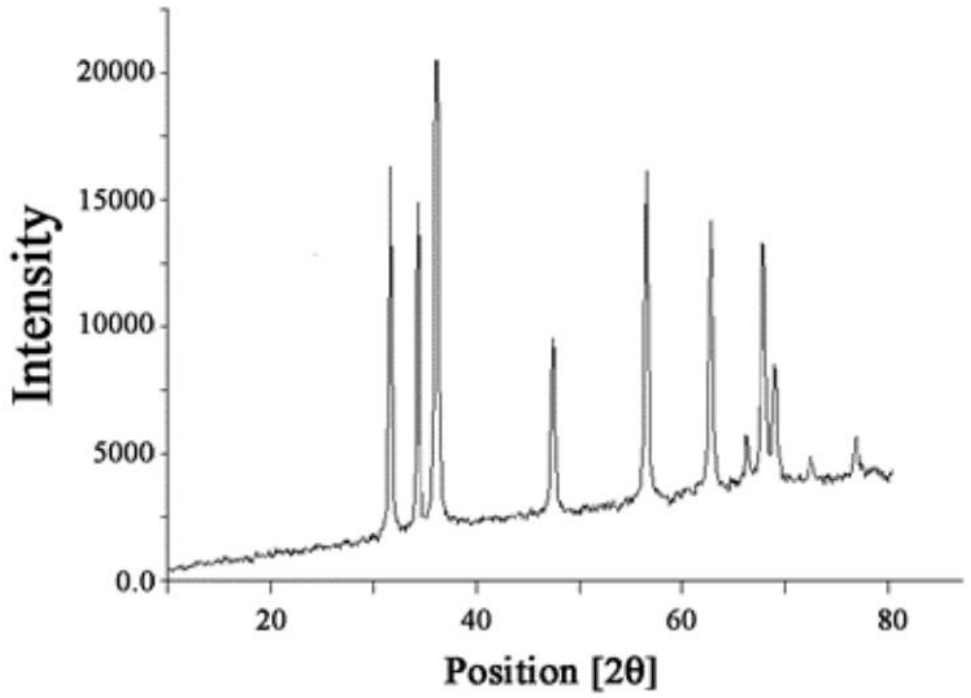

Figure 3-25 XRD patterns of ZnO nanoparticles.

Where λ is the wavelength (Cu K α), β is the full width at the half-maximum (FWHM) of the ZnO (101) line, and θ is the diffraction angle. A definite line broadening of the diffraction peaks is an indication that the synthesized materials are in nanometer range. The lattice parameters calculated were also in agreement with the reported values. The reaction temperature greatly influences the particle morphology of as prepared ZnO powders. Figure 1 show the XRD patterns of ZnO nanoparticles.

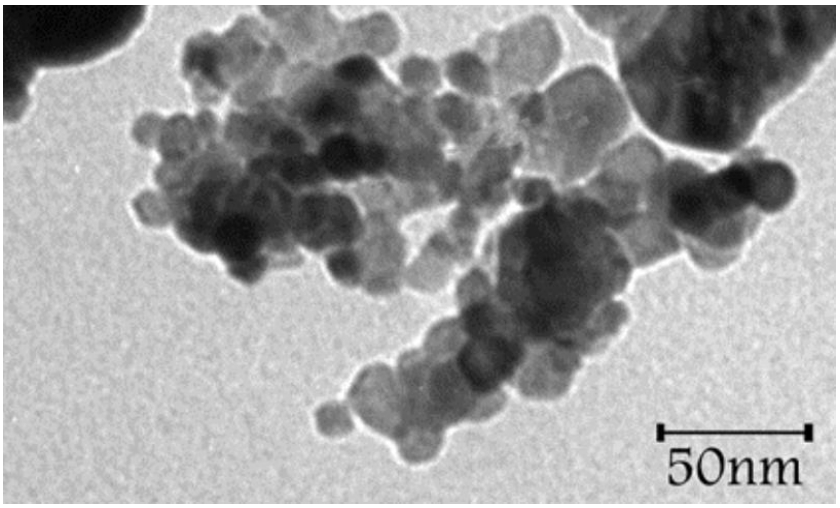

Figure 3-26 TEM image of ZnO nanoparticles.

The morphology of the as-grown nanostructures was characterized by TEM technique. Fig. 2 presents a typical TEM image of ZnO/NPs nanoparticle. It is clear that in this case, a ZnO nanoparticle was successfully prepared.

3.4.1. Electrochemical investigation for forth study

AA can be oxidized at positive potential depends on the electrode type and solution pH [11]. We anticipated that the oxidation of AA would be pH dependent. In order to ascertain this, the voltammetric response of AA at a surface of ZnO/NPs/IL/CPE was obtained in solutions with varying pH. Result shows, the peak potential of the redox couple was pH dependent with a slope of −52.0 mV/pH unit at 25 °C which was equal to the anticipated Nernstian value for a one-electron, one-proton electrochemical reaction. It can be seen that the maximum value of the peak current was appeared at pH 7.0 (Fig. 3), so this value was selected throughout the experiments.

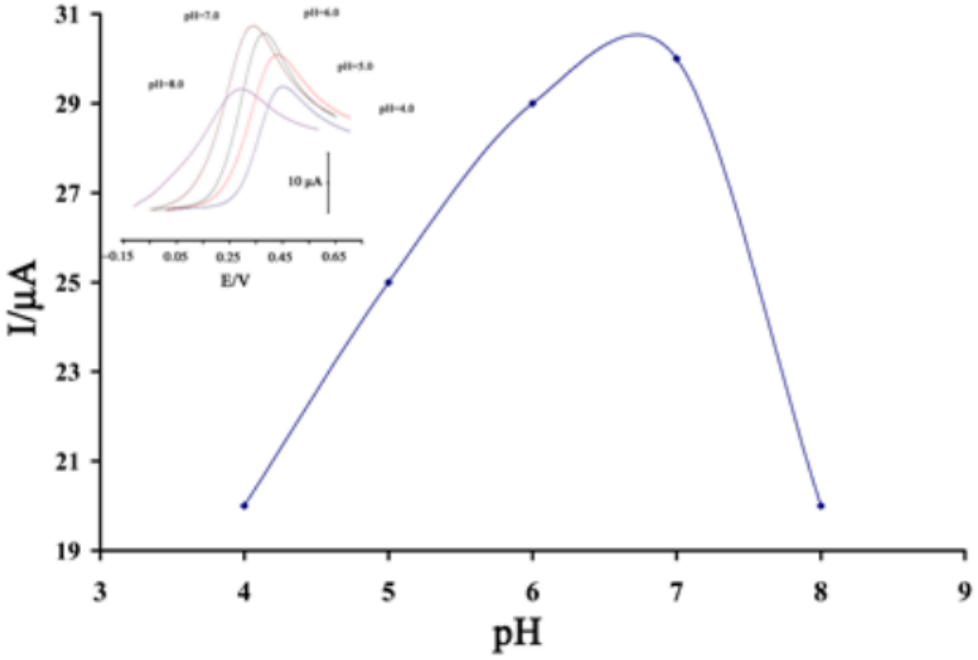

Figure 3-27 Current–pH curve for electrooxidation of 50.0 μM AA at ZnO/NP/IL/CPE with a scan rate of 50 mV s -1 . Inset) influence of pH on cyclic voltammograms of AA at a surface of the modified electrode, (pH 4, 5, 6, 7, and 8, respectively).

Figure 4 (inset) shows the current density derived from the cyclic voltammograms responses of 50 μM AA (pH 7.0) at the surface of different electrodes with a scan rate of 100 mV s^{-1}. The results show that the presence of ZnO/NPs and IL together cause increasing the active surface of the electrode. The direct electrochemistry of AA on the modified electrode was investigated by linear sweep voltammetry. Figure 4 showed the typical linear voltammogram responses of 50 μM AA at pH 7.0 at the surface of different electrodes with a scan rate of 100 mV s^{-1}. ZnO/NPs/IL/CPE exhibited significant oxidation peak current around 370 mV with the peak current of 33.4μA (Fig. 4, curve a). In contrast, low redox activity peak was observed at ZnO/NP/CPE (Fig. 4, curve c) and at unmodified CPE (Fig. 4 curve d) over the same potential range. The AA oxidation peaks potential at ZnO/NP/CPE and at CPE observed around 450 and 460 mV vs. the Ag/AgCl/KClsat reference electrode with the oxidation peaks current of 11.5 and 4.5 μA, respectively. In addition, at the surface of bare IL/CPE, the oxidation peak appeared at 370 mV with the peak current was 19.0 μA (Fig. 4, curve b), which indicated the presence of ILs in CPE could enhance the peak currents and decrease the oxidation potential (decreasing the

overpotential). A substantial negative shift of the currents starting from oxidation potential for AA and dramatic increase of current of AA indicated the catalytic ability of ZnO/NP/ILCPE to AA oxidation. The results indicated that the presence of ZnO/NPs on ZnO/NPs/IL/CPE surface had great improvement with the electrochemical response, which was partly due to excellent characteristics of ZnO/NPs such as good electrical conductivity, high chemical stability, and high surface area. The suitable electronic properties of ZnO/NPs together with the ionic liquid gave the ability to promote charge transfer reactions, good anti-fouling properties, especially when mixed with a higher conductive compound such as ILs when used as an electrode.

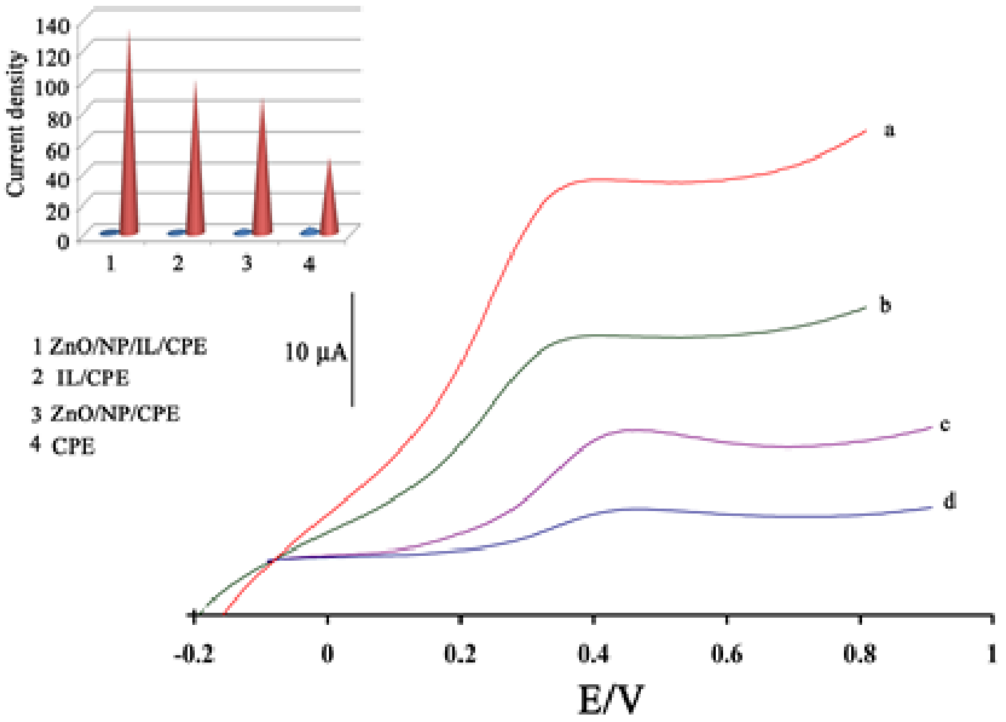

Figure 3-28 Cyclic voltammograms of a) at ZnO/NP/IL/CPE, b) IL/CPE, c) at ZnO/NP/CPE and d) CPE in presence of 100 µM AA at a pH 7.0, respectively. Inset: the current density derived from cyclic voltammograms responses of 100 µM AA at pH 7.0 at the surface of different electrodes with a scan rate of 50 mV s^{-1}.

The influence of potential scan rate (ν) on I p of 50 µM AA at the ZnO/NP/IL/CPE was studied by linear sweep voltammetry at various sweep rates (Fig. 5 inset). As shown in Fig. 5, the peak currents of AA grow with the increasing of scan rates and there are good linear relationships between the peak currents and ν 1/2 (Fig. 5). The regression equation is I pa = 5.9717 - 25.0670 ν

1/2 (I pa : μA, ν: mVs −1 , R 2 = 0.9911), indicating the redox process of 50 μM AA at the ZnO/NP/IL/CPE was diffusion-controlled.

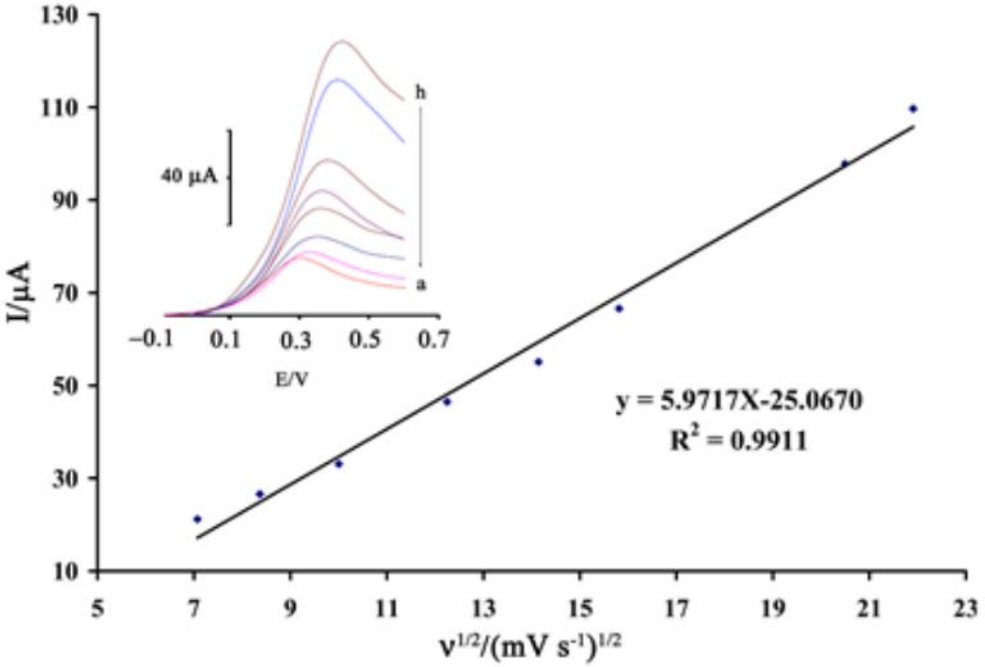

Figure 3-29 Plot of I pa versus ν 1/2 for the oxidation of AA at ZnO/NP/IL/CPE. Inset shows cyclic voltammograms of AA at ZnO/NP/IL/CPE at different scan rates of 50, 70, 100, 150, 200, 250, 420 and 480 mV s –1 in 0.1 M phosphate buffer, pH 7.0.

To obtain further information on the rate determining step, a Tafel plot was developed for the AA at a surface of ZnO/NP/IL/CPE using the data derived from the raising part of the current–voltage curve (Fig. 6). The slope of the Tafel plot is equal to n(1−α)F/2.3RT which comes up to 0.1908 V decade −1 . We obtained α as 0.8.

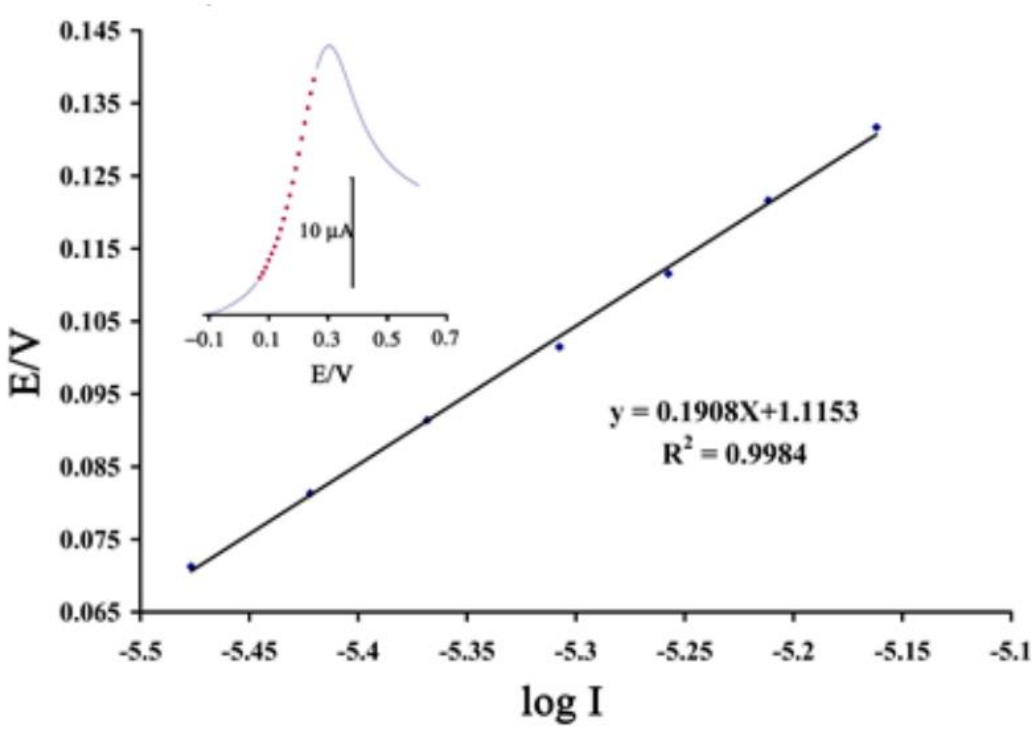

Figure 3-30 Tafel plot for ZnO/NP/IL/CPE in 0.1 M PBS (pH 7.0) with a scan rate of 50 mV s −1 in the presence of 50 μM AA

Chronoamperometric measurements of AA at ZnO/NP/IL/CPE were carried out by setting the working electrode potential at 400 mV vs. Ag/AgCl/KClsat for the various concentration of AA in buffered aqueous solutions (pH 7.0) (Fig. 7A). For an electroactive material (AA in this case) with a diffusion coefficient of D, the current observed for the electrochemical reaction at the mass transport limited condition is described by the Cottrell equation. Experimental plots of I vs. $t^{-1/2}$ were employed, with the best fits for different concentrations of AA (Fig. 7B). The slopes of the resulting straight lines were then plotted vs. AA concentration. From the resulting slope and Cottrell equation the mean value of the D was found to be 2.3×10^{-5} cm^2 /s.

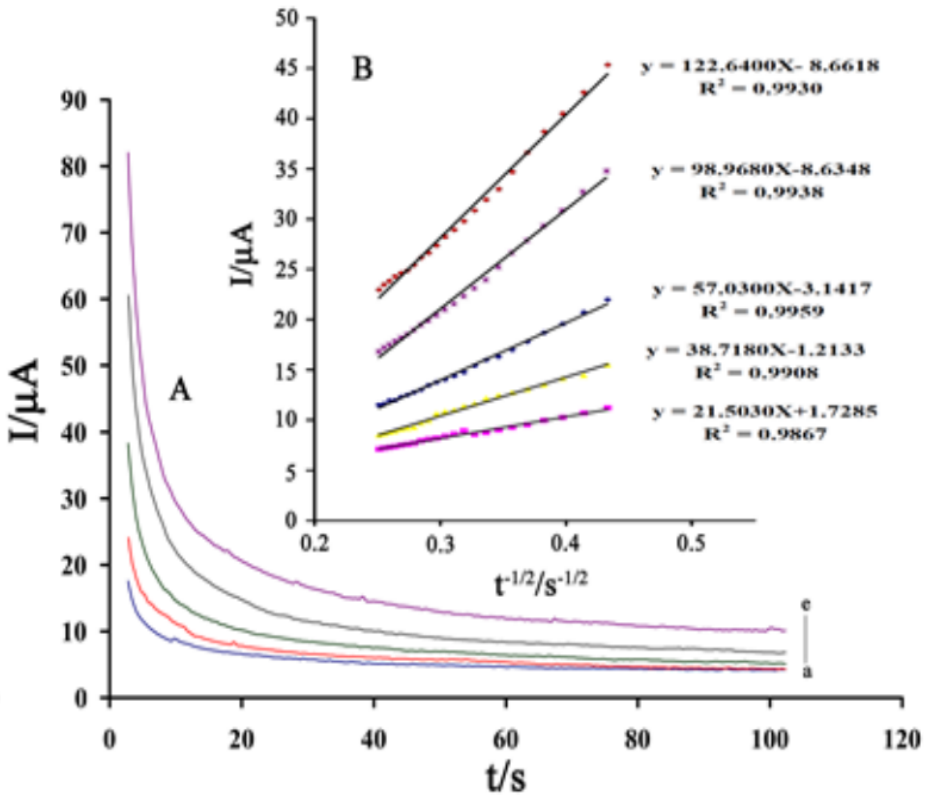

Figure 3-31 A) Chronoamperograms obtained at ZnO/NP/IL/CPE in the presence of a) 300; b) 400; c) 500; d) 600 and e) 700 µM AA in the buffer solution (pH 7.0). B) Cottrell's plot for the data from the chronoamperograms

3.4.2. Linear dynamic range and limit of detection for forth study

Square wave voltammetry (SWV) was used to determine AA concentrations. The SW voltammograms clearly show that the plot of peak current vs. AA concentration is linear for 0.08–350 µmol L −1 of AA, the regression equation being I_p (µA) = (0.6449±0.0120)C AA + (18.1350±0.8932) (r 2 = 0.9902, n = 10), where C is µM concentration of AA and I p is the peak current. The detection limit was 0.04 µM AA according to the definition of Y LOD = Y B +3σ.

3.4.3. Stability and reproducibility for forth study

The repeatability and stability of ZnO/NP/IL/CPE was investigated by square wave voltammetric measurements of 10.0 µM AA. The relative standard deviation (RSD%) for ten successive assays was 0.94%. When using four different electrodes, the RSD% for seven measurements was 1.5%.

When the electrode stored in the laboratory, the modified electrode retains 97% of its initial response after a week and 94% after 45 days. These results indicate that ZnO/NP/IL/CPE has good stability and reproducibility, and could be used for AA.

3.4.4. Interference study for forth study

In order to evaluate the selectivity of the proposed method in the determination of AA the influence of various foreign species on the determination of 10.0 µM AA was investigated. Tolerance limit was taken as the maximum concentration of foreign substances that caused an approximate relative error of ±5%. The results given in Table 1 show that the peak current of AA is not affected by all conventional cations, anions, and organic substances.

Table 3-9 Interference study for the determination of 10.0 µM AA under the optimized conditions

Species	Tolerant limits ($W_{Substance}/W_{AA}$)
Glucose, Sacarose, , Lactose, Feroctose	900
Li^{+} , Br^{-} , Al^{3+} , K^{+} , ClO^{4-} , Na^{+} , Cl^{-} , CO_3^{-2} , Ca^{2+} , Mg^{2+} , SO_4^{2-}	750
Thiourea, Glutamic acid, Tryptophan, Lucine, L-Threonine, L-Phenylalanine, Glycine, Methionine, Alanine, Valine, Histidine	600
Cysteine	400
Starch	Saturation

3.5. Real sample analysis for forth study

In order to evaluate the analytical applicability of the proposed method, also it was applied to the determination of AA in tablet, fruit juice and vegetable juice samples. Based on the repeated differential pulse voltammetric responses (n=3) of the diluted analyte and the samples that were spiked with specified concentration of AA, measurements were made for determination of AA concentrations in food samples. The results are listed in Table 2. In addition, a published electrochemical method [20] was used for the analysis to confirm the accuracy of the proposed method with a standard procedure. The results presented in Table 2 indicate that the modified

electrode retained its efficiency for the determination of AA in real samples with satisfactory results.

Table 3-10 Determination of AA in real samples (n=3)

Sample	AA Added (μM)	Found (AA) Proposed method (μM)	Found (AA) Official method (μM)	F_{ex} [a]	F_{tab}	t_{ex} [b]	$t_{tab(95\%)}$
Tablet	5.0	5.35±0.45[c]	4.22±0.45	5.4	19.0	1.2	3.8
	10.0	9.74±0.55	10.65±0.72	-	-	-	-
	20.0	19.84±0.33	20.45±0.55	-	-	-	-
Fruit Juices	-	-	-	-	-	-	-
Orange "	-	150.66±1.22	151.11±1.47	11.9	19.0	3.5	3.8
Kiwi "	-	80.22±0.85	79.88±1.33	10.5	19.0	3.2	3.8
Apple "	-	25.35±0.65	24.95±0.95	9.2	19.0	3.0	3.8
Lemon	-	55.23±0.45	54.95±0.83	8.2	19.0	2.7	3.8
Vegetable juices	-	-	-	-	-	-	-
Pimento	-	45.33±0.75	45.22±0.85	10.0	19.0	3.1	3.8
Dill	-	90.32±0.25	90.25±0.32	4.9	19.0	1.1	3.8

[a] Fex Calculated F-value; Reported F value from F-test table with 95% confidence level and 2/2 degree of freedom;
[b] tex Calculated t; ttab (95%) Reported t value from t-student test table with 95% confidence level.
[c] ±Shows the standard deviation.

3.5.1. X-Ray diffraction and TEM of NiO nanoparticles for fifth study

The X-ray diffraction (XRD) data were recorded using Cu K α radiation (1.5406 Å) (Fig. 1A). The intensity data were collected over a 2θ range of 10–80°. The average grain size of the samples was estimated with the help of Scherrer equation using the diffraction intensity of (200) peak. XRD studies confirmed that the synthesized materials were NiO, and all the diffraction peaks agreed with the reported Joint Committee on Powder Diffraction Standards (JCPDS) data, and no characteristic peaks were observed other than NiO [18]. The mean grain size (D = 23 nm) of the particles was determined from the XRD line broadening measurement using Scherrer equation:

$$D=K\lambda/(\beta \cos\theta) \quad (1)$$

Where λ is the wavelength (Cu Kα), β is the full width at the half-maximum (FWHM) of the NiO (200) line and θ is the diffraction angle. A definite line broadening of the diffraction peaks is an indication that the synthesized materials are in the nanometre range. The morphology of the as-grown nanostructures was characterized by scanning electron microscopy (SEM) technique.

Figure 2 shows the SEM image of the synthesized product. It is clear that in this case, a NiO nanoparticle was successfully prepared.

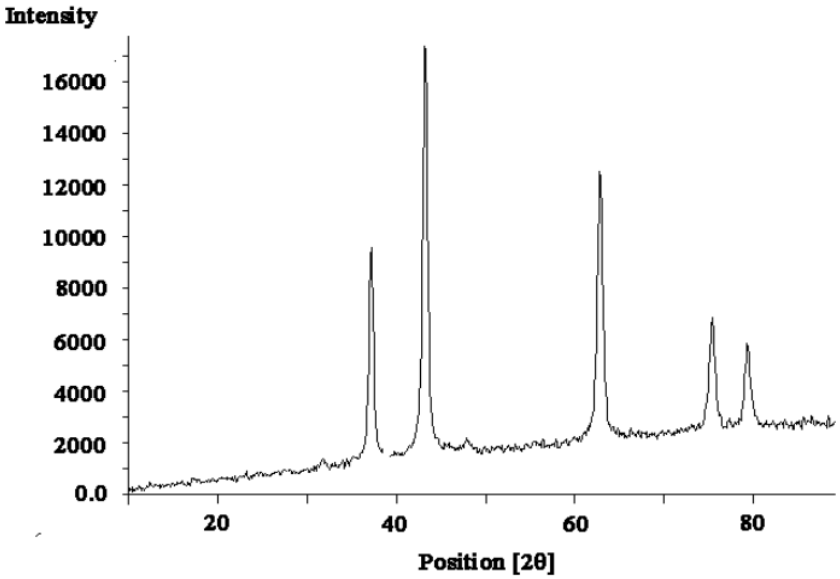

Figure 3-33 XRD patterns of as-synthesized NiO nanoparticle.

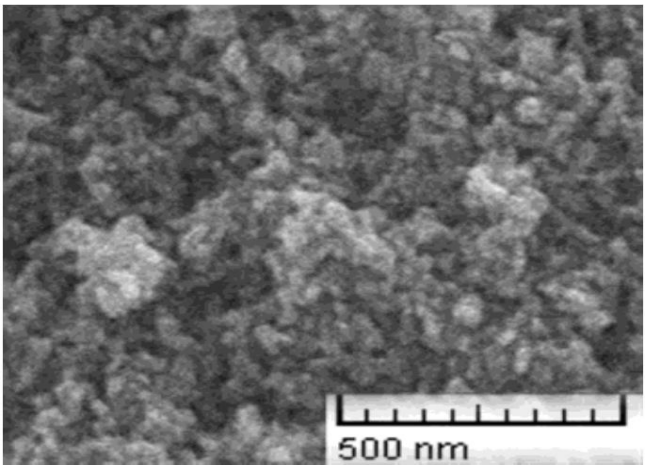

Figure 3-33 SEM image of NiO/NPs.

3.5.2. Electrochemical investigation for fifth study

The active surface areas of the working electrodes are estimated according to the slope of the IP versus $\nu^{1/2}$ plot for a known concentration of $K_4Fe(CN)_6$, based on the Randles–Sevcik equation:

$$I_p = 2.69\times10^5 n^{3/2} A D^{1/2} \nu^{1/2} C_O \quad (2)$$

Where I pa refers to the anodic peak current, n the electron transfer number, A the surface area of the electrode, D R the diffusion coefficient, C 0 the concentration of $K_4Fe(CN)_6$ and ν is the scan rate. For 1.0 mmol L^{-1} $K_4Fe(CN)_6$ in 0.10 mol L^{-1} KCl electrolyte with n = 1 and $D_R = 7.6\times10^{-6}$ cm s^{-1} and from the slope of the I_{pa}–$\nu^{1/2}$ relation, the microscopic areas were calculated. They were 0.15 and 0.09 cm^2 for NiO/NPs/CPE and CPE, respectively. Scheme 1 shows the electro-oxidation reaction of NB. According to Scheme 1, we anticipated that the oxidation of NB would be pH dependent.

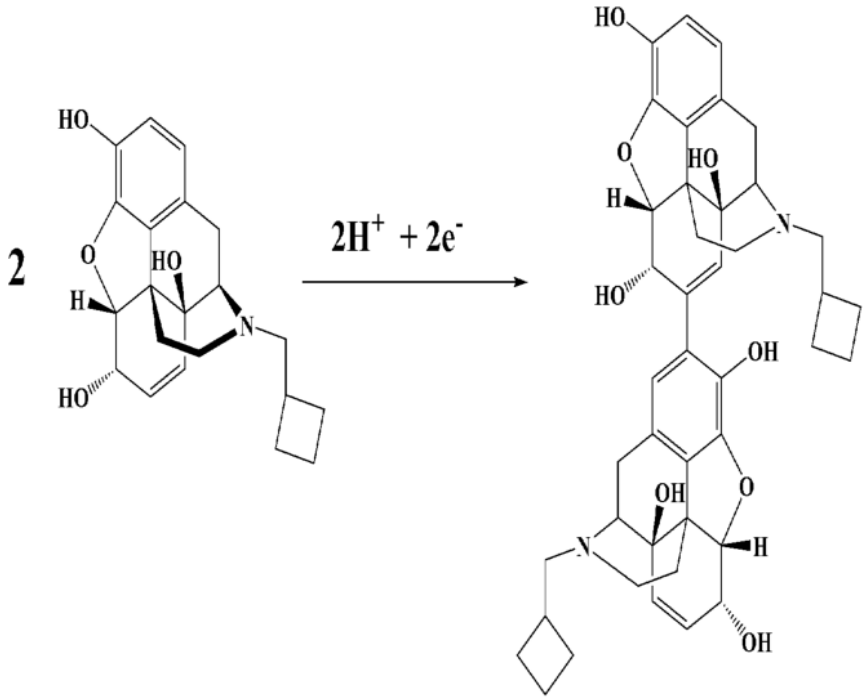

Figure 3-34 Mechanism for electro-oxidation of NB

The effect of pH was investigated using cyclic voltammetry technique for electro-oxidation of NB at a surface of NiO/NPs/CPE. It was found that the oxidation peak current increased gradually from pH 5.0 to 7.0, and then the current conversely decreased when the pH value increased from 7.0 to 8.0 (Fig. 3). According to the above point that pH 7.0 was chosen as the optimal experimental condition.

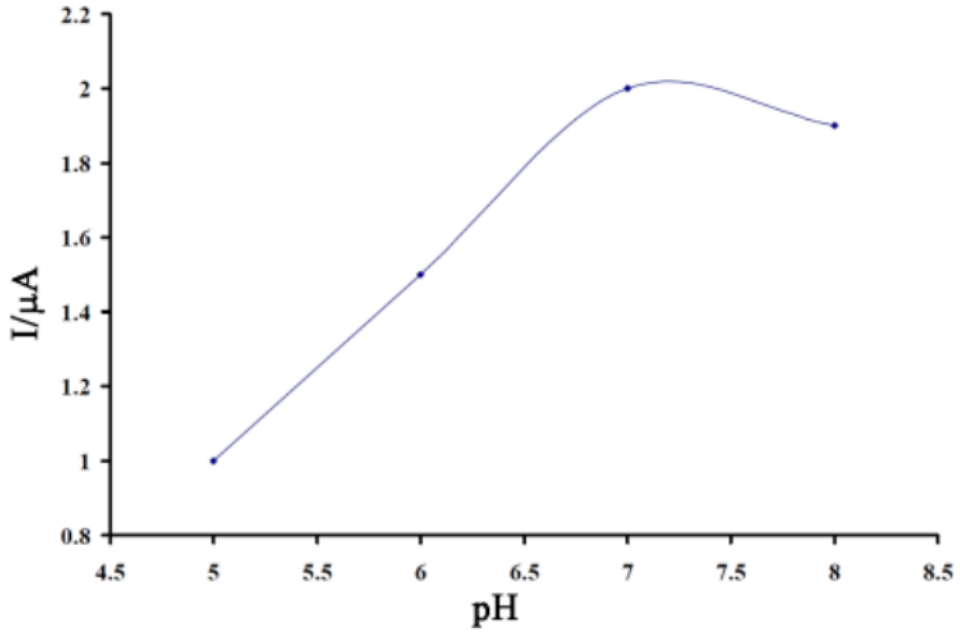

Figure 3-35 Current–pH curve for electro-oxidation of 100.0 μM NB at NiO/NPs/CPE with a scan rate of 50 mV s^{-1}

Fig. 4 (curves a & b) showed the electrochemical responses of NiO/NPs/CPE, and CPE in 100 μM NB in PBS solution (pH 7.0), respectively. At NiO/NPs/CPE, and CPE, NB showed an irreversible oxidation peak, with oxidation peak potential (E pa) of 0.57 V, and 0.60 V, respectively. However, the peak current of NB at NiO/NPs/CPE was much larger than that at the CPE; it was about 1.7 times larger than CPE by cyclic voltammetry. Thus, the modified electrode exhibited a catalytic activity toward the oxidation of NB. This further testified the superiority of NiO/NPs/CPE to CPE and indicated that the use of NiO/NPs as modifier facilitated the electron transfer between NB and electrode.

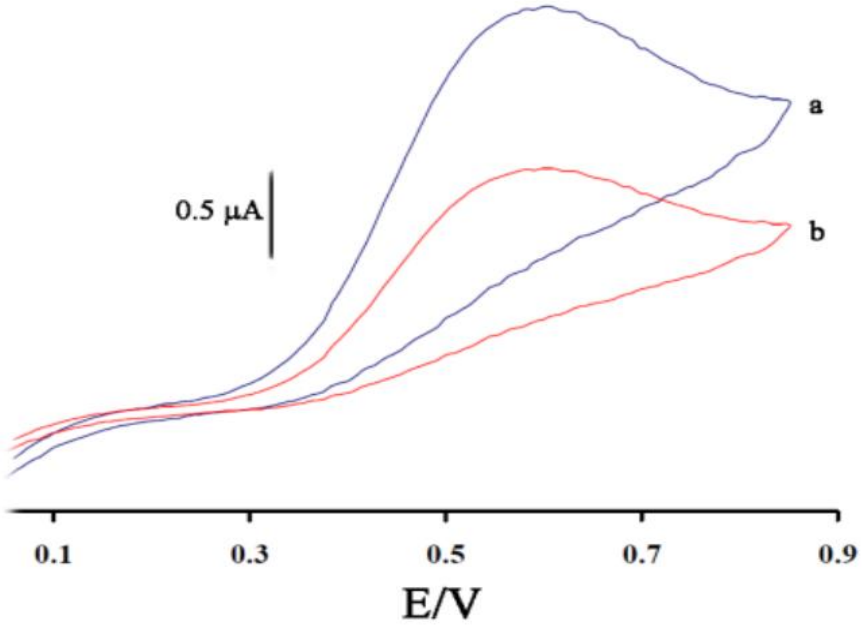

Figure 3-36 Cyclic voltammograms of (a) NiO/NPs/CPE, and (b) CPE in the presence of 100 µM NB at pH 7.0, respectively.

To obtain information about the rate-determining step, the Tafel plot was drawn, as derived from points in the Tafel region of the cyclic voltammogram. The slope of the Tafel plot was equal to 2.3 RT/n(1−α)F , which came up to 0.3064 V decade −1 for scan rate 50 mV s −1 (Fig. 5). Therefore, we obtained the mean value of α, which is equal to 0.8.

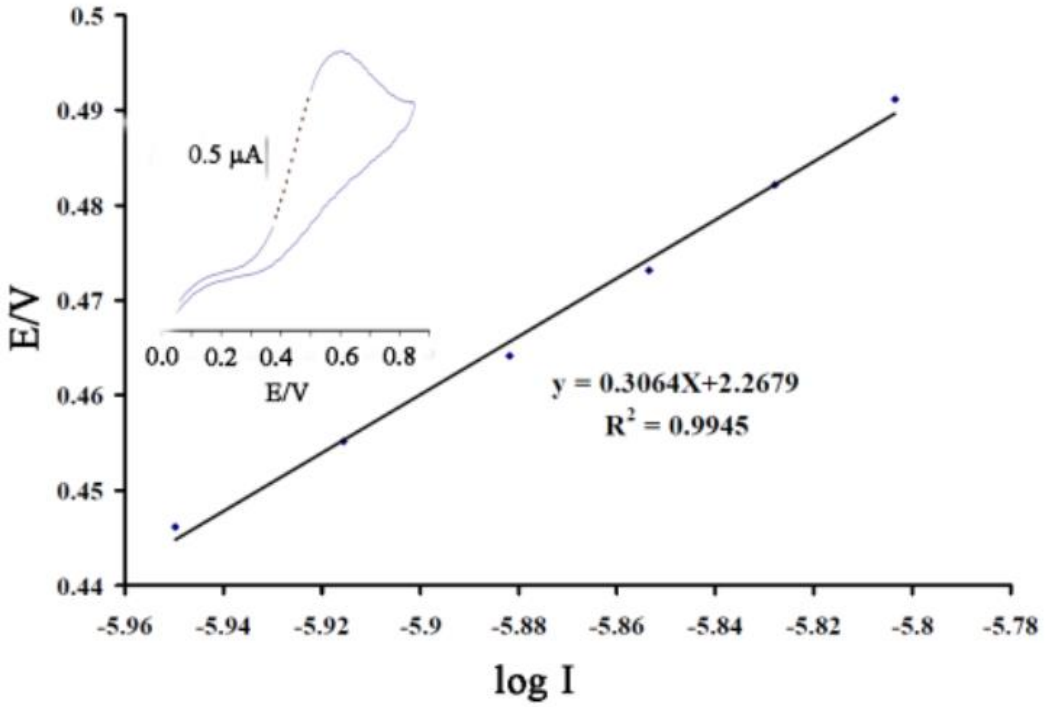

Figure 3-37 Tafel plot for NiO/NPs/CPE in 0.1 MPBS (pH 7.0) at the scan rateof 50 mV s −1 in the presence of 100.0 μM NB

The chronoamperometry as well as the other electrochemical methods was employed for the investigation of electro-oxidation of NB at NiO/NPs/CPE. Chronoamperometric measurements of NB at NiO/NPs/CPE were done (not shown) for various concentrations of NB. For an electroactive material (NB in this case) with a diffusion coefficient of D, the current for the electrochemical reaction (at a mass transport limited rate) is described by the Cottrell equation [19]:

$$I = nFAD^{1/2} C b \pi^{-1/2} t^{-1/2} \quad (3)$$

Under diffusion control, a plot of I versus $t^{-1/2}$ will be linear, and from the slope the value of D can be obtained. The mean value of the D was found to be 1.0×10^{-4} cm^2 /s. The repeatability and stability of NiO/NPs/CPE were investigated by linear sweep voltammetric measurements of 10.0 μM NB. The relative standard deviation (RSD%) for six successive assays was 0.95%.

When using five different electrodes, the RSD% for five measurements was 1.6%. When the electrode stored in the laboratory, the modified electrode retains 96% of its initial response after a week and 93% after 35 days. These results indicate that NiO/NPs/CPE has a good stability and reproducibility, and could be used for NB analysis. The influence of various substances as potentially interfering compounds for the determination of NB was studied under the optimum conditions with 10.0 μM NB at pH 7.0. The potential interfering substances were chosen from the group of substances commonly found with NB in pharmaceuticals and/or in biological fluids. The tolerance limit was defined as the maximum concentration of the interfering substance that caused an error of less than ±5% for the determination of NB.

After the experiments, we found that neither 1000-fold of glucose, sucrose, lactose and fructose, nor 750-fold of K^+ , Li^+ , Ca^{2+} , Mg^{2+} , Al^{3+} , NH^{4+} , SO_4^{2-} , Cl^- and ClO_4^- ,nor 500-fold phenylalanine, valine, tryptophan, histidine and glycine affected the selectivity. Nor did saturation solution of starch; neither 400-fold of urea and thio-urea were interfered with the determination of NB.

Since square wave voltammetry has a much higher current sensitivity than linear sweep voltammetry, it was used for the determination of nb (Fig. 6 inset). The SW voltammograms clearly show that the plot of peak current vs. NB concentration is linear for 0.8–400 μM of NB with slope of 0.1835 μA μM -1 (Figure 6). According to the method mentioned in Ref. [20], the lower detection limit, C_m , was obtained by using the equation $C_m = 3_{sb}/m$, where s b is the standard deviation of the blank response (μA) and m is the slope of the calibration plot. The data analysis presents the value of lower limit detection of NB to be 0.5 μM.

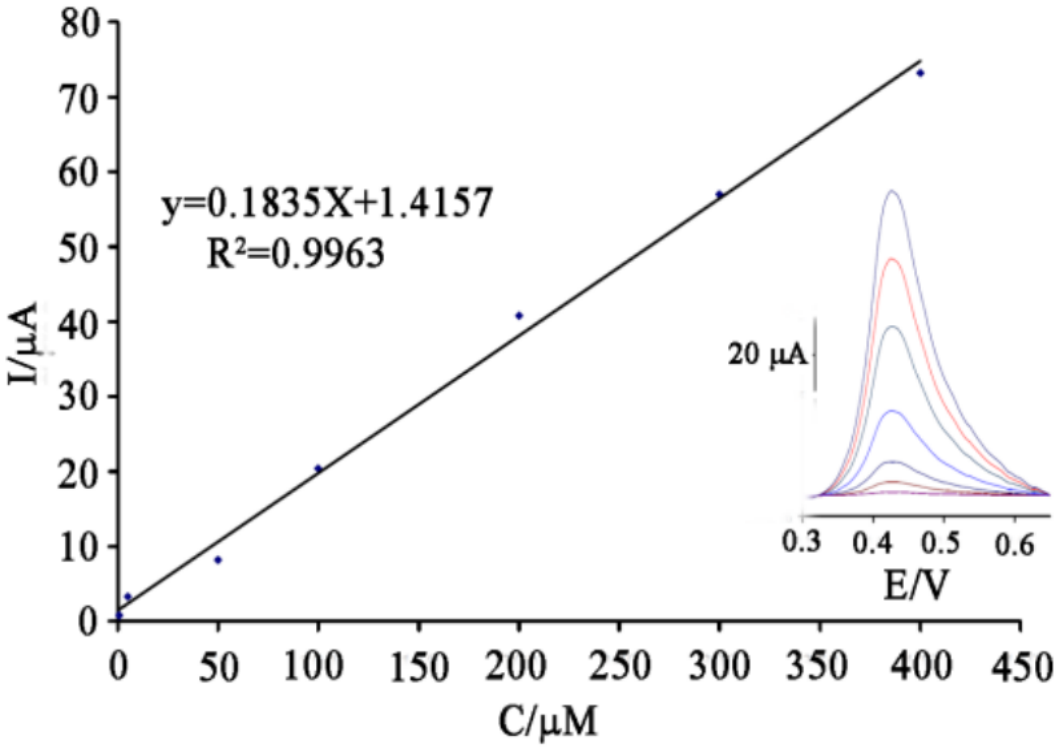

Figure 3-38 The plots of the electrocatalytic peak current as a function of NB concentration. Inset shows the SWVs of NiO/NPs/CPE in 0.1 M phosphate buffer solution (pH 7.0) containing different concentrations of NB. From inner to outer correspond to 0.8, 5.0, 50.0

In order to demonstrate the ability of the modified electrode to the determination of NB in real samples, determinations of NB in pharmaceutical and in urine samples were examined. The results are given in Table 1. These results demonstrated the ability of NiO/NPs/CPE for voltammetric determination of NB with high selectivity and good reproducibility.

Table 3-11 Ability of propose sensor for determination of NB in real samples

Sample	Added (μM)	Expected (μM)	Founded (μM)	Recovery %
Urine	---	---	<LOD	---
	5.00	5.00	4.87±0.62	97.40
Serum	---	---	<LOD	---
	10.00	10.00	10.45±0.55	104.50
Water	---	---	<LOD	---
	20.00	20.00	20.65±0.75	103.25

3.6. Molecular geometry for sixth study

The geometry of Droxidopa and the numbering of atoms and the geometrical parameters of selected parameters in VAC and in the five solvents are given in figure 1 and table 1, respectively.

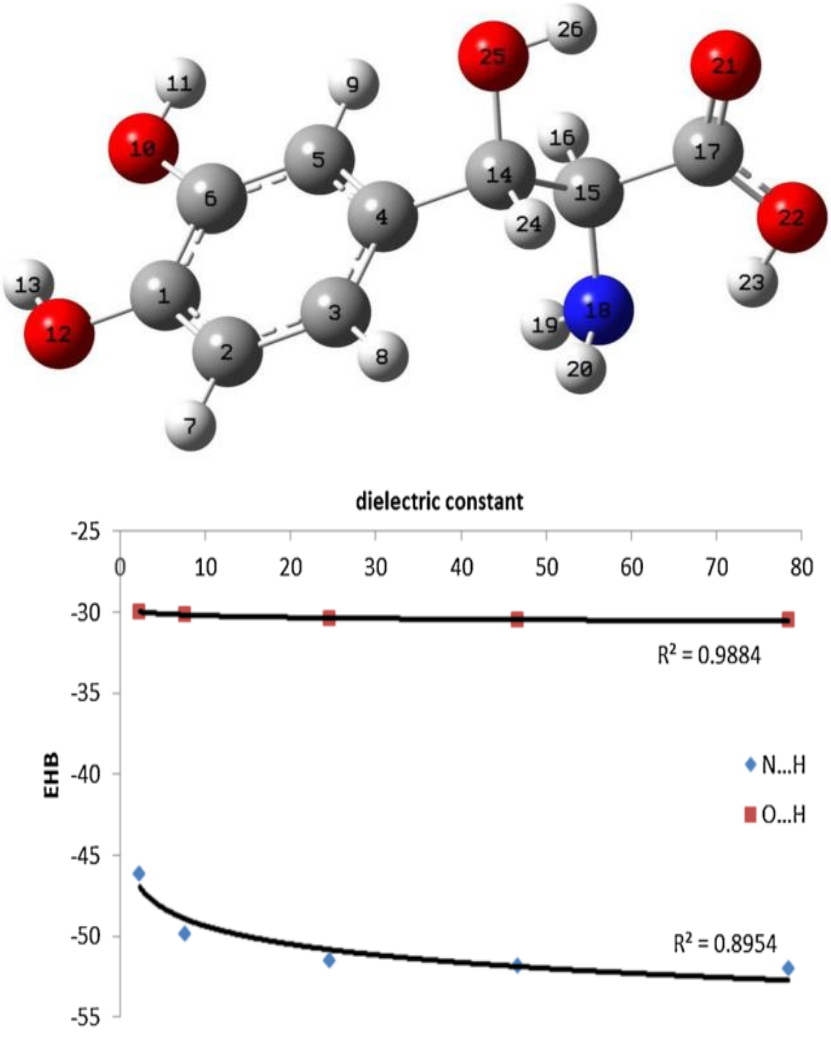

Figure 3-39 The relationship between the E HB (in kJ/mol) and dielectric constant.

Table 3-12 The geometrical parameters (bond distance in Å and bond angle in◦) of Droxidopa in vacuum and in five solvents.

Environment	O21-C17	C14-O25	O25-H26	O21...H26	C17-O22	O22-H23	C15-N18	N18...H23	O22-H23-N18	O25-H26-O21
VAC	1.210	1.417	0.972	1.938	1.332	0.985	1.468	1.904	124.57	139.57
CC	1.213	1.421	0.972	1.937	1.330	0.989	1.467	1.875	125.58	140.38
THF	1.216	1.426	0.972	1.933	1.328	0.993	1.466	1.849	126.45	141.27
ET	1.217	1.429	0.972	1.930	1.326	0.995	1.466	1.837	126.86	141.60
DMSO	1.217	1.429	0.972	1.930	1.326	0.995	1.466	1.835	126.93	141.68
AQ	1.217	1.430	0.972	1.929	1.326	0.995	1.466	1.834	126.96	141.72

The same atom numbering as for the study in VAC is utilized for all the environments to facilitate the comparisons. The geometrical parameters showed that the N...H, O...H distances and θ (O−H...N) , θ (O−H...O) in Droxidopa molecule are in the range of 1.834–1.904, 1.929–1.938-Å and 124.57–126.96, 139.57–141.72 degree, respectively. It is well-known that the geometrical parameters of the HB reflect the strength of the bond. In many cases, there is a clear relationship between these parameters and the strength of hydrogen bond.

The smaller the N...H and O...H distances and the larger θ (O−H...N) and θ (O−H...O) angle in the Droxidopa in vacuum and in the five solvents, the stronger is intramolecular hydrogen bonds. Results in table 1 show that in AQ solution, the θ (O−H...N) and θ (O−H...O) angles are larger and both N...H and O...H intramolecular hydrogen bonds are stronger than the other solutions. These parameters in CC solution are closed to VAC environment, because the dielectric constant of CC is very small. As shown in this table, analysis of bond lengths indicates that r C−O are lengthened, with respect to the Droxidopa molecule in VAC. These lengthening of single bonds could be attributed to the increasing quantification of electron delocalization, which in turn causes the hydrogen bond to become stronger than that for Droxidopa molecule in VAC. Therefore, among the environments studied in this work, the lengthening of C–O bonds is observed in solution. Alternatively, the main solvent effect is shortening the N...H and O...H distances compared with the corresponding value in VAC. These structural changes in Droxidopa suggest a stronger hydrogen bond in solutions than that in VAC.

3.6.1. H-bond energies for sixth study

One of the most important features of intramolecular H-bond is its strength. The IHB energy plays a significant role in conformational preference, in which its value mainly depends on the choice of the resonance state. Many authors have devised various methods to estimate the energy of IHB. In the Schuster method [32] it is assumed that the energy difference between the close (with HB) and open (without HB) conformers is equal to HB energy. But this energy gap also contains some conformational contributions that cannot be a direct measure of the HB energy. In recent years, the powerful method of Espinosa [33] is often applied for the estimation of H-bond energy. In this method, the H-bond energies may be estimated from the properties of bond

critical points. Espinosa and co-workers have pro- posed a simple relationship between the hydrogen bond energy and the local electron potential energy density $V(r_{CP})$ at ρ_O(N)...H :

$E_{HB} = 1/2\ V(r_{CP})$ (1)

Corresponding to the Abramov's relation 34 at the critical point:

$G(r_{CP}) = (\frac{3}{10})(3\pi^2)^{2/3} \rho^{5/3}(r_{CP}) + (\frac{1}{6})\nabla^2 \rho(r_{CP})$(2)

The local potential energy density $V(r_{CP})$ can be obtained from the viral equation:

$2G(r_{CP}) + V(r_{CP}) = (\frac{1}{4})\nabla^2 \rho(r_{CP})$(3)

All values in the relations mentioned above are expressed in atomic units. E HB energies calculated from the potential energy densities of O...H and N...H contacts are included in table 2. These values suggest that the H-bond strength in solutions is relatively stronger than VAC, which is in agreement with calculated geometrical parameters (table 1).

It is worth mentioning that E HB correlates to the geometrical parameters, which are usually assumed to be good descriptors of the H-bond strength. The linear correlation coefficient for the dependency of E HB versus r O...H and r N...H is 0.989 and 0.998, respectively. It means that E HB is a good description of the H-bond strength. Furthermore, as shown in figure 2, there are very excellent logarithmic correlation coefficients for the dependency of E HB versus dielectric constant (ε) as the following equations for both N...H and O...H hydrogen bond strength:

$E_{HB} = -0.16\ln\varepsilon - 29.86$for O-H...O IHB

And

$E_{HB} = -1.63\ln\varepsilon - 45.62$for O-H...N IHB

3.6.2. Charge Density Properties for sixth study

The precise mapping of the distribution of charge density in H-bonded systems is a classical topic in structural chemistry, with a large number of individual studies reported. Currently, quantum theory of atom in molecule (QTAIM) [35] is the most frequently used formalism in theoretical analyses of charge density. Here, each point in space is characterized by a charge

density ρ(r), and further quantities such as the gradient of ρ(r), the Laplacian function of ρ(r),and the matrix of the second derivatives of ρ(r) (Hessian matrix). The relevant definitions and the topology of ρ(r) in a molecule or molecular complexes can be best understood with the help of an illustration. If there is a chemical bond between two atoms (such as HB), they are directly connected by a trajectory called the 'bond path.' The point with the minimal ρ value along the bond path is called the BCP, which represents a saddle point of ρ(r). Strictly speaking, trajectories terminate at the BCP, so that the bond path represents a pair of trajectories, each of which connects a nucleus with the BCP. Figures 3 and 4 present the molecular graph and contour map of Droxidopa obtained from the B3LYP/6-311++G(d,p) wave function, respectively.

The calculated electron density, ρ, and its second derivative, $\nabla^2 \rho$ were used for describing the nature of the intra-molecular O−H...O and O-H...N bonds. The calculated electron density (ρ), its Laplacian ($\nabla^2\rho$) at bond critical points and charge density at ring critical point (ρ_{RCP}), and its Laplacian $\nabla^2\rho_{RCP}$) for Droxidopa in VAC and in the five solvents are given in table 2 and shown in figure 3.

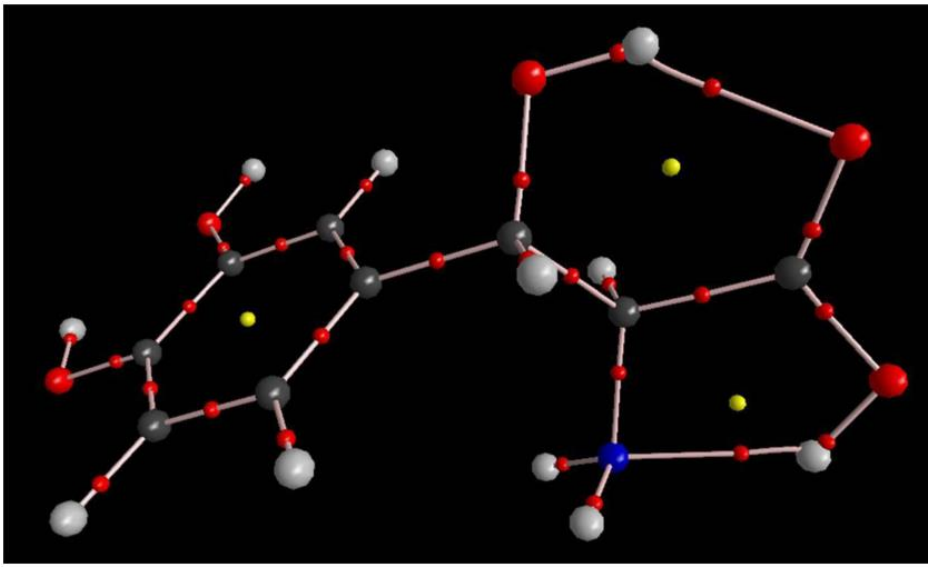

Figure 3-40 The molecular graphs of Droxidopa obtained from the B3LYP/6-311++G(d,p) wave function.

The calculated electron density properties of Droxidopa in VAC and in the five solvents demonstrate that the O...H bonding has a low ρ (ranging from 0.02793 to 0.02828), and positive $\nabla^2\rho$ values (ranging from 0.09722 to 0.09815). Similarly, the calculated electron density

properties of Droxidopa in VAC and in the five solvents show that the N...H bonding has low ρ (ranging from 0.03676 to 0.04307), and positive $\nabla^2\rho$ values (ranging from 0.10743 to 0.1063). These properties are typical for closed-shell interactions as HBs and indicate electrostatic character of the O...H and N...H bonding. With considering calculated topological parameters, we can conclude that the main solvent effect is an increase in electronic densities at the ring critical points (ρ_{RCP}). This fact indicates that the hydrogen-bond strength in solution is stronger than that of the VAC. Another topic analyzed here is the existence of the ring critical point (RCP) for closed configurations. The $\nabla^2\rho_{RCP}$ is a point of the minimum electron density within the ring surface and a maximum on the ring line [36].

As shown in figure 4, the density value is arbitrarily terminated at the positions of the carbon, oxygen, and nitrogen nuclei. The lower maps illustrate the trajectories traced out by ρ, the gradient vectors of the density. The contour map is overlaid with the trajectories of ρ associated with the bond cps that define the bond paths and the intersection of the interatomic surfaces with the plane of the diagram.

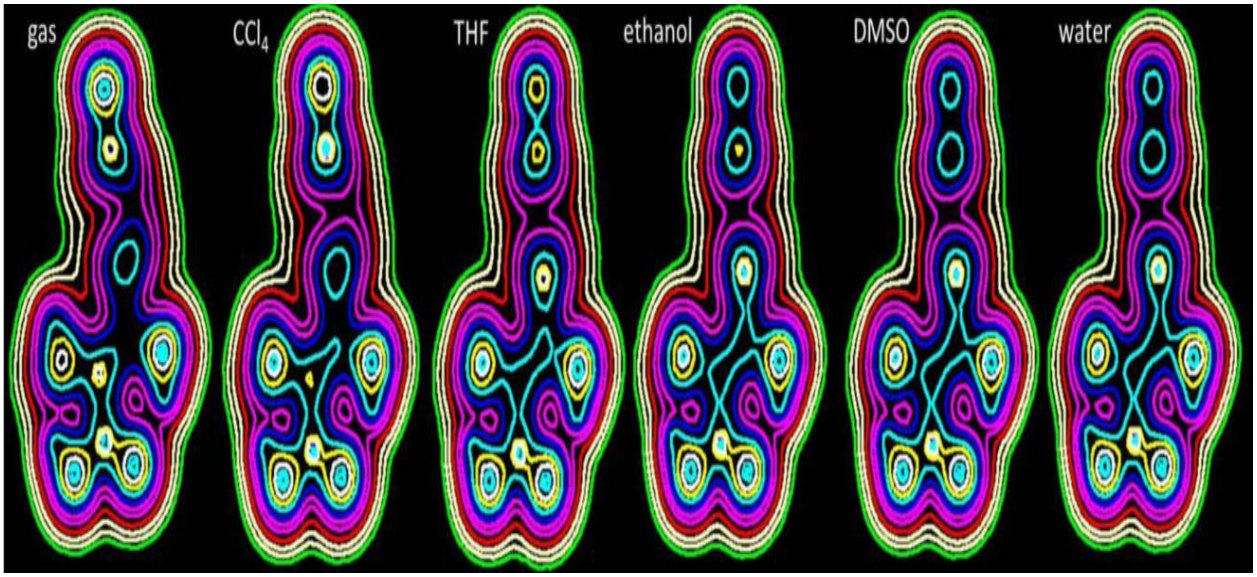

Figure 3-41 The contour map of Droxidopa in vacuum and in five solvents obtained from the B3LYP/6 311++G(d,p) wave function in plane with three selected points: A(2.42, 3.06, 2.07), B(7.33, 1.88, 0.82), and C(7.97, −1.56, −1.52).

It has been mentioned recently that for IHB, there is a correlation between the electron density at the bond critical point corresponding to the contact within the H-bridge and the electron density

at the RCP [11]. There is a linear relationship between E_{HB} and $\nabla^2\rho$ at the RCP. The corresponding correlation coefficient amounts to 0.998 for N...H bond (with equation as E_{HB}=−554.1 $\nabla^2\rho$ RCP +49.234). This implies that the properties of the RCP values could be very useful to estimate the strength of IHB. Their values permit us to have a better understanding of these novel correlations. The derived relationships from these graphs empower us to acquire other physically meaningful results.

3.6.3. NBO analysis for sixth study

The natural bond orbital (NBO) analyses were applied to evaluate the hydrogen bond strength in the Droxidopa in VAC and in the five solvents. The NBO method shows that for typical hydrogen bonding, a two-electron n B →σ ∗ XH intermolecular donor–acceptor interaction exists where electron density from the lone pair n B of the H-acceptor delocalizes into the unfilled σ ∗ XH anti-bonding orbital of the H-donor. The n B →σ ∗ XH orbital overlap is characteristic for hydrogen bonding interaction. The hydrogen bond formation leads to an increase in the occupancy of the σ ∗ XH anti-bond orbital and hence the weakening and lengthening of the X–H bond. This leads to the red-shifted ν X−H stretching frequency. Therefore, electron delocalization or charge transfer (CT) effects between n B and σ ∗ XH may be estimated by second-order perturbation theory:

$$E(2) = -2\frac{\langle n_B \left| F \right| \sigma^*_{XH} \rangle^2}{\varepsilon(\sigma^*_{XH}) - \varepsilon(n_B)}$$

Where $\langle n_B \left| F \right| \sigma^*_{XH} \rangle$ is the Fock matrix element between the n B and σ ∗ XH orbitals, ε(σ ∗ XH)−ε(n B) is the orbital energy difference (the difference of diagonal Fock matrix element). It is worth mentioning that the CT and the corresponding lowering of energy are attributed to hydrogen bonding interactions. In other words, the second-perturbation energies E(2) lowering is responsible for the orbital interaction of H-bond, the larger E(2) values correspond to stronger CT interaction occurring in the H-bond. The results of NBO analysis are listed in table 3.

In the NBO analysis of hydrogen bond system, the charge transfer between the lone pairs of proton acceptor and antibonds of the proton donor is the most important parameter. The results of NBO analysis illustrate that in the structure of Droxidopa, two lone pairs of oxygen atom (n 2 O) and a lone pair of nitrogen atom (n N) participate as donors and the σ* O−H interactions behave as acceptors in relatively strong intramolecular charge transfer interactions with the energy values presented in table 3. The energy corresponds to the n 2 O(nN)→σ* O−H interaction, which is connected with the maximum n 2 O(nN)→σ* O−H overlap, leading to a linear, or nearly so, geometry of the O-H...O and N-H...O hydrogen-bonded system, respectively.

Hydrogen bonding causes an increase of the occupancy of the σ* O−H anti-bond orbital and further weakening and lengthening of the O-H bond. These orders of energy values again support the calculated intra-molecular hydrogen bonds strength values in Droxidopa in VAC and in the five solvents.

It is worth mentioning that the NBO energy connected with n2O(nN)→σ* O−H overlap nicely correlating with other geometrical and topological parameters. Moreover, we found out that there is an excellent correlation between E HB versus n2O→σ* O−H and nN→σ* O−H with correlation coefficient of 0.955 and 1.00, respectively. These kinds of correlations are important, because they permit us to quantitatively dictate the strength of such interactions and provide a physical explanation for the process. Eventually, the NBO and AIM analyses show that the strength of the IHB increases with the increase of the solvent dielectric constant.

Chapter Four

Conclusion

4.1. First study

In this study, the 1-methyl-3-butylimidazolium chloride modified NiO/CNTs carbon paste electrode was used to investigate the electrochemical behaviors of morphine. The IL/NiO/CNTCPE showed great improvement to the electrode process of morphine compared to the traditional carbon paste electrode. The modified electrode successfully resolves the overlapped voltammetric peaks of morphine and diclofenac by ≈ 180 mV, so that the modified electrode displays high selectivity in the SWV measurement of morphine and diclofenac in their mixture solutions. The electrode was successfully used for the de- termination of morphine in injection solution and urine samples.

4.2. Second study

The novel IL/NiO/NPs/CPE electrochemical sensor was developed for the rapid determination of NADH. The IL/NiO/NPs/CPE showed great improvement to the electrode process of NADH compare to the traditional carbon paste electrode. Compared with traditional CPE, a decrease of over-potential of oxidation of NADH was about 70 mV with 4.0-fold increment in the oxidation peak current when using IL/NiO/NPs/CPE. Under the optimum conditions, the oxidation peak current was proportional to the NADH concentration in the range of 0.03–900 μmol L^{-1} with the detection limit of 9.0 nmol L^{-1}. Finally, the propose sensor was successfully used for the determination of NADH in real samples.

4.3. Third study

In this study we report synthesis of ZnO/CNT nanocomposite as a high sensitive sensor for voltammetric determination of NE using carbon paste electrode. The synthesized nanocomposite was characterized with different methods such as SEM, TEM, XRD, and EDAX. ZnO/CNTs/IL/CPE combines the features of ZnO/CNT nanocomposite and room temperature ionic liquid to play a good voltammetric sensor. Hence it shows high sensitivity and reproducibility in sensing of NE. Compared with traditional CPE, a decrease of over-potential of oxidation of NE was about 130 mV with 7.5-fold increment in the oxidation peak current when

using ZnO/CNTs/IL/CPE. Under the optimum conditions, the oxidation peak current was proportional to the NE concentration in the range of 0.05 to 450 μmol L^{-1} with the detection limit of 0.85 μmol L^{-1} . The proposed method was successfully applied to the NE detection in real samples such as drug and urine.

4.4. Forth study

In this investigation, we describe synthesis of ZnO/NPs as a high sensitive sensor for voltammetric determination of AA using carbon paste electrode. The synthesized nanoparticle was characterized with different methods such as TEM and XRD. The direct electrochemistry of AA at a surface of ZnO/NP/IL/CPE was assessed by cyclic voltammetry, chronoamperometry and square wave voltammetry methods. The presence 1,3- dipropylimidazolium bromide and ZNO nanoparticles helped AA to have a favored orientation and reduce the effective electron transfer distance. Finally, the propose sensor was successfully used for the determination of AA in food samples.

4.5. Fifth study

This work describes the ability of the modified NiO/NPs carbon paste electrode for determination of NB. The voltammetric investigation demonstrates that electrooxidation of NB at the surface of NiO/NPs/CPE showed very distinct characteristics which due to the presence of NiO/NPs layer on the surface of electrode. The proposed modified electrode presented a low detection limit and good linear range and reproducibility which make it a suitable NB sensor for practical applications.

4.6. Sixth study

We have examined two types of IHBs for Droxidopa in vacuum and five solvents using B3LYP level of theory at the 6311++G(d,p) basis set. The results obtained from the DFT calculations

and the topological parameters derived from the Bader theory suggest that the stronger HB can lead to lengthening the O-H bond and shortening the N...H and the O...H distances. Our calculated RCP values are useful descriptors of the strength of IHBs, emphasizing that there is a correlation between E_{HB} and the other parameters such as solvent dielectric constant. Moreover, the calculated electron densities and Laplacian properties of Droxidopa in vacuum and five solvents illustrate that O(N)...H bonding have lower ρ and positive $\nabla^2 \rho$ values. These properties are typical for closed-shell interactions as HBs that indicate electrostatic characters of the O(N)...H bondings. NBO analysis indicates that there is an excellent linear correlation between E_{HB} and $n_2O(nN) \rightarrow \sigma^* O-H$ charge transfer in vacuum and five solvents. Overall, our theoretical calculations show that the strength of the IHB increases with the increase of the solvent dielectric constant and we found a good correlation between these parameters.

References:

[1] A. Reyhani, S.Z. Mortazavi, A.Z. Moshfegh, A. Nozad Golikand, M. Amiri, Enhanced electrochemical hydrogen storage by catalytic Fe-doped multi-walled carbon nano-tubes synthesized by thermal chemical vapor deposition, J. Power Sources 188 (2009) 404–410.

[2] A. Reyhani, S.Z. Mortazavi, S. Mirershadi, A. Nozad Golikand, A.Z. Moshfegh, H 2 adsorption mechanism in Mg modified multi-walled carbon nanotubes for hydrogen storage, Int. J. Hydrogen Energy 37 (2012) 1919–1926.

[3] A. Reyhani, S.Z. Mortazavi, S. Mirershadi, A.Z. Moshfegh, P. Parvin, A. Nozad Golikand, Hydrogen storage in decorated multiwalled carbon nanotubes by Ca, Co, Fe, Ni, and Pd nanoparticles under ambient conditions, J. Phys. Chem. C 115 (2011) 6994–7001.

[4] E.Afsharmanesh,H.Karimi-Maleh, A. Pahlavan,J.Vahedi, Electrochemical behaviorof morphineatZnO/CNTnanocompositeroomtemperatureionicliquidmodifiedcarbon paste electrode and its determination in real samples, J. Mol. Liq. 181 (2013) 8–13.

[5] H. Karimi-Maleh, P. Biparva, M. Hatami, A novel modified carbon paste electrode based on NiO/CNTs nanocomposite and (9,10-dihydro-9,10-ethanoanthracene- 11,12-dicarboximido)-4-ethylbenzene-1,2-diol as a mediator for simultaneous determination of cysteamine, nicotin amide adenine dinucleotide and folic acid, Biosens. Bioelectron. 48 (2013) 270–275.

[6] M. Roodbari Shahmiri, A. Bahari, H. Karimi-Maleh, R. Hosseinzadeh, N. Mirnia, Ethynylferrocene–NiO/MWCNT nanocomposite modified carbon paste electrode as a novel voltammetric sensor for simultaneous determination of glutathione and acetaminophen, Sens. Actuators B 177 (2013) 70–77.

[7] A.A. Ensafi, H. Bahrami, B. Rezaei, H. Karimi-Maleh, Application of ionic liquid–TiO 2 nanoparticlemodified carbon paste electrode forthe voltammetricdetermination of benserazide in biological samples, Mater. Sci. Eng. C 33 (2013) 831–835.

[8] S. Reddy, B.E. Kumara Swamy, U. Chandra, B.S. Sherigara, H. Jayadevappa, Synthesis of CdO nanoparticles and their modified carbon paste electrode for determination of dopamine and ascorbic acid by using cyclic voltammetry technique, Int. J. Electrochem. Sci. 5 (2010) 10–17.

[9] http://en.wikipedia.org/wiki/Morphine.

[10] F. Benedetti, A. Pollo, L. Colloca, Opioid-mediated placebo responses boost pain endurance and physical performance: is it doping in sport competitions? J. Neurosci. 27 (2007) 11934–11939.

[11] F. Tagliaro, D. Franchi, R. Dorizzi, M. Marigo, High-performance liquid chromato- graphic determination of morphine inbiological samples: anoverviewof separation methods and detection techniques, J. Chromatogr. 488 (1989) 215–228.

[12] Q.C. Meng, M.S. Cepeda, T. Kramer, H. Zou, D.J. Matoka, J. Farrar, High performance liquidchromatographicdeterminationofmorphineandits3-and6-glucuronideme- tabolites by two-step solid-phase extraction, J. Chromatogr. B 742 (2000) 115–123.

[13] M.E. Soares, V. Seabra, M.D.A. Bastos, Comparative study of different extractive procedures to quantify morphine in urine by HPLC-UV, J. Liq. Chromatogr. 15 (1992) 1533–1541.

[14] A.M. Bermejo, I. Ramos, P. Fernandez, M. Lopezrivadulla, A. Cruz, M. Chirotti, N. Fucci, R. Marsilli, Morphine determination bygas chromatography/mass spectroscopy in human vitreous humor and comparison with radioimmunoassay, J. Anal. Toxicol. 16 (1992) 372–374.

[15] J.G. Guillot, M. Lefebvre, J.P. Weber, Determination of heroin, 6-acetylmorphine, and morphine in biological fluids using their propionyl derivatives with ion trap GC–MS, J. Anal. Toxicol. 21 (1997) 127–133.

[16] P. Glare, T. Walsh, C. Pippenger, A simple, rapid method for the simultaneous determination of morphine and its principal metabolites in plasma using high performance liquid chromatography and fluorometric detection, Ther. Drug Monit. 13(1991) 226–232.

[17] S. Hara, S. Mochinaga, M. Fukuzawa, O.N.T. Kuroda, Direct injection of edible oils as micro emulsions in a micellar mobile phase applied to the liquid chromatographic determination of synthetic antioxidants, Anal. Chim. Acta. 387 (1999) 121–134.

[18] X.X. Zhang, J. Li, J. Gao, L. Sun, W.B. Chang, Determination of morphine by capillary electrophoresis immunoassay in thermally reversible hydrogel-modified buffer and laser-induced fluorescence detection, J. Chromatogr. A 895 (2000) 1–7.

[19] R. Dams, T. Benijts, W.E. Lambert, A.P. De Leenheer, Simultaneous determination of in total 17 opium alkaloids and opioids in blood and urine by fast liquid chromatography – diode-array detection – fluorescence detection, after solid-phase extraction, J. Chromatogr. B 773 (2002) 53–61.

[20] N.W. Barnett, S.W. Lewis, D.J. Tucker, Determination of morphine in process streams by sequential injection analysis with chemiluminescence detection, Fresenius, J. Anal. Chem. 355 (1996) 591–595.

[21] N.W. Barnett, C.E. Lenehan, S.W. Lewis, D.J. Tucker, K.M. Essery, Determination of morphine in water immiscible process streams using sequential injection analysis coupled with acidic permanganate chemiluminescence detection, Analyst 123 (1998) 601–605.

[22] S.W. Lewis, P.S. Francis, K.F. Lim, G.E. Jenkins, X.D. Wang, Pulsed flow chemistry: a new approach to solution handling for flow analysis coupled with chemi-luminescence detection, Analyst 125 (2000) 1869–1874.

[23] G. Sakai, K. Ogata, T.U. da, N. Miura, N. Yamazoe, A surface plasmon resonance based immune sensor for highly sensitive detection of morphine, Sensors Actuators B 49 (1998) 5–12.

[24] F. Xu, M. Gao, L. Wang, T. Zhou, L. Jin, J. Jin, Amperometric determination of morphine on cobalt hexacyanoferrate modified electrode in rat brain microdialysates, Talanta 58 (2002) 427–432.

[25] A. Salimi, R. Hallaj, G.R. Khayatian, Amperometric detection of morphine at preheated glassy carbon electrode modified with multiwall carbon nanotubes, Elec- troanalysis 17 (2005) 873–879.

[26] F. Li, J. Song, D. Gao, Q. Zhang, Han, L. Niu, Simple and rapid voltammetric determination of morphine at electrochemically pretreated glassy carbon electrodes, Talanta 79 (2009) 845–850.

[27] K.C. Ho, C.Y. Chen, H.C. Hsu, L.C. Chen, S.C. Shiesh, X.Z. Lin, Amperometric detection of morphine at a Prussian blue-modified indium tin oxide electrode, Biosens. Bioelectron. 20 (2004) 3–8.

[28] M.H. Pournaghi-Azar, A. Saadatirad, Simultaneous voltammetric and amperometric determination of morphine and codeine using a chemically modified-palladized aluminum electrode, J. Electroanal. Chem. 624 (2008) 293–298.

[29] A.Mokhtari, H. Karimi-Maleh,A.A.Ensafi, H. Beitollahi, Application of modified multiwall carbon nanotubes paste electrode for simultaneous voltammetric determination of morphine and diclofenac in biological and pharmaceutical samples, Sensors Actuators B 169 (2012) 96–105.

[30] A. Niazia, J.B. Ghasemi, M. Zendehdel, Simultaneous voltammetric determination of morphine and noscapine by adsorptive differential pulse stripping method and least-squares support vector machines, Talanta 74 (2007) 247–254.

[31] A.A. Ensafi, M. Izadi, B. Rezaei, H. Karimi-Maleh, N-hexyl-3-methylimidazolium hexafluoro phosphate/multiwall carbon nanotubes paste electrode as a biosensor for voltammetric detection of morphine, J. Mol. Liq. 174 (2012) 42–47.

[32] W. Thongchai, B. Liawruangrath, C. Thongpoon, T. Machan, High performance thin layer chromatographic method for the determination of diclofenac sodium in pharmaceutical formulation, Chiang Mai J. Sci. 33 (2006) 123–128.

[33] J.Emami, N.Ghassami, R. Talari,A rapid and sensitive modified HPLC method for determination of diclofenac in human plasma and its application in pharmacokinetic studies, DARU 15 (2007) 132–138.

[34] M.S. Morton, K.O. Brien, Analgesic efficacy of paracetamol and diclofenac in children receiving PCA morphine, Br. J. Anaesth. 82 (1999) 715–717.

[35] T. Tavana, M.A. Khalilzadeh, H. Karimi-Maleh, A.A. Ensafi, H. Beitollahi, D. Zareyee, Sensitive voltammetric determination of epinephrine in the presence of acetaminophen at a novel ionic liquid modified carbon nanotubes paste electrode, J. Mol. Liq. 168 (2012) 69–74.

[36] M. Ansari, S. Kazemi, M.A. Khalilzadeh, H. Karimi-Maleh, M.B. Pasha Zanousi, Sensitive and stable voltammetric measurements of norepinephrine at ionic liquid–carbon nanotubes paste electrodes, Int. J. Electrochem. Sci. 8 (2013) 1938–1948.

[37] H. Beitollah, M. Goodarzian, M.A. Khalilzadeh, H. Karimi-Maleh, M. Hassanzadeh, M. Tajbakhsh, Electrochemical behaviors and determination of carbidopa on carbon nanotubes ionic liquid paste electrode, J. Mol. Liq. 173 (2012) 137–143.

[38] S. Salmanpour, T. Tavana, A. Pahlavan, M.A. Khalilzadeh, A.A. Ensafi, H. Karimi-Maleh, H. Beitollahi, E. Kowsari, D. Zareyee, Voltammetric determination of norepinephrine in the presence of acetaminophen using a novel ionic liquid/multiwall carbon nanotubes paste electrode, Mater. Sci. Eng. C 32 (2012) 1912–1918.

[39] M. Bijad, H. Karimi-Maleh, M.A. Khalilzadeh, Application of ZnO/CNTs nano- composite ionic liquid paste electrode as a sensitive voltammetric sensor for determination of ascorbic acid in food samples, Food Anal. Methods (2013), http://dx.doi.org/10.1007/s12161-013-9585-9.

[40] J. Vahedi, H. Karimi-Maleh, M. Baghayeri, A.L. Sanati, M.A. Khalilzadeh, M. Bahrami, A fast andsensitive nanosensor basedon MgO nanoparticle room-temperature ionic liquid carbon paste electrode for determination of methyldopa in pharmaceutical and patient human urine samples, Ionics (2013), http://dx.doi.org/10.1007/ s11581-013-0940-z.

[41] A.A. Ensafi, H. Karimi-Maleh, Voltammetric determination of isoproterenol using multiwall carbon nanotubes-ionic liquid paste electrode, drug test, Analysis 3 (2011) 325–330.

[42] R. Moradi, S.A. Sebt, H. Karimi-Maleh, R. Sadeghi, F. Karimi, A. Bahari, H. Arabi, Synthesis and application of FePt/CNTs nanocomposite as a sensor and novel amide ligand as a mediator for simultaneous determination of glutathione, nicotinamide adenine dinucleotide and tryptophan, Phys. Chem. Chem. Phys. 15 (2013) 5888–5897.

[43] H. Beitollahi, H. Karimi-Maleh, H. Khabazzadeh, Nanomolar and selective determination of epinephrine in the presence of norepinephrine using carbon paste electrode modified with carbon nanotubes and novel 2-(4-oxo-3-phenyl-3,4 dihydroquinazolinyl)-N′-phenyl-hydrazinecarbothioamide, Anal. Chem. 80

(2008) 9848–9851.

[44] A.A. Ensafi, H. Karimi-Maleh, Modified multiwall carbon nanotubes paste electrode as a sensor for simultaneous determination of 6-thioguanine and folic acid using ferrocenedicarboxylic acid as a mediator, J. Electroanal. Chem. 640 (2010) 75–83.

[45] R. Sadeghi,H. Karimi-Maleh, M.A. Khalilzadeh, H. Beitollahi, Z. Ranjbarha, M.B. Pasha Zanousi, A new strategy for determination of hydroxylamine and phenol in water and waste water samples using modified nanosensor, Environ. Sci. Pollut. Res. (2013), http://dx.doi.org/10.1007/s11356-013-1733-7.

[46] M. Keyvanfard, R. Shakeri, H. Karimi-Maleh, K. Alizad, Highly selective and sensitive voltammetric sensor based on modified multiwall carbon nanotube paste electrode for simultaneous determination of ascorbic acid, acetaminophen and tryptophan, Mater. Sci. Eng. C 33 (2013) 811–816.

[47] R.S. Nicholson, I. Shain, Theory of stationary electrode polarography. single scan and cyclic methods applied to reversible, irreversible, and kinetic systems, Anal. Chem. 36 (1964) 706–723.

[48] H.R. Zare, N. Nasirizadeh, M. Mazloum-Ardakani, M. Namazian, Electrochemical properties and electrocatalytic activity of hematoxylin modified carbon paste electrode toward the oxidation of reduced nicotinamide adenine dinucleotide (NADH), Sens. Actuators B 120 (2006) 288–294.

[49] L.M. Smyth, J. Bobalova, M.G. Mendoza, C. Lew, V.N. Mutafova-Yambolieva, Release of beta-nicotinamide adenine dinucleotide upon stimulation of post- ganglionic nerve terminals in blood vessels and urinary bladder, J. Biol. Chem. 279 (2004) 48893–48903.

[50] R.A. Billington, S. Bruzzone, A. De Flora, A.A. Genazzani, F. Koch-Nolte, M. Ziegler, E. Zocchi, Emerging functions of extracellular pyridine nucleotides, Mol. Med. 12 (2006) 324–327.

[51] C. Shan, H. Yang, D. Han, Q. Zhang, A. Ivaska, L. Niu, Electrochemical determination of NADH and ethanol based on ionic liquid-functionalized grapheme, Biosens. Bioelect. 25 (2010) 1504–1508.

[52] L. Zhang, Y. Li, L. Zhang, D.W. Li, D. Karpuzov, Y.T. Long, Electrocatalytic oxidation of NADH on graphene oxide and reduced graphene oxide modified screen-printed electrode, Int. J. Electrochem. Sci. 6 (2011) 819–829.

[53] D. Gligor, Y. Dilginb, I. Catalin Popescua, L. Gorton, Poly-phenothiazine derivative-modified glassy carbon electrode for NADH electrocatalytic oxidation, Electrochim. Acta 54 (2009) 3124–3128.

[54] Y. Sha, Q. Gao, B. Qi, X. Yang, Electropolymerization of Azure B on a screen-printed carbon electrode and its application to the determination of NADH in a flow injection analysis system, Microchim. Acta 148 (2004) 335–341.

[55] T. Jamali, H. Karimi-Maleh, M.A. Khalilzadeh, A novel nanosensor based on Pt:Co nanoalloy ionic liquid carbon pasteelectrode for voltammetric determination of vitamin B 9 in food samples, LWT – Food Sci. Technol. 57 (2014) 679–685.

[56] M. Najafi, M.A. Khalilzadeh, H. Karimi-Maleh, A new strategy for determination of bisphenol A in the presence of Sudan I using a ZnO/CNTs/ionic liquid paste electrode in food samples, Food Chem. 158 (2014) 125–131.

[57] M. Ansari, S. Kazemi, M.A. Khalilzadeh, H. Karimi-Maleh, M.B. Pasha Zanousi, Sensitive and stable voltammetric measurements of norepinephrine at ionic liquid–carbon nanotubes paste electrodes, Int. J. Electrochem. Sci. 8 (2013) 1938–1948.

[58] A.A. Ensafi, M. Izadi, H. Karimi-Maleh, Sensitive voltammetric determination of diclofenac using room-temperature ionic liquid-modified carbon nanotubes paste electrode, Ionics 19 (2013) 137–144.

[59] A.A. Ensafi, H. Karimi-Maleh, Voltammetric determination of isoproterenol using multiwall carbon nanotubes-ionic liquid paste electrode, Drug Test Anal. 3 (2011) 325–330.

[60] A.A. Ensafi, M. Izadi, B. Rezaei, H. Karimi-Maleh, N-hexyl-3-methylimidazolium hexafluoro phosphate/multiwall carbon nanotubes paste electrode as a biosensor for voltammetric detection of morphine, J. Mol. Liq. 174 (2012) 42–47.

[61] A. Pahlavan, V.K. Gupta, A.L. Sanati, F. Karimi, M. Yoosefian, M. Ghadami, ZnO/CNTs nanocomposite/ionic liquid carbon paste electrode fordetermi- nation of noradrenaline in human samples, Electrochim. Acta 123 (2014) 456–462.

[62] V.K. Gupta, R. Sadeghi, F. Karimi, A novel electrochemical sensor based on ZnO nanoparticle and ionicliquid binder for square wave voltammetric determination ofdroxidopa in pharmaceutical and urine samples, Sens. Actuators B 186 (2013) 603–609.

[63] W. Sun, Y. Li, Y. Duan, K. Jiao, Direct electrocatalytic oxidation of adenine and guanine on carbon ionic liquid electrode and the simultaneous determination, Biosens. Bioelect. 24 (2008) 988–993.

[64] F. Xiao, C. Ruan, J. Li, L. Liu, F. Zhao, B. Zeng, Voltammetric determination of xanthine with a single-walled carbon nanotube-ionic liquid paste modified glassy carbon electrode, Electroanalysis 20 (2008) 361–366.

[65] M. Bijad, H. Karimi-Maleh, M.A. Khalilzadeh, Application of ZnO/CNTs nanocomposite ionic liquid paste electrode as a sensitive voltammetric sensor for determination of ascorbic acid in food samples, Food Anal. Methods 6 (2013) 1639–1647.

[66] M. Elyasi, M.A. Khalilzadeh, H. Karimi-Maleh, High sensitive voltammetric sensor based on Pt/CNTs nanocomposite modified ionic liquid carbon paste electrode for determination of Sudan I in food samples, Food Chem. 141 (2013) 4311–4317.

[67] A.L. Sanati, H. Karimi-Maleh, A. Badiei, P. Biparva, A.A. Ensafi, A voltammetric sensor based on NiO/CNTs ionic liquid carbon paste electrode for determination of morphine in the presence of diclofenac, Mater. Sci. Eng. C 35 (2014) 379–385.

[68] T. Tavana, M.A. Khalilzadeh, H. Karimi-Maleh, A.A. Ensafi, H. Beitollahi, D. Zareyee, Sensitive voltammetric determination of epinephrine in the presence of acetaminophen at a novel ionic liquid modified carbon nanotubes paste electrode, J. Mol. Liq. 168 (2012) 69–74.

[69] J. Vahedi, H. Karimi-Maleh, M. Baghayeri, A.L. Sanati, M.A. Khalilzadeh, M. Bahrami, A fast and sensitive nanosensor based on MgO nanoparticle room-temperature ionic liquid carbon paste electrode for determination of methyldopa in pharmaceutical and patient human urine samples, Ionics 19 (2013) 1907–1914.

[70] S. Salmanpour, T. Tavana, A. Pahlavan, M.A. Khalilzadeh, A.A. Ensafi, H. Karimi- Maleh, H. Beitollahi, E. Kowsari, D. Zareyee, Voltammetric determination of norepinephrine in the presence of acetaminophen using a novel ionic liquid/multiwall carbon nanotubes paste electrode, Mater. Sci. Eng. C 32 (2012) 1912–1918.

[71] A.A. Ensafi, H. Bahrami, B. Rezaei, H. Karimi-Maleh, Application of ionic liquid-TiO 2 nanoparticle modified carbon paste electrode for the voltammetric determination of benserazide in biological samples, Mater. Sci. Eng. C 33 (2013) 831–835.

[72] R. Sadeghi, H. Karimi-Maleh, A. Bahari, M. Taghavi, A novel biosensor based on ZnO nanoparticle/1,3-dipropylimidazolium bromide ionic liquid- modified carbon paste electrode for square-wave voltammetric determination of epinephrine, Phys. Chem. Liq. 51 (2013) 704–714.

[73] H. Beitollah, M. Goodarzian, M.A. Khalilzadeh, H. Karimi-Maleh, M. Has- sanzadeh, M. Tajbakhsh, Electrochemical behaviors and determination of carbidopa on carbon nanotubes ionic liquid paste electrode, J. Mol. Liq. 173 (2012) 137–143.

[74] E. Afsharmanesh, H. Karimi-Maleh, A. Pahlavan, J. Vahedi, Electrochemical behavior of morphine at ZnO/CNT nanocomposite room temperature ionic liquid modified carbon paste electrode and its determination in real samples, J. Mol. Liq. 181 (2013) 8–13.

[75] M. Fouladgar, H. Karimi-Maleh, Ionic liquid/multiwall carbon nanotubes paste electrode for square wave voltammetric determination of methyldopa, Ionics 19 (2013) 1163–1170.

[76] M. Yoosefian, Z. Barzgari, J. Yoosefian, Ab initio study of Pd-decorated single- walled carbon nanotube with C-vacancy as CO sensor, Struct. Chem. 25 (2014) 9–19.

[77] A.A. Ensafi, H. Karimi-Maleh, S. Mallakpour, B. Rezaei, Highly sensitive voltam- metric sensor based on catechol-derivative-multiwall carbon nanotubes for the catalytic determination of captopril in patient human urine samples, Colloids Surf. B 87 (2011) 480–488.

[78] A.A. Ensafi, H. Karimi-Maleh, S. Mallakpour, M. Hatami, Simultaneous determination of N-acetylcysteine and acetaminophen by voltammetric method using N-(3,4-dihydroxyphenethyl)-3,5-dinitrobenzamide modified multiwall carbon nanotubes paste electrode, Sens. Actuators B 155 (2011) 464–472.

[79] A.A. Ensafi, H. Karimi-Maleh, Modified multiwall carbon nanotubes paste electrode as a sensor for simultaneous determination of 6-thioguanine and foliacid using ferrocenedicarboxylic acid as a mediator, J. Electroanal. Chem. 640 (2010) 75–83.

[80] C. Luyo, R. Ionescu, L.F. Reyes, Z. Topalian, W. Estrada, E. Llobet, C.G. Granqvist, P. Heszler, Gas sensing response of NiO nanoparticle films made by reactive gas deposition, Sens. Actuators B 138 (2009) 14–20.

[81] M. Roodbari Shahmiri, A. Bahari, H. Karimi-Maleh, R. Hosseinzadeh, N. Mirnia, Ethynylferrocene–NiO/MWCNT nanocomposite modified carbon paste electrode as a novel voltammetric sensor for simultaneous determination of glutathione and acetaminophen, Sens. Actuators B 177 (2013) 70–77.

[82] H. Karimi-Maleh, P. Biparva, M. Hatami, A novel modified carbon paste electrode based on NiO/CNTs nanocomposite and (9,10-dihydro-9,10- ethanoanthracene-11,12-dicarboximido)-4-ethylbenzene-1,2-diol as a mediator for simultaneous determination of cysteamine, nicotinamide adenine dinucleotide and folic acid, Biosens. Bioelect. 48 (2013) 270–275.

[83] H. Teymourian, A. Salimi, R. Hallaj, Electrocatalytic oxidation of NADH at electrogenerated NAD+ oxidation product immobilized onto multiwalled carbon nanotubes/ionic liquid nanocomposite: application to ethanol biosensing, Talanta 90 (2012) 91–98.

[84] Q. Wang, H. Tang, Q. Xie, L. Tan, Y. Zhang, B. Li, S. Yao, Room-temperature ionic liquids/multi-walled carbon nanotubes/chitosan composite electrode for electrochemical analysis of NADH, Electrochim. Acta 52 (2007) 6630– 6637.

[85] A. Salimi, S. Lasghari, A. Noorbakhash, Carbon nanotubes-ionic liquid and chloropromazine modified electrode for determination of NADH and fabrication of ethanol biosensor, Electroanalysis 22 (2010) 1707–1716.

[86] L.A. Saghatforoush, M. Hasanzadeh, S. Sanati, R. Mehdizadeh, Ni(OH) 2 and NiO nanostructures: synthesis, characterization and electrochemical performance, Bull. Korean Chem. Soc. 33 (2012) 2613–2618.

[87] C.E. Banks, A. Crossley, C. Salter, S.J. Wilkins, R.G. Compton, Carbon nano- tubes contain metal impurities which are responsible for the “Electrocatalysis” seen at some nanotube-modified electrodes, Angew. Chem. Int. Ed. 45 (2006) 2533–2537.

[88] M. Mazloum-Ardakani, A. Khoshroo, High performance electrochemical sensor based on fullerene-functionalized carbon nanotubes/ionic liquid: determination of some catecholamines, Electrochem. Commun. 42 (2014) 9–12.

[89] R.S. Nicholson, I. Shain, Theory of stationary electrode polarography, Anal. Chem. 36 (1964) 706–723.

[90] B.J. Sanghavi, A.K. Srivastava, Simultaneous voltammetric determination of acetaminophen, aspirin and caffeine using an in situ surfactant-modified multiwalled carbon nanotube paste electrode, Electrochim. Acta 55 (2010) 8638–8648.

[91] B.J. Sanghavi, A.K. Srivastava, Adsorptive stripping differential pulse voltammetric determination of venlafaxine and desvenlafaxine employing Nafion–carbon nanotube composite glassy carbon electrode, Electrochim. Acta 56 (2011) 4188–4196.

[92] R. Moradi, S.A. Sebt, H. Karimi-Maleh, R. Sadeghi, F. Karimi, A. Bahari, H. Arabi, Synthesis and application of FePt/CNTs nanocomposite as a sensor and novel amide ligand as a mediator for simultaneous determination of glutathione, nicotinamide adenine dinucleotide and tryptophan, Phys. Chem. Chem. Phys. 15 (2013) 5888–5897.

[93] A.A. Ensafi, H. Karimi-Maleh, S. Mallakpour, A new strategy for the selective determination of glutathione in the presence of nicotinamide adenine dinucleotide (NADH) using a novel modified carbon nanotube paste electrode, Colloids Surf. B 104 (2013) 186–193.

[94] A.A. Ensafi, H. Karimi-Maleh, M. Ghiaci, M. Arshadi, Characterization of Mn-nanoparticles decorated organo-functionalized SiO 2 –Al 2 O 3 mixed-oxide as a novel electrochemical sensor: application for the voltammetric determination of captopril, J. Mater. Chem. 21 (2011) 15022–15030.

[95] V.K. Gupta, A.K. Jain, G. Maheshwari, Novel Aluminum (III) selective potentiometric sensor based on morin in poly (vinyl chloride) matrix, Talanta 72 (4) (2007) 1469–1473.

[96] V.K. Gupta, M.R. Ganjali, P. Norouzi, H. Khani, A. Nayak, Shilpi Agarwal, Electrochemical Analysis of some Toxic Metals and Drugs by Ion Selective Electrodes, Crit. Rev. Anal. Chem. 41 (2011) 282–313.

[97] V.K. Gupta, A.K. Jain, S. Agarwal, G. Maheshwari, An iron (III) ion-selective sensor based on a m bis (tridentate) ligand, Talanta 71 (2007) 1964–1968.

[98] R. Jain, V.K. Gupta, N. Jadon, K. Radhapyari, Voltammetric Determination of Cefixime in pharmaceuticals and Biological Fluidss, Anal. Biochem. 407 (2010) 79–88.

[99] V.K. Gupta, A.K. Singh, S. Mehtab, B. Gupta, A Cobalt (II) selective PVC membrane based on a Schiff base complex of N, N'-bis (salicylidene)-3, 4-diaminotoluene, Anal. Chim. Acta 566 (2006) 5–10.

[100] R.N. Goyal, V.K. Gupta, S. Chatterjee, Electrochemical oxidation of 2', 3'-dideoxyadenosine at pyrolytic graphite electrode, Electrochim. Acta 53 (2008) 5354–5360.

[101] V.K. Gupta, A.K. Singh, M. Al Khayat, Barkha Gupta, Neutral carriers based poly431 meric membrane electrodes for selective determination of Mercury (II), Anal. Chim. Acta 590 (2007) 81–90.

[102] V.K. Gupta, R. Prasad, R. Mangla, P. Kumar, New nickel (II) selective potentiometric sensor based on 5, 7,12,14-tetramethyldibenzotetraazaannulene in a poly (vinyl chloride) matrix, Anal. Chim. Acta 420 (2000) 19–27

[103] R.N. Goal, V.K. Gupta, S. Chatterjee, Simultaneous determination of adenosine and inosine using single-wall carbon nanotubes modified pyrolytic graphite electrode, Talanta 76 (2008) 662–668.

[104] V.K. Gupta, Imran Ali, A. Tawfik, Saleh, Arunima Nayak, Shilpi Agarwal, Chemical Treatment Technologies for Wastewater Recycling –a Review, RSC Adv. 2 (2012) 6380–6388.

[105] R.N. Goyal, V.K. Gupta, S. Chatterjee, Voltammetric biosensors for the determination of paracetamol at carbon nanotube modified pyrolytic graphite electrode, Sensor. Actuat. B-Chem. 149 (2010) 252–258.

[106] H. Beitollahi, H. Karimi-Maleh, H. Khabazzadeh, Nanomolar and selective determination of epinephrine in the presence of norepinephrine using carbon paste electrode modified with carbon nanotubes and novel 2-(4-oxo-3-phenyl-3,4- dihydroquinazolinyl)-N ? -phenyl-hydrazinecarbothioamide, Anal. Chem. 80 (2008) 9848–9851.

[107] http://www.wisegeek.org/what-is-noradrenaline.htm; 26, May, 2013.

[108] H. Seol, H. Jeong, S. Jeon, A selective determination of norepinephrine on the glassy carbon electrode modified with poly (ethylenedioxypyrrole dicarboxylic acid) nanofibers, J. Solid State Electrochem. 13 (2009) 1881–1887.

[109] H. Beitollahi, A. Mohadesi, S. Khalilizadeh Mahani, H. Karimi-Maleh, A. Akbari,New voltammetric strategy for simultaneous determination of norepinephrine, acetaminophen, and folic acid using a 5-amino-3 ? ,4 ? -dimethoxy-biphenyl-2-ol/carbon nanotube paste electrode, Ionics 18 (2012) 703–710.

[110] H.Jeong, H. Kim, S. Jeon, Modified glassy carbon electrode by electropoly-merization of tetrakis-(2-aminopheny)porphyrin for the determination ofnorepinephrine in the presence of ascorbic acid, Microchem. J. 78 (2004)181–186.

[111] A.R. Taheri, A. Mohadesi, D. Afzali, H. Karimi-Maleh, H. Mahmoudi Moghad- dam, H. Zamani, Z. rezayati zad, Simultaneous voltammetric determination of norepinephrine and folic acid at the surface of modified carbon nanotube paste electrode, Int. J. Electrochem. Sci. 6 (2011) 171–180.

[112] H. Seol, H. Jeong, S. Jeon, Selective determination of norepinephrine on the glassy carbon electrode modified with poly (ethylenedioxypyrrole dicarboxylic acid) nanofibers, J. Solid State Electrochem. 13 (2009) 1881–1887.

[113] W. Chen, X. Lin, H. Luo, L. Huang, Electrocatalytic oxidation and determination of norepinephrine at poly(cresol red) modified glassy carbon electrode, Electroanalysis 17 (2005) 941–945.

[114] A.A. Ensafi, H. Karimi-Maleh, Modified multiwall carbon nanotubes paste electrode as a sensor for simultaneous determination of 6-thioguanine and folic acid using ferrocenedicarboxylic acid as a mediator, J. Electroanal. Chem. 640 (2010) 75–83.

[115] H. Karimi-Maleh, P. Biparva, M. Hatami, A novel modified carbon paste electrode based on NiO/CNTs nanocomposite and (9,10-dihydro- 9,10-ethanoanthracene-11, 12-dicarboximido)-4-ethylbenzene-1,2-diol as a mediator for simultaneous determination of cysteamine, nicotin amide adenine dinucleotide and folic acid, Biosens. Bioelect. 48 (2013) 270–275.

[116] G.S. Lai, H.L. Zhang, C.M. Jin, Electrocatalysis and voltammetric determination of dopamine at a calix[4]arene crown-4 ether modified glassy carbon electrode, Electroanalysis 19 (2007) 496–501.

[117] A.A. Ensafi, H. Karimi-Maleh, S. Mallakpour, B. Rezaei, Highly sensitive voltammetric sensor based on catechol-derivative-multiwall carbon nanotubes for the catalytic determination of captopril in patient human urine samples, Coll. Surf. B 87 (2011) 480–488.

[118] A.A. Ensafi, H. Karimi-Maleh, S. Mallakpour, M. Hatami, Simultaneous determination of N-acetylcysteine and acetaminophen by voltammetric method using N-(3,4-dihydroxyphenethyl)-3,5-dinitrobenzamide modified multiwall carbon nanotubes paste electrode, Sens. Actuators B 155 (2011) 464–472.

[119] A. Kutluay, M. Aslanoglu, Electrocatalytic oxidation of isoproterenol and its voltammetric determination in pharmaceuticals and urine samples using a poly(1-methylpyrrole)-DNA modified electrode, Acta Chim. Slov. 57 (2010) 157–162.

[120] A. Mokhtari, H. Karimi-Maleh, A.A. Ensafi, H. Beitollahi, Application of modified multiwall carbon nanotubes paste electrode for simultaneous voltammetric determination of morphine and diclofenac in biological and pharmaceutical samples, Sens. Actuators B 16 (2012) 96–105.

[121] S. Kharian, N. Teymoori, M.A. Khalilzadeh, Multi-wall carbon nanotubes and TiO2 as a sensor for electrocatalytic determination of epinephrine in the presence of p-chloranil as a mediator, J. Solid State Electrochem. 16 (2012) 563–568.

[122] M. Suchea, S. Christoulakis, K. Moschovis, N. Katsarakis, G. Kiriakidis, ZnO transparent thin films for gas sensor applications, Thin Solid Films 515 (2006) 551–554.

[123] R.N. Goyal, V.K. Gupta, M. Oyama, N. Bachheti, Gold nanoparticles modified indium tin oxide electrode for the simultaneous determination of dopamine and serotonin: application in pharmaceutical formulations and biological fluids, Talanta 72 (2007) 976–983.

[124] S. Shahrokhian, E. Jokar, M. Ghalkhani, Electrochemical determination of piroxicam on the surface of pyrolytic graphite electrode modified with a film of carbon nanoparticle-chitosan, Microchim Acta 170 (2010) 141–146.

[125] B. Rezaei, S. Damiri, Using of multi-walled carbon nanotubes electrode for adsorptive stripping voltammetric determination of ultratrace levels of RDX explosive in the environmental samples, J. Hazard. Mater. 83 (2010) 138–144.

[126] F. Ghorbani-Bidkorbeh, S. Shahrokhian, A. Mohammadi, R. Dinarvand, Electro- chemical determination of naltrexone on the surface of glassy carbon electrode modified with Nafion-doped carbon nanoparticles: Application to determinations in pharmaceutical and clinical preparations, J. Electroanal. Chem. 638 (2010) 212–217.

[127] C.E. Banks, A. Crossley, C. Salter, S.J. Wilkins, R.G. Compton, Carbon nano- tubes contain metal impurities which are responsible for the electrocatalysis seen at some nanotube-modified electrodes, Angew. Chem. Int. Ed. 45 (2006) 2533–2537.

[128] Y. Pan, L. Li, S.H. Chan, J. Zhao, Correlation between dispersion state and electrical conductivity of MWCNTs/PP composites prepared by melt blending, Composites: Part A 41 (2010) 419–426.

[129] S. Kazemi, H. Karimi-Maleh, R. Hosseinzadeh, F. Faraji, Selective and sensitive voltammetric sensor based on modified multiwall carbon nanotubes paste electrode for simultaneous determination of L-cysteine and folic acid, Ionics 19 (2013) 933–940.

[130] J.B. Raoof, Reza. Ojani, S.R. Hosseini, A novel, effective and low cost catalyst for methanol oxidation based on nickel ions dispersed onto poly(o- toluidine)/Triton X-100 film at the surface of multi-walled carbon nanotube paste electrode, J. Power Sour. 196 (2011) 1855–1863.

[131] R. Moradi, S.A. Sebt, H. Karimi-Maleh, R. Sadeghi, F. Karimi, A. Bahari, H. Arabi,

Synthesis and application of FePt/CNTs nanocomposite as a sensor and novel amide ligand as a mediator for simultaneous determination of glutathione, nicotinamide adenine dinucleotide and tryptophan, Phys. Chem. Chem. Phys. 15 (2013) 5888–5897.

[132] S. Shahrokhian, M. Ghalkhani, M. Adeli, M.K. Amini, Multi-walled carbon nano- tubes with immobilised cobalt nanoparticle for modification of glassy carbon electrode: Application to sensitive voltammetric determination of thioridazine, Biosens. Bioelect. 24 (2009) 3235–3241.

[133] A.A. Ensafi, M. Ghiaci, M. Arshadi, H. Karimi-Maleh, Synthesis and character- ization of

ferrocenecarboxaldehyde immobilized on modified SiO 2 –Al 2 O 3 in nanoscale, application for determination of penicillamine, J. Nanopart. Res. 15 (2013) 1610.

[134] Y. Zhang, J. Zheng, Sensitive voltammetric determination of rutin at an ionic liquid modified carbon paste electrode, Talanta 77 (2008) 325–330.

[135] Pandurangachar, M., Kumara Swamy, B.E., Chandrashekar, B.N., Gilbert, O., Sherigara, B.S., Electrochemical deposition of 1-butyl-4-methyl-pyridinium tetrafluroborate ionic liquid on carbon paste electrode and its application for the simultaneous determination of dopamine, ascorbic acid and uric acid Vol. 165 (2012) 168–172.

[136] Fouladgar, M., Karimi-Maleh, H., Ionic liquid/multiwall carbon nanotubes paste electrode for square wave voltammetric determination of methyldopa vol. 19, pp. 1163-1170.

[137] D.V. Chernyshov, N.V. Shvedene, E.R. Antipova, I.V. Pletnev, Ionic liquid-based miniature electrochemical sensors for the voltammetric determination of cat- echolamines, Anal. Chim Acta 621 (2008) 178–184.

[138] M.R. Ganjali, H. Khoshsafar, A. Shirzadmehr, M. Javanbakht, F. Faridbod, Improvement of carbon paste ion selective electrode response by using room temperature ionic liquids (RTILs) and multi-walled carbon nanotubes (MWC- NTs), Int. J. Electrochem. Sci. 4 (2009) 435–443.

[139] T. Tavana, M.A. Khalilzadeh, H. Karimi-Maleh, A.A. Ensafi, H. Beitollahi, D. Zareyee, Sensitive voltammetric determination of epinephrine in the presence of acetaminophen at a novel ionic liquid modified carbon nanotubes paste electrode, J. Mol. Liq. 168 (2012) 69–74.

[140] H. Beitollah, M. Goodarzian, M.A. Khalilzadeh, H. Karimi-Maleh, M. Has- sanzadeh, M. Tajbakhsh, Electrochemical behaviors and determination of carbidopa on carbon nanotubes ionic liquid paste electrode, J. Mol. Liq. 173 (2012) 137–143.

[141] S. Salmanpour, T. Tavana, A. Pahlavan, M.A. Khalilzadeh, A.A. Ensafi, H. Karimi-Maleh, H. Beitollahi, E. Kowsari, D. Zareyee, Voltammetric determination of norepinephrine in the presence of acetaminophen using a novel ionic liquid/multiwall carbon nanotubes paste electrode, Mat. Sci. Eng. C 32 (2012) 1912–1918.

[142] E. Afsharmanesh, H. Karimi-Maleh, A. Pahlavan, J. Vahedi, Electrochemical behaviors and determination of carbidopa on carbon nanotubes ionic liquid paste electrode, J. Mol. Liq. 173 (2012) 137–143.

[143] W. Sun, Y. Li, H. Gao, K. Jiao, Direct electrochemistry of double stranded DNA on ionic liquid modified carbon paste electrode, Microchim Acta 165 (2009) 313–317.

[144] M. Elyasi, M.A. Khalilzadeh, H. Karimi-Maleh, High sensitive voltammetric sensor based on Pt/CNTs nanocomposite modified ionic liquid carbon paste electrode for determination of Sudan I in food samples, Food Chem. 141 (2013) 4311–4317.